THE PRODUCTION OF THERMALLY CONDUCTIVE THERMOPLASTIC POLYMERS WITH METALLIC OR CARBON FILLERS

by

Tankut TÜREL

B.S., Chemistry, Boğaziçi University, 2013

Submitted to the Institute for Graduate Studies in
Science and Engineering in partial fulfillment of
the requirements for the degree of
Master of Science

Graduate Program in Chemistry
Boğaziçi University

2015

To my family

and

To my precious nephew Marvin

ACKNOWLEDGEMENTS

First of all, I would like to express my sincerest gratitude for Prof. Selim Küsefoğlu for his guidance, encouragement and tolerance. It was a great pleasure for me to be one of the group members of his research group. I believe that I gained self-confidence and numerous experiences by studying and working with him. I am also thankful to him for his life advices for my life style and my future.

I would like to express special thanks to committee members Inst. Ediz Taylan, Prof. İlknur Doğan, Prof. Duygu Avcı Semiz and Assoc. Prof. Nuri Ersoy for giving their valuable time in reviewing this thesis and for all their advices and comments on the final manuscripts.

My special thanks go to especially Gizem Kırevliyası and Hazal Pekcan for their most precious friendships, support on everything. Without their friendship and supports, it would be very difficult to overcome all kinds of problems I had faced with in life and during the writing period of this thesis. I would like to thank Jesmi Çavuşoğlu for her technical support on the instruments, some software and laboratory work. In addition, I would also like to thank to all of my friends in chemistry department especially Merve Seçkin Altuncu, Eren Esen, Nur Çiçek Kekeç and Duygu Tuncel for their endless friendship and morale support.

My deepest appreciations go to my family members, my father Serdar Türel, my mother Perihan Türel and my sister Burcu Türel Diem for their labors in my growth, their helps in my successes and future plans and supports on everything. I am grateful to them for being the best family ever. I want also thank to my uncle Serhat Türel for his guidance in some important life experiences and his morale support on the worst days we had faced with. I am also thankful to my grandparents for their labors in my growth.

Last but not the least; I am grateful to the founder of the Republic of Turkey, Mustafa Kemal Atatürk. Without his revolutions, it would be impossible for us to advance in science.

ABSTRACT

THE PRODUCTION OF THERMALLY CONDUCTIVE THERMOPLASTIC POLYMERS WITH METALLIC OR CARBON FILLERS

Thermal conductivity values of organic polymers are extremely low. Therefore, they are used as thermal insulating materials in many applications. In recent years, especially in electrical and electronics industry, plastic materials are used due to their corrosion resistance, ease of manufacture and low price. However, to be able to remove the heat generated by the electronic circuits, the plastic used must have a high thermal conductivity. In this project, composites were made from a polymer containing carboxylic acid groups (ethylene-metacrylic acid copolymer Surlyn®) filled with highly thermally conductive fillers such as spherical aluminum, aluminum flakes, graphite flakes or carbon fiber in different weight ratios. Alkali metal surface of aluminum gives an acid-base neutralization reaction with carboxylic acid groups of Surlyn® by forming an ionic bond and, this creates an interface with high interfacial adhesion. When graphite used as filler material with Surlyn®, the possibility of having an interaction between the filler and the polymer matrix is very low; however, when carbon fiber is used as a filler material with Surlyn®, it is expected that there is a good interaction between the filler and the polymer matrix although carbon fiber has the same structure with graphite because during manufacturing of carbon fiber, it is partially oxidized to 1,4-diketone, quinone, hydroquinone, dicarboxylic acid structures on the edge groups. In these composites, polymer matrix-filler material interfacial interaction properties were determined by scanning electron microscope. It is the objective of this work to enhance the adhesion of filler to polymer matrix by using coupling agents and surface treatment of the fillers. The increase in the thermal conductivity of the composites produced was determined by the thermal camera experiments. At the end of this study, the thermal conductivity of Surlyn® was increased from 0.24 W/m·K to 6.8 W/m·K by the incorporation of 40% by weight graphite.

ÖZET

TERMAL OLARAK İLETKEN METAL VEYA KARBON DOLGULU TERMOPLASTİK POLİMERLERİN ÜRETİMİ

Organik polimerlerin termal geçirgenlik değerleri çok düşüktür. Bu nedenle birçok uygulamada termal yalıtım malzemesi olarak kullanılmaktadırlar. Son yıllarda özellikle elektrik ve elektronik sanayinde daha ucuz, kolay üretim ve paslanmaz özellikler gibi avantajlara sahip oldukları için plastik malzemeler kullanılmaya başlanmıştır. Ancak, bu kullanılan plastik malzemelerin belirli bir değerin üzerinde termal geçirgenlik katsayısına sahip olması niteliği aranmaktadır. Böylece elektrik ve elektronik devrelerin yarattığı ısının cihazın dışına atılması ve cihazın soğuması amaçlanmaktadır. Bu projede karboksilik asit grubu içeren bir polimerin (etilen-metakrilik asit kopolimeri Surlyn®), küresel tanecikli alüminyum tozu, pul tanecikli alüminyum tozu, pul tanecikli grafit tozu ve karbon elyaf gibi yüksek termal iletkenliğe sahip dolgu maddeleri ile değişik ağırlık oranlarında kompozitleri üretilmiştir. Alkalin yüzeyli bir metal olan alüminyum, karboksilik asit grubu içeren Surlyn® ile asit-baz nötrleşme reaksiyonu vermesi sonucunda iyonik bağ kurarak güçlü bir ara yüzey oluşturmaktadır. Surlyn® ile dolgu olarak grafit kullanıldığında arada bir etkileşim görme olasılığı çok düşüktür. Ancak dolgu olarak grafitin kimyasal yapısının aynısı olmasına rağmen karbon elyaf kullanıldığı zaman ara yüzeylerinde güzel bir etkileşim beklenebilir çünkü karbon elyaf üretimi sırasında yüzeyde 1,4-diketon, kinon, hidrokinon, dikarboksilik asit yapılarına yükseltgenmiştir. Bu kompozitlerde polimer-dolgu ara yüzey yapışma özellikleri taramalı elektron mikroskobu ile belirlenmiştir. Dolgu maddesine uygulanan çeşitli bağlayıcı ajanlar ve çeşitli yüzey muameleleri ile ara yüzey bağ kuvveti artırılmıştır. Üretilen tüm kompozitlerin termal geçirgenlikteki artış termal kamera deneyleri ile saptanmıştır. Çalışma sonunda Surlyn® polimerinin termal iletkenliği 0.24 W/m·K iken, % 40 grafit dolgulu Surlyn® kompozitinin termal iletkenliği 6.8 W/m·K' e çıkarılmıştır.

TABLE OF CONTENTS

LIST OF FIGURES

LIST OF TABLES

LIST OF SYMBOLS

%	Percentage
(m·K/W)	Thermal Resistivity Unit
(W/m·K)	Thermal Conductivity Unit
(Ω·m)	Electrical Resistivity Unit
$(\Omega \cdot m)^{-1}$	Electrical Conductivity Unit
®	Registered in the U.S. Patent and Trademark Office
°C	Celcius, Temperature Unit
A	Cross-Sectional Area
Al	Aluminum
Al_2O_3	Alumina
AlN	Aluminum Nitride
BN	Boron Nitride
C_2H_5OH	Ethyl Alcohol
cm^{-1}	Wavelength Unit
C_p	Heat Capacity
Cu	Copper
dT	Change in Temperature
dx	Change in Position
H_2O	Water Molecule
H_2O_2	Hydrogen Peroxide
H_2SO_4	Sulfuric Acid
HAc	Acetic Acid
HCl	Hydrochloric Acid
l	Mean Free Path of Phonons
K	Kelvin, Temperature Unit
$KMnO_4$	Potassium Permanganate
kV	Kilovolts, Unit of Electric Potential
L	Length of the Material
m	Meter
Na^+	Sodium Ion

NaOH	Sodium Hydroxide
pH	Power of Hydrogen
q	Amount of Heat Transferred
SiC	Silicon Carbide
W	Watt, Power Unit
Zn^{2+}	Zinc Ion
ΔT	Temperature Difference
λ	Thermal Conductivity
ρ	Density
σ	Electrical Conductivity
υ	Average Sound Velocity
Ω	Ohm, Electrical Resistance Unit

LIST OF ACROYNMS / ABBREVIATIONS

2D	Two Dimensional
ASTM	American Society for Testing and Materials
ATR	Attenuated Total Reflectance
CNT	Carbon Nanotube
EDX	Energy Dispersive X-Ray Spectroscopy
EP	European
ESEM	Environmental Scanning Electron Microscopy
FEG	Field Emission Gun
FLIR	Forward Looking Infrared
FTIR	Fourier Transform Infrared Spectroscopy
HDPE	High Density Polyethylene
IR	Infrared
LDPE	Low Density Polyethylene
LED	Light Emitting Diode
PAN	Poly Acrylonitrile
PC	Poly Carbonate
PET	Polyethylene Terephthalate
PMMA	Poly (methyl methacrylate)
PP	Polypropylene
PS	Polystyrene
PTFE	Polytetrafluoroethylene
PVC	Polyvinyl chloride
RT	Room Temperature
SEM	Scanning Electron Microscopy
SI	International System of Units
US	United States

1. INTRODUCTION

1.1. Thermal Conductivity

The concept thermal conductivity plays a very significant role in human life. There are billions of people inhabiting the temperate and cold regions of the earth where keeping warm is necessary for their existence. The use of materials with low thermal conductivities, such as wool and animal skins, has kept people warm from the Stone Age to present. Using highly thermally conductive materials in house-heating radiators supplies the diffusion of the heat to the house with minimum energy loss. If the outer walls of a building are covered with thermal-insulation materials, the heat loss will significantly be prevented. Of course, these examples could be extended infinitely. In short, one can see that thermal conductivity of a material is very important for human existence.

How does a solid transfer heat? According to Fourier's law, the heat flow through a solid material is proportional to the temperature gradient along the material. When materials are subjected to a steady-state heat flow (q), a temperature gradient (dT/dx) is produced in the materials along the heat flow direction [1]. Heat flow and temperature gradient are combined in theorem 1.1 where λ is the thermal conductivity of the material, A is the cross sectional area of the sample, and the minus sign indicates that heat transfer occurs from hot to cold regions of a material:

Theorem 1.1. Fourier's Law for Heat Conduction.

$$q = -\lambda \cdot A \cdot \frac{dT}{dx}$$

The term thermal conductivity is used to express the ability of a material to conduct heat. Conduction occurs only if there is a temperature difference between two ends of the conducting medium. If the Fourier's law is redesigned for a uniform, insulated rod, then the amount of heat transfer by conduction through this rod is given by Equation 1.1 where

q is the amount of heat transferred, ΔT is the temperature difference between the ends of the sample and L is the length of the sample.

$$q = \lambda \cdot A \cdot \frac{\Delta T}{\mathrm{L}} \tag{1.1}$$

According to this equation, the amount of heat transfer is proportional to the temperature difference of the hotter and colder points, to the cross sectional area of the material, and inversely proportional to the distance between the hotter and the colder points of the material.

Thermal conductivity requires kinetic energy transfer between neighboring atoms or molecules and in this way, heat transmission is very similar to sound transmission. The term thermal conductivity is described by the Debye kinetic model where C_p is the heat capacity, ρ is the density, υ is the average sound velocity in the material, and l is the mean free path of phonons in the material [2]. Phonons can simply described as vibrational motions of atoms or molecules in a lattice.

Theorem 1.2. Debye Kinetic Model.

$$\lambda = \frac{Cp \cdot \rho \cdot \upsilon \cdot l}{3}$$

The average sound velocity depends on the material and is not related to temperature. However, the mean free path of phonons depends on the temperature. As temperature increases, the mean free path of phonons decreases because of intrinsic phonon-phonon interactions [3].

The process of energy transfer can be represented on an atomic scale as an exchange of kinetic energy between microscopic particles such as molecules, atoms and free electrons. Less energetic particles gain energy in collisions with more energetic particles. Consider a metal rod which is heated by a flame from one of the ends. As the flame heats the rod, the particles near the flame vibrate with increasing amplitudes. These particles, in turn, collide with neighboring particles and transfer some of their energy to their

neighbors. Slowly, the amplitudes of vibration of metal atoms and electrons farther and farther from the flame increase up to the other end of the rod [4].

In SI units, thermal conductivity is measured in watts per meter kelvin, ($W \cdot m^{-1} \cdot K^{-1}$). The reciprocal of thermal conductivity is called thermal resistivity and it can be defined as the ability of a material to resist heat flow. The SI unit of thermal resistivity is given as $K \cdot m \cdot W^{-1}$.

1.1.1. Thermally Conductive and Non-Conductive Materials

Materials that are good heat conductors have relatively larger thermal conductivity values, while good thermal insulators have extremely low thermal conductivity values. For this reason, highly thermally conductive materials are widely used in heat transfer applications; conversely, materials with low thermal conductivities are used in thermal insulation applications.

The rate of heat conduction depends on the properties of the material being heated. Solid materials, normally, have greater thermal conductivity when they are compared with liquid and gas materials. In solids, two main methods of heat transport exist: electron transport and phonon transport. Among the solid materials, generally, metals are better heat conductors compared to non-metals. The reason for this fact is that metals contain a large number of free electrons, which can easily move through the metals, and so they can transport energy over large distances. In other words, in a good conductor, such as copper and aluminum, conduction takes place by means of both the vibration of atoms and the motion of free electrons. When non-metallic materials are concerned, they have generally low thermal conductivity values except diamond, graphite, graphene, carbon fiber and carbon nanotube. The reason is that diamond is a highly crystalline compound, and graphite, graphene, carbon fiber and carbon nanotube has extended conjugation in their structure. Non-metals except the above mentioned ones are bad heat conductors. For instance; asbestos, concrete, wood, organic polymers have low thermal conductivity values due to the fact that they don’t have free electrons or extended conjugation, and that their crystallinity is low and that conduction takes place only by means of vibration of molecules. For example, it is possible to hold a piece of asbestos in a flame indefinitely;

however, when an aluminum piece is held in a flame for a little time, it is impossible to hold the piece without burning our hand. This shows that a very little energy is transported through the asbestos piece.

When liquids and gases are concerned, they are poorer heat conductors due to the fact that the separation distance between their particles is greater compared to solids. Water has a thermal conductivity value of 0.6 W/m·K, whereas the solid form of water, which is ice, has a thermal conductivity value of 2 W/m·K. Air has a very low thermal conductivity value, which is 0.024 W/m·K. Thermal conductivity values of some materials are listed in the following table [5]:

Table 1.1. Thermal Conductivity Values for Various Materials at RT.

Material	**Thermal Conductivity ($W \cdot m^{-1} \cdot K^{-1}$)**
Aluminum	234
Gold	315
Aluminum oxide	18
Aluminum nitride	200 – 320
Silicon carbide	611
Diamond	1,300 - 2,400
Carbon fiber	20 - 2000
Nickel	91
Copper	400
Iron	84 - 90
Boron nitride	110
CNT (single wall)	≈ 6,000
CNT (multi wall)	≈ 3,000
Graphite	600

1.1.1.1. Thermal Conductivity of Polymeric Materials. As stated above, organic polymers are not good thermal conductors, and their thermal conductivity values generally lie between 0.1-0.6 W/m·K. Polymers lack high thermal conductivity values due to their relatively low atomic density, weak interactions or chemical bonding, complex crystal structure and high anharmonicity in their vibrations [6]. For this reason, polymers are generally used as insulating materials.

Improvements in some electrical applications lead to the development of new materials. Polymers are good candidates for these kinds of materials due to their ease of production, corrosion resistivity, light weight, high strength-to-weight ratio, and low cost; however, polymers are thermally non-conductive; for this reason, there are a lot of studies on improving their thermal conductivity values. In general, polymers are filled with thermally conductive fillers in order to enhance their thermal conductivity. Thermally conductive polymer composites are very significant for many fields of engineering. This importance arises from the fact that the thermal properties of such composites are close to some characteristics of metals, whereas the mechanical properties and processing methods are typical for plastics.

For amorphous polymers, the mean free path of phonons, l, which is described on the Debye kinetic model, is an extremely small constant, i.e. a few angstroms, due to phonon scattering at numerous defects in the amorphous state, leading to a very low conductivity of polymers [7]. For example, HDPE is the linear form of polyethylene which has very few branches; LDPE is more branched form of polyethylene. HDPE has more crystalline structure compared to LDPE due to good packing of chains, and high intermolecular forces between the chains while LDPE is more amorphous compared to HDPE. According to Debye kinetic model, HDPE should have larger thermal conductivity value than LDPE due to the high crystallinity difference: The thermal conductivity value of LDPE is 0.33W/m·K, whereas thermal conductivity of HDPE is between 0.45-0.52 W/m·K.

Table 1.2 shows the thermal conductivity of some commercial unfilled polymers and composites filled with highly thermally conductive fillers at room temperature [8].

Table 1.2. Thermal Conductivity Values for Various Polymers and Thermally Conductive Composites at Room Temperature.

Material	**Thermal Conductivity ($W \cdot m^{-1} \cdot K^{-1}$)**
Low density polyethylene (LDPE)	0.33
High density polyethylene (HDPE)	0.45-0.52
Polypropylene (PP)	0.14
Polystyrene (PS)	0.04-0.14
Polyethylene terephthalate (PET)	0.29
Polymethyl methacrylate (PMMA)	0.15-0.25
Polytetrafluoroethylene (PTFE)	0.25
Polyvinyl chloride (PVC)	0.12-0.17
Polycarbonate (PC)	0.19
Epoxy	0.17-0.21
Nylon 6,6	0.25
Surlyn® 1601	0.24
Polyimide + Graphite 40 vol%	1.7
Epoxy + Boron Nitride 54.1 vol%	2.91
PP + Copper 30 vol%	1.25

Phonon transport is the main mechanism of heat transport in commercial unfilled polymers. A phonon is the quantum mechanical description of an elementary vibrational motion in which a lattice of atoms or molecules uniformly oscillates at a single frequency. Phonons transfer heat energy through interactions with each other and with subatomic particles [9]. That is to say, when a polymeric material is heated, one molecule that is near the edge of the material being heated receives the heat, and then begins to vibrate at a higher frequency, and *via* this vibration, transfers the heat to the neighboring molecule. Phonon scattering is one of the reasons responsible for low values of thermal conductivity in polymers. It occurs because of lattice imperfections such as air inclusions, voids, impurities and low crystallinity in the polymers. In a multi-phase system such as filled polymers, if there is no strong interaction between the polymeric matrix and the filler, the boundary separating those causes an interfacial heat resistance due to phonon scattering.

The way to overcome the problem of low thermal conduction is to incorporate thermally conductive fillers including graphite, carbon black, carbon fibers, metallic or ceramic particles in polymers. This may lead to a large enhancement in not only the thermal properties but also electrical and mechanical characteristics of polymers. Generally, ceramics are preferred due to their high thermal conductivity and low electrical conductivity. AlN, BN, SiC and Al_2O_3 can be given as examples of thermally conductive and electrically resistive ceramics.

There are many crucial points that have significant effects on the thermal conductivity of polymeric composites. These are matrix and filler thermal conductivity, filler size and shape, agglomerations of fillers, hybridization of fillers, surface modification of fillers and free volume in the matrix:

- Thermal conductivity of the polymer matrix has a significant role on the thermal conductivity of the composites. Mamunya *et al.*, 2002, showed that the thermal conductivity of Cu filled epoxy resin composites is larger than that of Cu filled polyvinylchloride composites at any filler volume content due to higher thermal conductivity of epoxy resin [10].

- In general, when two composites with the same matrix but different fillers are compared, it is observed that higher thermal conductivity of fillers leads to higher composite thermal conductivity for the same filler volume content [9].

- If two composites with the same constituents differing only in the filler particle size are compared, it is concluded that larger particle size of fillers may lead to a little enhancement of the composite thermal conductivity due to the larger number of agglomerations in the composite [9].

- Filler particle shape is one of the most important characteristics of the thermal conductivity of a polymer composite. The governing factor in the particle shape is called the aspect ratio. Aspect ratio of a particle is the ratio of the length of the particle to the diameter of the particle. The aspect ratio of the ideal spheres equals unity. As the particle shape changes from the spherical one to another shape, then the aspect ratio increases.

Among fiber shaped, platelet shaped and spherical shaped particles, fiber shaped particles have the greatest aspect ratio. In other words, in a composite, if the filler aspect ratio is high, then the average distance between the filler particles is low. Therefore, in larger aspect ratio particle filled composites, the high heat resistance regions, in this case polymer matrix is lower compared to that of smaller aspect ratio particle filled composites [9]. In short, lower percolation threshold values are obtained when higher aspect ratio filler in the composites. Figure 1.1 shows two composites differing only in the filler shapes. It is easily observed that the inter-particle distance is lower on the composite shown on the right, of which fillers have higher aspect ratio compared to the fillers of the composite shown on the left. Here, high aspect ratio fillers create an uninterrupted high thermal conductivity pathway for heat transfer. Heat will more easily conducted from one of the edges to the other edge of the composite shown on the right.

Figure 1.1. 2D Representation of Two Composites with Different Shapes of Fillers.

- If there is no interaction between the matrix and the filler, the boundary between them is a micro-void, free volume in the matrix. That causes phonon scattering at the boundary, which affects the thermal conductivity of the composite negatively. Surface modification of filler particles will result in a better interaction between the polymer matrix and the filler. If there is a good interaction between the matrix and the filler, then interfacial heat resistance decreases, suppressing phonon scattering [9]. Figure 1.2 shows simplified interfacial properties in the polymer composites. On the left picture, there is an interaction between the polymer matrix and the filler; however, on the composite on the right, it is easily observed that the adhesion is very poor leading to free volume in the matrix. The free volume acts as a highly thermally resistive region and prevents heat transfer.

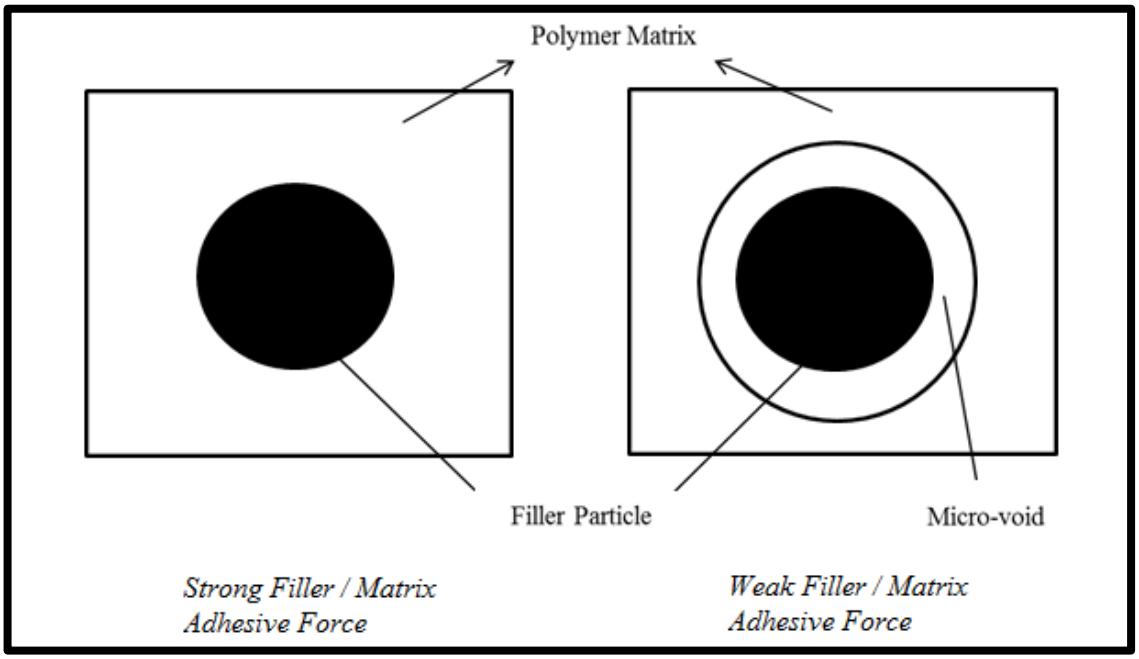

Figure 1.2. Imaginal Representation of Interfacial Properties.

- The use of hybrid fillers shows an enhancement on the thermal conductivity of the composites compared to the use of single fillers. Hybrid fillers are the combination of different kinds, shapes, or sizes of fillers in a composite. By using hybrid fillers, the filler packing density is increased, and therefore, the number of conductive pathways is improved, as well as a low percolation threshold is achieved, which also reduces cost [11].

Figure 1.3. 2D Representation of Composites with Single Fillers and Hybrid Fillers.

1.1.1.2. Advantages of Thermally Conductive Polymer Composites. Increasing the thermal conductivity of typically insulating polymers opens new markets. A thermally conductive resin can be used in heat sink applications. A heat sink is generally an object that absorbs and dissipates heat from another object using thermal contact; that is to say, a

heat sink is a material which has a very high thermal conductivity. Generally, metals were preferred as heat sink materials due to their excellent thermal conductivity values in the past; however, increasing demands on the heat sink materials from the electrical and electronic companies lead to the development of new heat sink materials such as thermally conductive polymers. Conductive resins with a thermal conductivity from approximately 1 to 30 W/m·K can be used in heat sink applications [12].

First, metals are more expensive compared to polymeric materials. The use of thermally conductive polymers as a heat dissipater in electrical and electronic devices will reduce the cost of the product. If wide manufacturing of this product is involved, the company will definitely have more profits when they use thermally conductive polymers instead of metals.

Second, metal molding is extremely expensive because of very high temperatures used when metal processing is desired. However, polymers are processed with an extruder and injection molding machine which are more affordable compared to metal injection molding device. Additionally, when polymers are processed, it is not necessary to reach very high temperatures as in metal molding because polymers have very low melting temperatures compared to metals. Therefore, using polymer processing machines instead of metal molding machines will lead to energy save in a company, so cost effective. Thermally conductive polymer composites are very easily manufactured by injection molding, and more complex shapes can be produced.

Another significant advantage of thermally conductive polymer composites over metals is that thermally conductive plastics have improved corrosion resistance; however, metals except platinum and gold do corrode when they are exposed to air, water, humidity or any corrosive chemical. Therefore, metal parts have to be coated, passivated and painted to protect against corrosion. Additionally, if a thermally conductive polymer composite is filled with metallic fillers, it is again susceptible to oxidation; in other words, metal fillers in the polymer composites may corrode; however, corrosion risk of thermally conductive metal filled composites is not as high as that of pure metals because polymer matrix forms a protective layer for metallic fillers. This is one of the disadvantages of metal filled composites over ceramic or carbon filled composites.

Moreover, conductive polymers are lighter compared to metals due to the fact that their densities are much lower than that of metals.

However, polymer composites have several disadvantages, too. Creep and thermal instability as well as high coefficient of thermal expansion are the most crucial ones.

1.2. Electrical Conductivity

In many applications in the electronics industry, it is desirable to have materials that are not only good thermal conductors but also electrical insulators. Therefore, a brief discussion of electrical conductivity is necessary.

Electrical conductivity is used to specify the electrical character of a material, and it is indicative of the ease with which a material is capable of conducting an electric current. The SI unit for electrical conductivity is reciprocal ohm-meters $(\Omega \cdot m)^{-1}$. Electrical conductivity is denoted by the Greek letter σ. Electrical resistivity is the reciprocal of electrical conductivity and it is an intrinsic property that quantifies how strongly a given material opposes the flow of electric current. Resistivity is represented with the letter ρ, and the SI unit of the electrical resistivity is Ω·m [13].

Solid materials have a broad range of electrical conductivity values. In solid materials, the electrical conductivity is governed by the movement of free electrons or electrically charged particles. According to the ease with which they conduct an electrical current, solid materials can be classified as conductors, semiconductors, and insulators. Metals are known to be good conductors of electricity. Electrons in the outer shell of a metal atom are free to move; therefore, they are called as free electrons. Because metals have a large number of these kinds of free electrons, they have a large conductivity values. Generally, their conductivity values are on the order of 10^{7} $(\Omega \cdot m)^{-1}$. Materials with intermediate conductivities are termed as semiconductors of which conductivity values range from 10^{-6} to 10^{4} $(\Omega \cdot m)^{-1}$. Metalloids can be given as examples of semiconductors. Lastly, insulators are materials with very low electrical conductivities. Most polymers belong to this group, and their electrical conductivities change from 10^{-10} to 10^{-20} $(\Omega \cdot m)^{-1}$.

The electrical properties of a solid material are a consequence of its electron band structure [14]. Figure 1.4 shows various possible electron band structures in solids at 0 K.

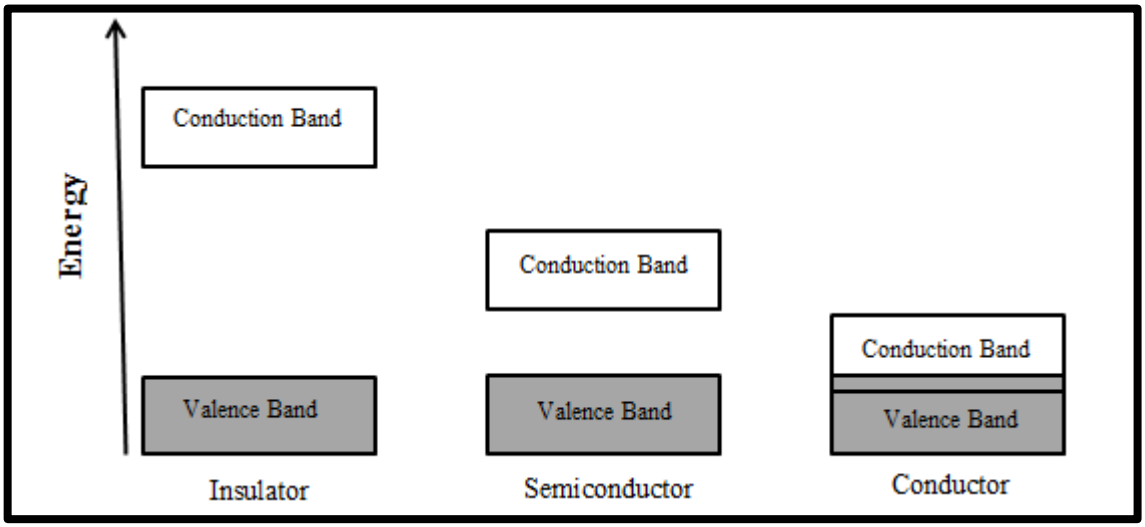

Figure 1.4. Possible Electron Band Structures in Solids at 0 K.

An electron can exist in either the conduction band or the valence band. It is impossible to have an electron in the forbidden band, or namely band gap. The forbidden gap is the energy difference between the conduction and valence bands. When sufficient energy is given to a material, the electrons move from the filled valence band to the unfilled conduction band so that an electric current is observed. In insulators i.e. polymers, the energy separation between the valence and the conduction bands is very high; therefore, they require a large amount of energy to obtain a small amount of current. Conversely, forbidden gap of a semiconductor material is relatively smaller; in this manner, when certain amount of voltage is applied, more current will flow in the semiconductor than in the insulator. In a good conductor such as a metal, the conduction band overlaps with the valence band, and there is no forbidden gap between the valence and conduction bands of a conductor; consequently, electrons move from valence to conduction band very easily when conductors are involved [15].

Electrical conductivity resembles thermal conductivity in such a way that they are both governed by the motion of free electrons. Generally, it is observed that materials having high electrical conductivity values also have high thermal conductivity values.

However, the relationship is not this simple. Thermal conductivity is also dependent on the lattice vibrations, in other words; transport of phonons. Ceramics such as AlN and BN have a high electrical resistivity but they are thermally conductive. In such ceramics, the heat is transported by the lattice vibrations rather than movement of free electrons. Table 1.3 shows typical room-temperature electrical conductivities for various materials at room temperature [14]:

Table 1.3. Electrical Conductivities of Various Materials at RT.

Material	**Electrical Conductivity $(\Omega \cdot m)^{-1}$**
Silver	6.8×10^7
Copper	6.0×10^7
Gold	4.3×10^7
Aluminum	3.8×10^7
Iron	1.0×10^7
Platinum	0.94×10^7
Stainless Steel	0.2×10^7
Graphite	$3 \times 10^4 - 2 \times 10^5$
Carbon fiber	$0{,}6 \times 10^5$
Aluminum oxide	$< 10^{-13}$
Diamond	$\approx 10^{-13}$
Boron Nitride	$10^{-8} - 10^{-13}$
Aluminum Nitride	10^{-14}

1.2.1. Electrical Conductivity of Polymeric Materials

Generally, polymers are known to be poor conductors of electricity due to the lack of free electrons in the conduction process described above.

There is a lot of number of attempts to enhance the electrical conductivity of commercial plastics. The goal of increasing the electrical conductivity of polymers is to combine processability and other attractive properties of polymers (such as easy

manufacturing by injection molding, low cost, resistance against corrosion, humidity and chemicals) with the electronic properties of conductors and semiconductors.

Electrically conducting polymers are actually divided into two main categories: They are inherently conducting polymers and polymer composites with electrically conductive fillers.

Inherently conducting polymers, also called synthetic metals, have repeating conjugated Π bonds on their backbones; however, in this state, they are insulating materials. In order to call them inherently conducting polymers, they should be doped with oxidative or reductive dopants. In undoped state, the forbidden gap between the valence band and the conduction band is as large as that of an insulating material. However, when they are doped with appropriate dopants, the Π electrons will be free to move; as a consequence, conductivities as high as 1.5×10^{7} $(\Omega \cdot m)^{-1}$ will be achieved; however, these kinds of polymers have several disadvantages. Firstly, they are insoluble in any solvent because of the inflexibility of the backbone. Secondly, they cannot be melted, their processing is very hard. Last but not the least; they are very unstable under normal conditions. They lose conductivity within several hours under open air [16]. There are numerous studies to overcome all these drawbacks.

The main application areas of these kinds of polymers are rechargeable batteries, antistatic coatings for clothing, electromagnetic screening materials, and electronic devices.

Figure 1.5 shows the most common inherently conducting polymers in undoped state, among which polyacetylene is the first synthesized organic conducting polymer [14].

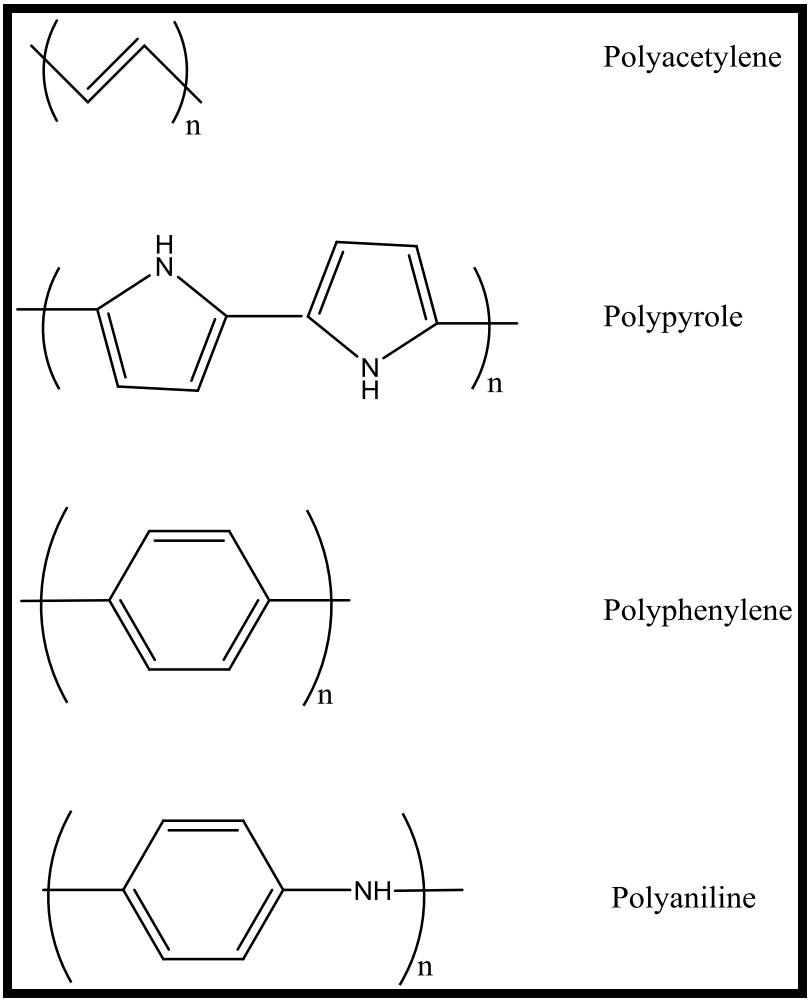

Figure 1.5. Most Common Inherently Conducting Polymers in Undoped State.

Commercial unfilled polymers that have no conjugated Π electrons on their backbones generally have extremely low electrical conductivities due to the lack of free electrons on their structures; however, their electrical conductivities can be enhanced *via* the addition of highly electrically conductive fillers in the polymer matrix. Before the critical volume fraction of conductive filler, the overall conductivity of the polymer composite increases very slowly with increasing concentration of fillers. At this region, a network of conductive filler starts to be formed. As the filler loading reaches a critical point, the conductivity suddenly increases. This point is called the percolation volume, or percolation threshold meaning that filler is added just enough to make a continuous conductive phase within the composite. After this critical volume region, the conductivity again increases slowly showing the growth of the conductive network [17]. Figure 1.6 demonstrates dependence of electrical conductivity on conductive filler content.

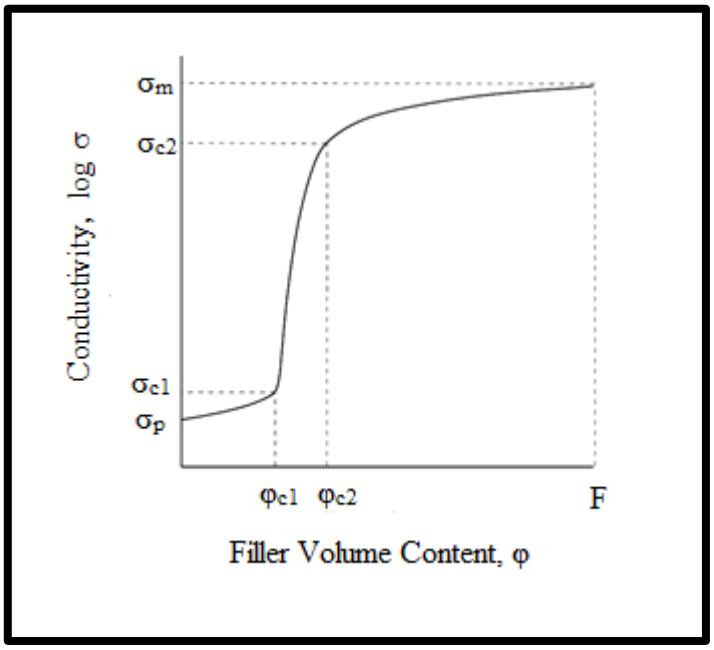

Figure 1.6. Typical Dependence of Logarithm of Electrical Conductivity on Conductive Filler Volume Content.

However, in the case of thermal conductivity of a polymer composite, there is no sharp increase in the overall thermal conductivity at the percolation threshold. This is due to the fact that the thermal conductivities of the polymer matrix and the filler are comparable to each other; their ratio is not more than 10^3, whereas the electrical conductivity of conductive filler is 10^{10} - 10^{20} greater than that of the polymer matrix, which is the actual reason for percolation behavior [18].

There are a lot of models estimating the thermal conductivity of polymer composites. The common point of all theoretical models is that as the volume percentage of conductive filler increases in the composite, there will be an increase in the overall thermal conductivity as in the case of electrical conductivity except percolation behavior.

Table 1.4 indicates the electrical conductivities for some common polymeric materials at room temperature [19-21]:

Table 1.4. Electrical Conductivities of Various Polymeric Materials at RT.

Material	**Electrical Conductivity $(\Omega \cdot m)^{-1}$**
Phenol-formaldehyde	$10^{-9} – 10^{-10}$
Poly(methyl methacrylate)	$< 10^{-12}$
Nylon 6,6	$10^{-12} – 10^{-13}$
Polystyrene	$< 10^{-14}$
Polyethylene	$10^{-15} – 10^{-17}$
Polytetrafluoroethylene	$< 10^{-17}$
Polyacetylene	$10^{3} – 1.7 \times 10^{5}$
Polypyrole	$10^{2} – 7.5 \times 10^{3}$
Polyaniline	30 - 200
Poly(paraphenylene)	100 - 1000
Poly(p-phenylene vinylene)	3 - 5000
Polythiophene	10 - 1000
20 wt % expanded graphite + HDPE	5.5×10^{-6}
55 wt % carbon black + HDPE	588

1.3. Previous Works

There are numerous articles and patents about thermally conductive polymer composites. One of these patents, United States Patent, US 4869954 A by Vincent Squitieri, states that there are some irregularities between the surfaces of the electronic components or devices and their heat sinks; and the older thermal interface materials which fill up these irregularities have the problems of creep and adherence of conformal coatings. In this patent, a urethane based thermal interface material which has a high thermal conductivity, and is resistant to creep is able to act as conformal coatings. This urethane based composite comprises of a urethane resin, a urethane curing agent, and one or more thermally conductive fillers selected from zinc oxide, aluminum oxide, magnesium oxide, aluminum nitride or boron nitride [22].

Another patent, European Patent, EP 2254940 B1 by Robert Hendrik Catharina Janssen and Franciscus Vehmendahl Van, describes a heatsink of thermally conductive

plastic materials. In this patent, it is stated out that heatsinks can be made of a thermally conductive plastic materials comprising at least 20 weight % expanded graphite or having in-plane thermal conductivity value at least 7.5 W/m·K. However, using a plastic in the heatsinks of LED devices may be risky without using a flame retardant additive, which will have adverse effects on the overall thermal conductivity of the composites. By using at least 20 weight % expanded graphite in the composite, flame retardancy is also improved without any use of additive and so without any significant loss of good heat conduction property [23].

United States Patent, US 20140182063 A1 by Mark L. Crawford, Bruce W. Peterson, and Matthew D. McKnight, explains enhanced thermally-conductive cushioning foams by addition of graphite. In this patent, it is stated out that polyurethane foams, latex foams and melamine foams have typically low thermal conductivities and they are used as insulators. As a person sleeps on a cushion and mattress, the compressed foam underneath the head and the body causes reduction in air flow paths inside the cushion and mattress; therefore, heat flow in the region below the body should be in the form of conduction. If no thermally conductive filler is used in the foam of the mattress, due to low thermal conductivity of the foam, heat flow will be very slow and require a large temperature difference to conduct heat at a rate similar to the heat production in a person's body, which causes a large region of hot foam around the body making the foam uncomfortable. For this reason, thermal conductivity of the foam is improved by the addition of kinds of graphite materials such as natural flake graphite, powder graphite, graphene sheets, graphene, synthetic graphite, graphite-based particulates, and combinations thereof. The thermally conductive foam consists of such graphite materials in the range about 0.1 % by weight to about 75 % by weight [24].

In one of the articles by Zengbin Wang, the use of ceramics, which are generally brittle, expensive and difficult to manufacture, in the base board of insulated gate bipolar transistors is discussed. Generally, ceramics are used because of their high thermal conductivity, and good electrical resistivity; however, they have the above mentioned drawbacks. Consequently, they provide the use of thermally conductive epoxy composites which are filled with highly thermally conductive, electrically insulative additives. Thermal conductivity values as high as 2.91 W/m·K, 3.95 W/m·K, and 10.1 W/m·K are

obtained with epoxy resin composites filled with hexagonal boron nitride, cubic boron nitride and conglomerated hexagonal boron nitride, respectively. These values may be further improved to 5.26 W/m·K, 5.94 W/m·K, and 12.3 W/m·K, respectively, by the addition of extra small aluminum nitride to fill the voids in sample [25].

In one study by Erik H. Weber, carbon black, synthetic graphite and carbon fiber are used as thermally conductive fillers in polycarbonate and nylon 6,6 matrixes. Upon the addition of such fillers, there is a certain improvement in the overall thermal conductivities; however, it is concluded that carbon fiber is the most effective in increasing the thermal conductivity in the longitudinal direction due to its higher aspect ratio, whereas graphite is the most effective in increasing the thermal conductivity in the transversal direction due to its lower aspect ratio; in other words, its larger diameter in the transverse direction [26].

Of course, there are infinite number of examples and patents in the literature. In this work, it is the objective to produce thermally conductive parts for outdoor lighting fixtures because the use of metals has the disadvantage of corrosion under open atmosphere, humidity or garden chemicals. This work is partially supported by EMFA Elektrik Fabrikası A.Ş. through a TÜBİTAK-TEYDEB grant.

2. RESEARCH OBJECTIVES

The purposes of this project are first to enhance the thermal conductivity of commercially available poly (ethylene-co-methacrylic acid) polymer by making its composites with highly thermally conductive fillers. Achieving an understanding of the interfaces between the polymer matrix and fillers is also an objective. The next aim of the project is to improve the interaction at the interface by using coupling agents or by oxidizing the surface of the fillers; in this manner, thermal conductivity value of the polymer composite should be higher due to less interfacial phonon scattering and suppressed interfacial heat resistance in the interfacial area.

The polymer used in this project is Surlyn® 1601, which is a DuPont™ product. Simply, it is a random copolymer of poly (ethylene-co-methacrylic acid). During the processing of Surlyn® 1601 resins, the carboxylic acid groups are partially neutralized with NaOH, so it has not only methacrylic acid groups but also methacrylate groups with sodium counter ions. It is hoped that Surlyn® as polymer matrix with its carboxylic acid functional groups will have an ionic interaction or a covalent linkage with the fillers. Additionally, the fillers used are aluminum, graphite and carbon fiber, respectively.

The proposed reaction between non-coated aluminum filler and the Surlyn® matrix is an acid-base reaction. The surface of the aluminum is prone to oxidation due to high contact with air and humidity so that aluminum metal contains hydroxides on the surface. This is a metallic hydroxide and can act as a base towards the methacrylic acid groups of Surlyn®. This reaction is given on Figure 2.1.

Graphite and carbon fiber are composed of parallel graphene sheets. There are numerous successive aromatic carbon rings in the structure of graphene; and for the fact that it is composed of aromatic rings, it is planar. Graphite has higher ratio of carbon in its structure, whereas carbon fiber is generally oxidized to 1,4 diketone, quinone, hydroquinone and dicarboxylic acid like structures on the edge groups during manufacture; therefore, the carbon ratio of carbon fiber is not as high as virgin graphite. Consequently, there may be a linkage between carbon fiber and Surlyn® matrix but the adhesion between

pristine graphite and Surlyn® needs to be improved. Figure 2.2, Figure 2.3 and Figure 2.4 show the possible reactions and interactions between the Surlyn® matrix and carbon fiber.

Thermal conductivity of the composites will be determined with the help of a thermal camera and a thermal conductivity comparator, which is a home-made device. Furthermore, the nature of the interfacial interactions between the polymer matrix and the fillers will be determined by scanning electron microscopy.

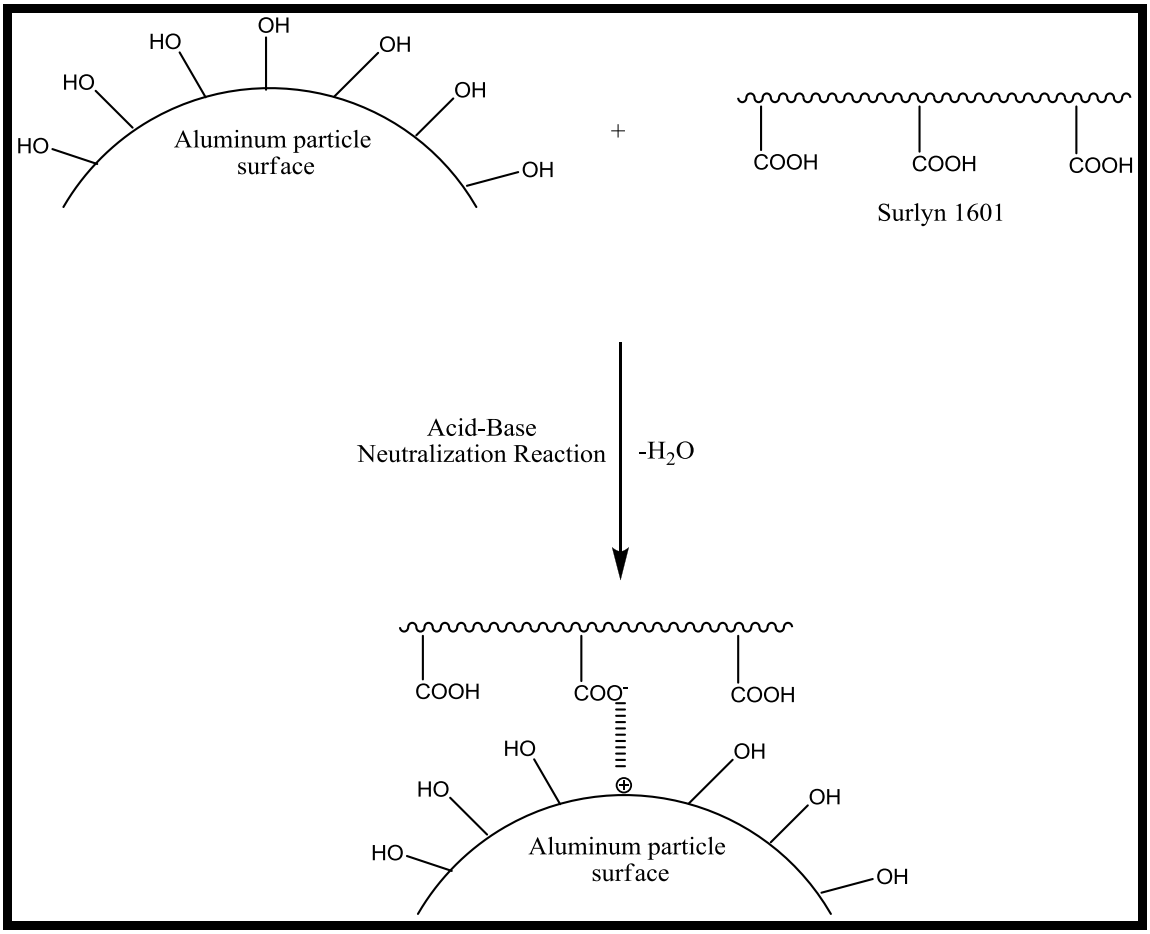

Figure 2.1. Proposed Acid- Base Reaction between Pristine Aluminum and Surlyn® 1601.

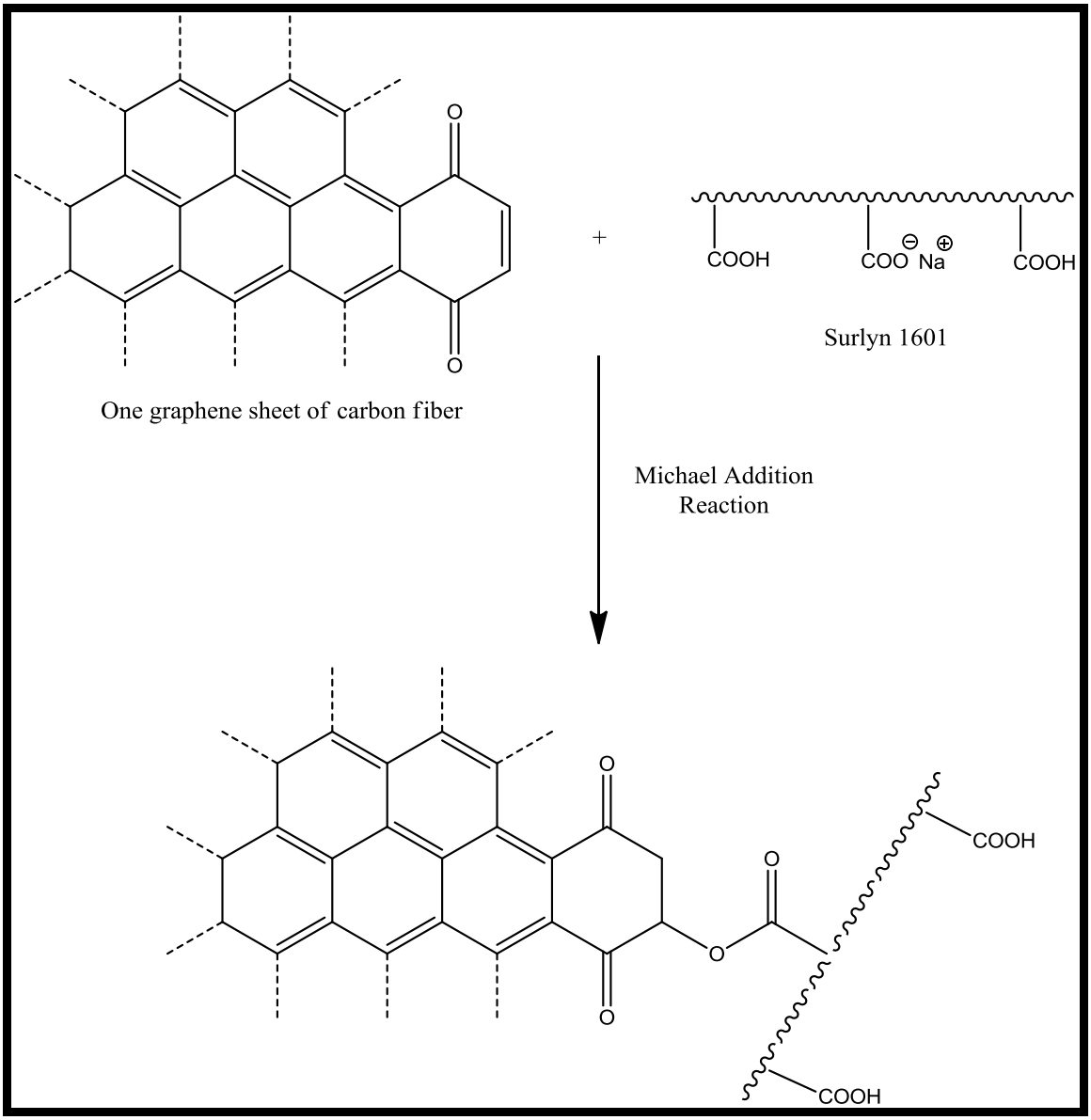

Figure 2.2. Proposed Michael Addition Reaction between Non-Coated Carbon Fiber and Surlyn® 1601.

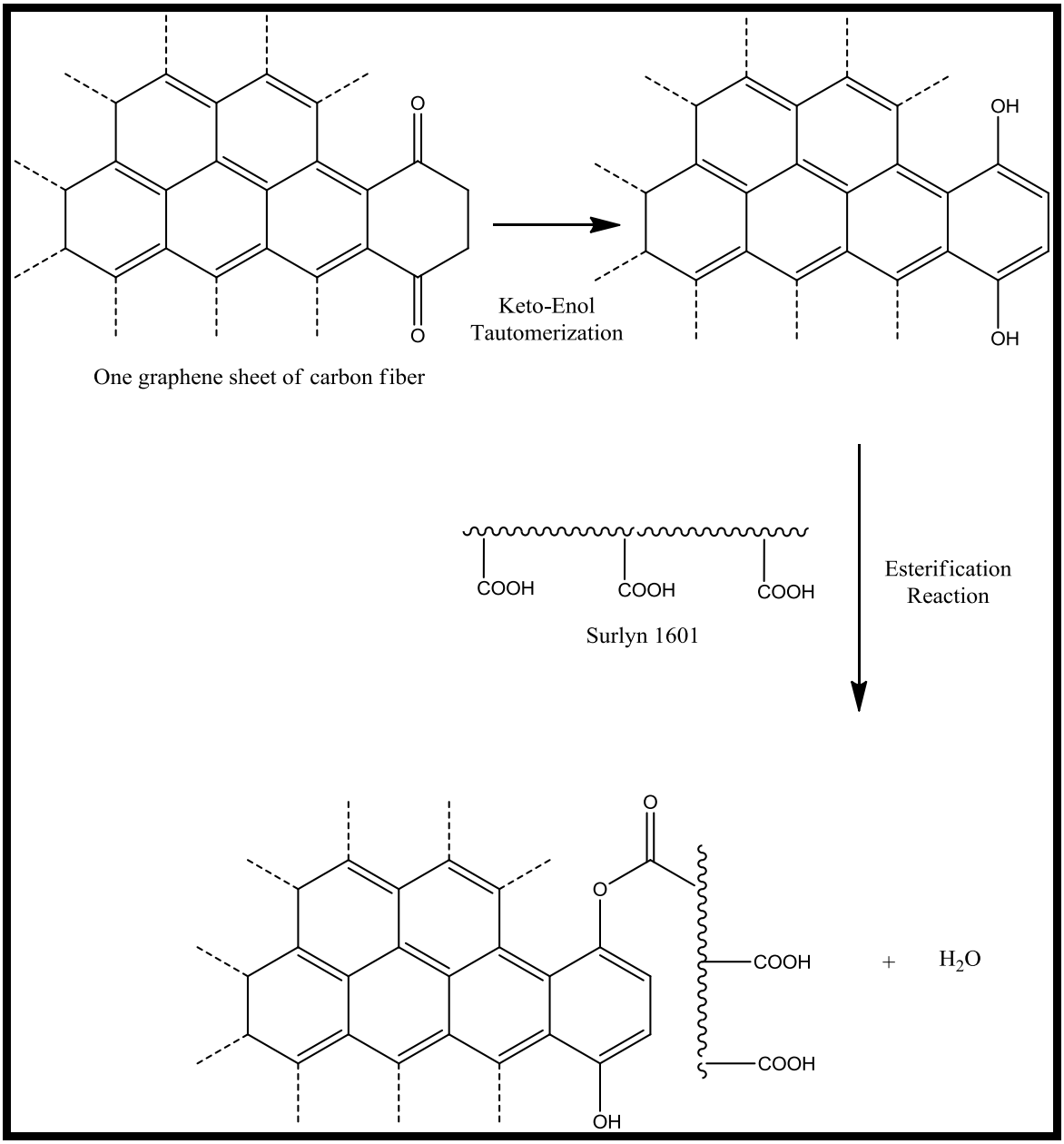

Figure 2.3. Proposed Esterification Reaction between Non-Coated Carbon Fiber and Surlyn® 1601.

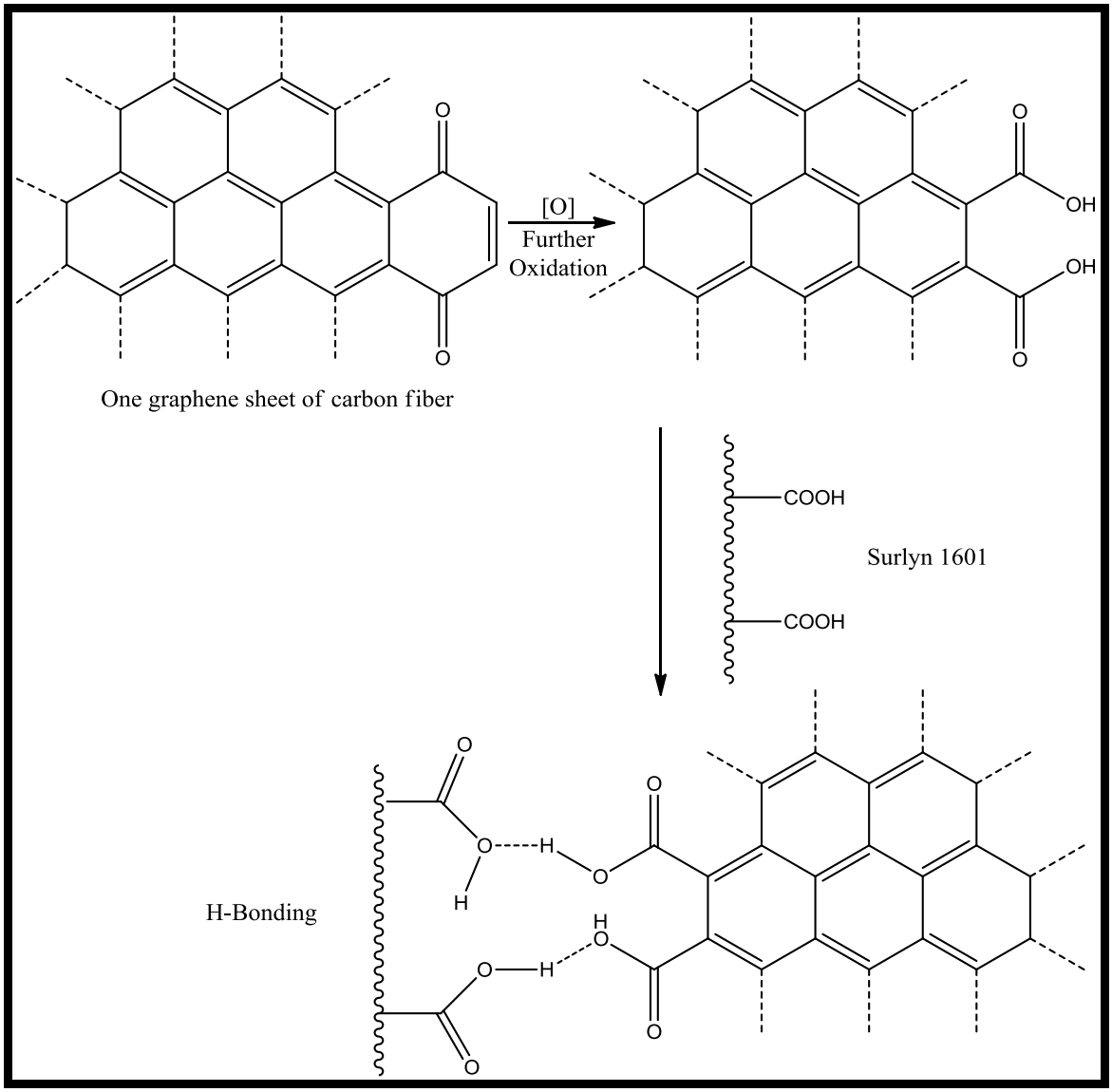

Figure 2.4. Proposed H-Bonding Interactions between Non-Coated Carbon Fiber and Surlyn®1601.

3. EXPERIMENTAL

3.1. Materials and Apparatus

3.1.1. Materials

As the polymer matrix in the thermally conductive composite samples, Surlyn® 1601 was chosen. Surlyn® is a DuPont™ product which is a thermoplastic ionomer resin, and Surlyn® is the trade name of this product. Actually, it is a random copolymer consisting of poly (ethylene-co-methacrylic acid), and it contains 5.4 mol % methacrylic acid [27]. At the last step of its processing, it is neutralized with either alkali metal hydroxides or zinc hydroxide; for this reason, it has also methacrylate groups partially neutralized by alkali metal ions or Zn^{2+} ions on its chains [28]. DuPont™ produces different grades of Surlyn®. This difference comes from the base used during neutralization [29]. Surlyn® 1601 has Na^{+} ions as counter-ions. Surlyn® 1601 is synthesized from free radical polymerization of ethylene and methacrylic acid monomers, and then neutralized with NaOH. Figure 3.1 shows the structure of Surlyn® 1601.

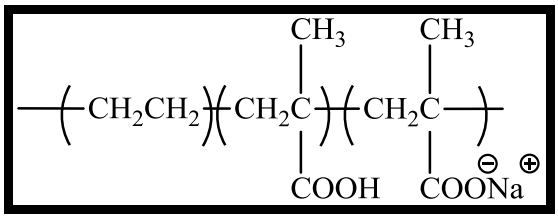

Figure 3.1. The Structure of Surlyn® 1601.

As fillers, spherical aluminum powder, aluminum flakes, graphite flakes and carbon fiber were chosen. Spherical aluminum powder was obtained from Akçay Paint Ltd.; the aluminum particles were sieved into pieces smaller than 5 micrometers in their diameters. Aluminum flakes were obtained from Akçay Paint Ltd. Thermal conductivity value of aluminum is given to be 234 W/m·K. Electrical conductivity of aluminum is 3.8 x 10^{7} $(\Omega \cdot m)^{-1}$. Graphite flakes were obtained from Faber Türk A.Ş. Thermal conductivity of graphite is 600 W/m·K whereas electrical conductivity of graphite is 2 x 10^{5} $(\Omega \cdot m)^{-1}$.

Finally, carbon fiber was obtained from AKSA, fiber diameter is 7.2 micrometers, and fibers are chopped to 6 millimeters in length. Carbon percentage is 95% in the fiber structure. Thermal conductivity of carbon fiber is given to be 20 W/m·K and its electrical conductivity is 0,6 x 10^5 $(\Omega \cdot m)^{-1}$.

As coupling agents; 3-Aminopropyltriethoxysilane, Michem® Prime 4983R and 1,6-Diamino-hexane were used. 3-Aminopropyltriethoxysilane was obtained from Cam Elyaf A.Ş. and it was used as received. It is an aminosilane generally used in the process of amino functionalization of the hydroxylated surfaces. This amino functionality of the aminosilane brings basicity to the functionalized surface, and therefore, aminosilane functionalized surface becomes reactive towards acids. Michem® Prime 4983R was purchased from Michelman™ and was used as obtained. Michem® Prime 4983R is an emulsion and is a copolymer of ethylene and acrylic acid. 3-Aminopropyltriethoxysilane and Michem® Prime 4983R were used in aluminum coupling reactions. The optimum pH that aminosilanes can work best is 5.5. Therefore, the pH of the media is adjusted to 5.5 with acetic acid, which is purchased from Akkimya. 1,6-Diamino-hexane was purchased from Sigma-Aldrich, and used as received. 1,6-Diamino-hexane was used to have a linkage between graphite oxide and Surlyn® 1601matrix. Diethyl ether, which was a product of Merck, was used to dissolve 1,6-Diamino-hexane. The reason for using graphite oxide instead of graphite in the coupling with matrix is that graphite has no functional groups on its structure; for that reason, it is not possible to observe a linkage between graphite and Surlyn® 1601 matrix. Therefore, graphite is oxidized with a method called Modified Hummers by the help of chemicals listed below. Table 3.1 shows the chemicals used in graphite oxidation process and the companies that these chemicals were purchased from.

Table 3.1. Chemicals Used in Oxidation of Graphite with Modified Hummers Method.

Chemical	**Company**
98 % H_2SO_4	Akkimya
$KMnO_4$	Fisher Scientific Company
50% H_2O_2	Akkimya
Concentrated HCl	Tekkim

Graphite oxide has several functional groups, such as carboxylic acid groups and alcohol groups which may have a linkage with polymer matrix by the help of some coupling agents. Instead of graphite oxidation method, surface of graphite is also tried to be oxidized by another method called Fenton oxidation. In this oxidation process, the chemicals used and the suppliers of these chemicals are listed in Table 3.2.

Table 3.2. Chemicals Used in Fenton Oxidation of Graphite.

Chemical	**Company**
Toluene	Merck
Pentane	Lab Scan
$FeSO_4.7H_2O$	Bereket Kimya
50% H_2O_2	Akkimya
Ethanol	Merck

3.1.2. Apparatus

Thermal conductivity values of the composites were determined by a FLIR E 40 thermal imaging camera and a home-made thermal conductivity comparator which is produced at EMFA A.Ş., which is the electrical and electronic devices company supporting the project. FLIR E 40 thermal imaging camera is an IR based device showing the temperature of all the points of a sample. Scanned surface is a 4 mm x 4 mm square. It is actually similar to the cameras forming images with visible light; however, a thermal camera uses infrared radiation to form these images. After an image of an object is obtained with this camera, different colors in the different regions of that image show different temperatures. Black and dark blue color shows the coolest regions, red color shows the warmer, yellow and white show the hottest points; additionally, FLIR software converts these colors into temperatures. In order to get the thermal conductivity values of the composites, FLIR thermal camera is not enough, it should be used with homemade thermal conductivity comparator. Figure 3.2 demonstrates the 2D representation of the thermal conductivity comparator together with standard and composite samples.

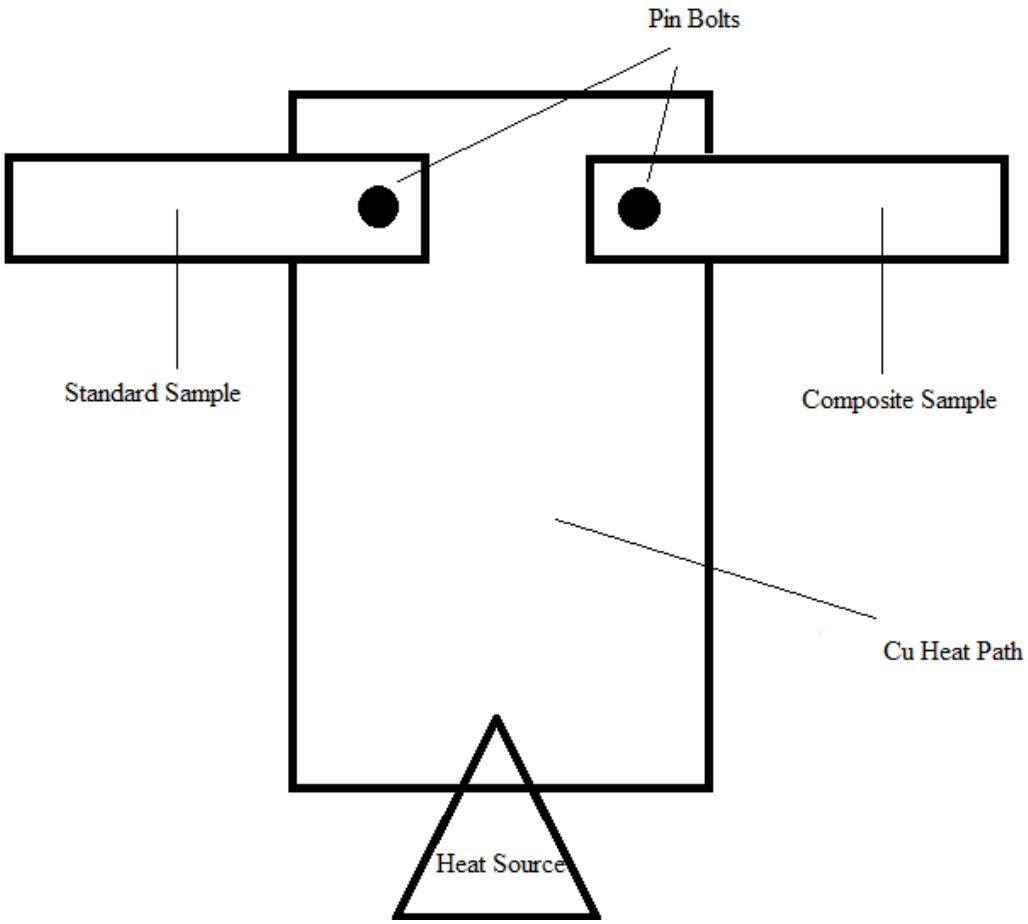

Figure 3.2. 2D Representation of Home-Made Thermal Conductivity Comparator.

The device is heated from the heat source, and the temperature is adjusted to the desired temperature. While heat resistance heats the device, the energy is given upwards on the copper heat path, which has a very low thermal resistivity. Then, heat is transferred to both the standard and the composite samples. The standard sample is a stainless steel part which has a thermal conductivity value of 16 W/m·K, the test piece has dimensions that are identical to the standard sample. The thermal conductivity of the experimental composite sample is measured with comparison method using Equation 1.1. The dimensions should be exactly the same for the standard and the experimental composite samples in order to get a real comparison. After this system reaches equilibrium, that is to say, after the heat given to samples from heat path is equal to the heat given from the samples to the environment, two isothermal points are chosen on both of the samples. The ratio of the distances of these points to the edges touching the heat path should be equal to the ratio of

the thermal conductivity values of these samples. Because the amount of heat given is equal ($q_1=q_2$) at equilibrium, redesigning Equation 1.1 gives Equation 3.1:

$$\frac{\lambda_1 \cdot A_1 \cdot \Delta T_1}{L_1} = \frac{\lambda_2 \cdot A_2 \cdot \Delta T_2}{L_2} \tag{3.1}$$

Due to the fact that the parts are identical ($A_1=A_2$), and the points chosen on both of the sample are isothermal ($\Delta T_1=\Delta T_2$) at equilibrium, then the Equation 3.1 is reduced to Equation 3.2:

$$\frac{\lambda_1}{L_1} = \frac{\lambda_2}{L_2} \tag{3.2}$$

The fracture surface morphologies of the composites were obtained with Scanning Electron Microscopy (SEM) in combination with Energy Dispersive X-ray analysis on an ESEM-FEG/EDAX Philips XL-30 instrument operating at either 5 kV or 10 kV using composite parts which are coated with carbon and having all the dimensions nearly 1 cm supported on carbon tape.

The FTIR analyses were performed with Nicolet 380 FTIR spectrometer with a Smart Diamond ATR.

3.2. Preparation of Surlyn® 1601 Composites with Untreated Fillers

10%, 20%, 30%, 40%, 50% by weight aluminum powder containing Surlyn® 1601 composites were prepared by firstly mechanical mixing of adequate amount of aluminum particulate powder and Surlyn® 1601 resins in a beaker, successively, this beaker was transferred into an oil-bath that was nearly at 200°C, which is actually very close to the processing temperature of Surlyn® 1601, 204°C [30]. They were mixed approximately 30 minutes in order to get homogenous composites at this temperature.

30% and 50% by weight aluminum flake containing Surlyn® 1601 composites were prepared in the same way.

10%, 20%, 30%, 40% by weight graphite flake containing Surlyn® 1601 composites were prepared with exactly the same procedure as aluminum powder filled composites.

5%, 10%, 15%, 20% by weight carbon fiber containing Surlyn® 1601 composites were prepared in the same way.

3.3. Preparation of Surlyn® 1601 Composites with Surface Treated Fillers

30% by weight aminosilane treated aluminum flake filled Surlyn® 1601 composite, 30% by weight aminosilane and Michem® Prime 4983R treated aluminum flake filled Surlyn® 1601 composite, additionally, 30% by weight oxidized graphite filled Surlyn® 1601 composite and 30% by weight Fenton hydroxylated graphite filled Surlyn® 1601 composite were prepared in such a way that composites with pristine fillers were prepared.

3.3.1. Aminosilane Treatment of Aluminum Flakes

3% by weight 3-Aminopropyltriethoxysilane aqueous solution is prepared by vigorous agitation. Then, the pH of this solution is adjusted to 5.5 with sufficient amount of acetic acid with the help of a pH meter. 5 grams of aluminum flake is treated in that solution in a homogenizer for 15 minutes. Successively, it is filtered, and then dried in an oven at 130°C for 1 hour. Finally, it is finely powdered by the help of a mortar.

3.3.2. Aminosilane and Michem® Prime 4983R Treatment of Aluminum Flakes

3% by weight 3-Aminopropyltriethoxysilane, and 4% by weight Michem® Prime 4983R aqueous solution is prepared with vigorous agitation. After that, the pH of the medium is adjusted to 5.5 with sufficient amount of acetic acid *via* a pH meter. 5 grams of aluminum flake is treated in that solution in a homogenizer for 15 minutes. Then, the mixture is filtered by vacuum filtration, and then dried in an oven at 130°C for 1 hour. At last, it is finely powdered with the help of a mortar.

3.3.3. Graphite Oxidation by Modified Hummers Method and 1,6-Diaminohexane Treatment of Graphite Oxide

Figure 3.3 shows FTIR analysis of pure graphite. Since graphite is a really good IR absorbent material, its IR spectra cannot be excellent. At 1606.33 cm^{-1}, there is a peak of an aromatic C=C stretch. There is no evidence that any other functionality can be observed from this figure. The peaks between 2277.57 and 2002.11 cm^{-1} belong to aromatic overtones. At 1017.41 cm^{-1}, there is a peak of in-plane –C-H bending.

The first step is the oxidation of graphite flakes by Modified Hummers Method [31]. 3 grams of graphite powder is added to 70 mL of concentrated H_2SO_4 under stirring in an ice-bath for 1.5 hr. Under vigorous agitation, 9 grams of $KMnO_4$ is added slowly to keep the temperature of the suspension lower than 20°C. Successively, the reaction system is transferred to a 40°C oil bath and vigorously stirred for about 30 minutes. Then, 150 mL of water is added slowly, and the solution is stirred for 15 minutes at 95°C. After this step, 500 mL of water is added. Then, 6mL of distilled water is added onto 9 mL of 50% H_2O_2 in order to get 30% 15 ml of H_2O_2. This solution should be added slowly on the suspension, turning the color of the suspension from dark brown to yellow. The mixture is filtered. After that, 83 mL of concentrated HCl, which is actually 30% by volume, is diluted to 250 mL with distilled water in order to get 10% by volume HCl. Then, this HCl solution is used to wash the filtrate to remove the metal ions. The washed filtrate is transferred to vacuum oven at 100°C for drying for 30 minutes. Finally, the dried product is finely powdered by the help of a mortar. The final product is graphite oxide. IR analysis of the final product shows broad –O-H stretching peak at 3312.95 cm^{-1}, strong –C-H stretching peaks at 2923.48 cm^{-1} and 2847.49 cm^{-1}, CO_2 stretches at 2356.73 cm^{-1} and 2334.56 cm^{-1}, strong C=O stretching peak at 1717.15 cm^{-1}, aromatic C=C stretching peak at 1615.83 cm^{-1}. Figure 3.4 shows the IR spectrum of graphite oxide before 1,6-Diamino-hexane treatment.

In the second step, 2 grams of 1,6-Diamino-hexane is dissolved in 50 mL of diethyl ether. Then, all graphite oxide produced at the previous step is treated with this ether solution for 30 minutes under vigorous agitation. Successively, diethyl ether is completely

vaporized in a steam bath. The final product is 1,6-Diamino-hexane coupled graphite oxide powder.

3.3.4. Fenton Oxidation of Graphite

Fenton oxidation is a method of hydroxylation of aromatic compounds. The procedure is as follows [32]: 6 grams of graphite is mixed with 100 ml of toluene in a 250 ml beaker and this suspension is stirred using an ultrasonic horn for 45 minutes. The resulting suspension was then filtered and washed with 30 ml of n-pentane and then dried under vacuum at 80°C for 1 hour. These steps are needed for the removal of organic residues from the surface of graphite. Then, all of this horn-sonicated graphite is added to 200 ml of distilled water, and then dispersed using an ultrasonic bath for 30 minutes. After that, 1.5 grams of $FeSO_4.7H_2O$ is added to the suspension, and stirred magnetically until all of the $FeSO_4.7H_2O$ solid dissolves. Then, 30 ml of 50% H_2O_2 is diluted to 50 ml with 20 ml of distilled water in order to get 50 ml of 30%H_2O_2. Successively, 50 mL of 30% H_2O_2 is added very slowly and carefully onto the suspension with continuous stirring. After stirring on a magnetic stirrer continuously for 24 hours, the suspension is filtered and then washed with first 25 ml of distilled water and then 25 ml ethanol. The product is then dried under vacuum at 80°C for 1 hour. The final product is hydroxylated graphite.

Figure 3.5 shows the FTIR analysis of the final product, which shows broad –O-H stretch at 3375.2 cm^{-1}, strong C=O stretching peak at 1746.4 cm^{-1}, aromatic C=C stretching peak at 1619.0 cm^{-1}. The peak at 1049.0 cm^{-1} belongs to C-O stretch. One can see again CO_2 stretches nearly at the same frequencies.

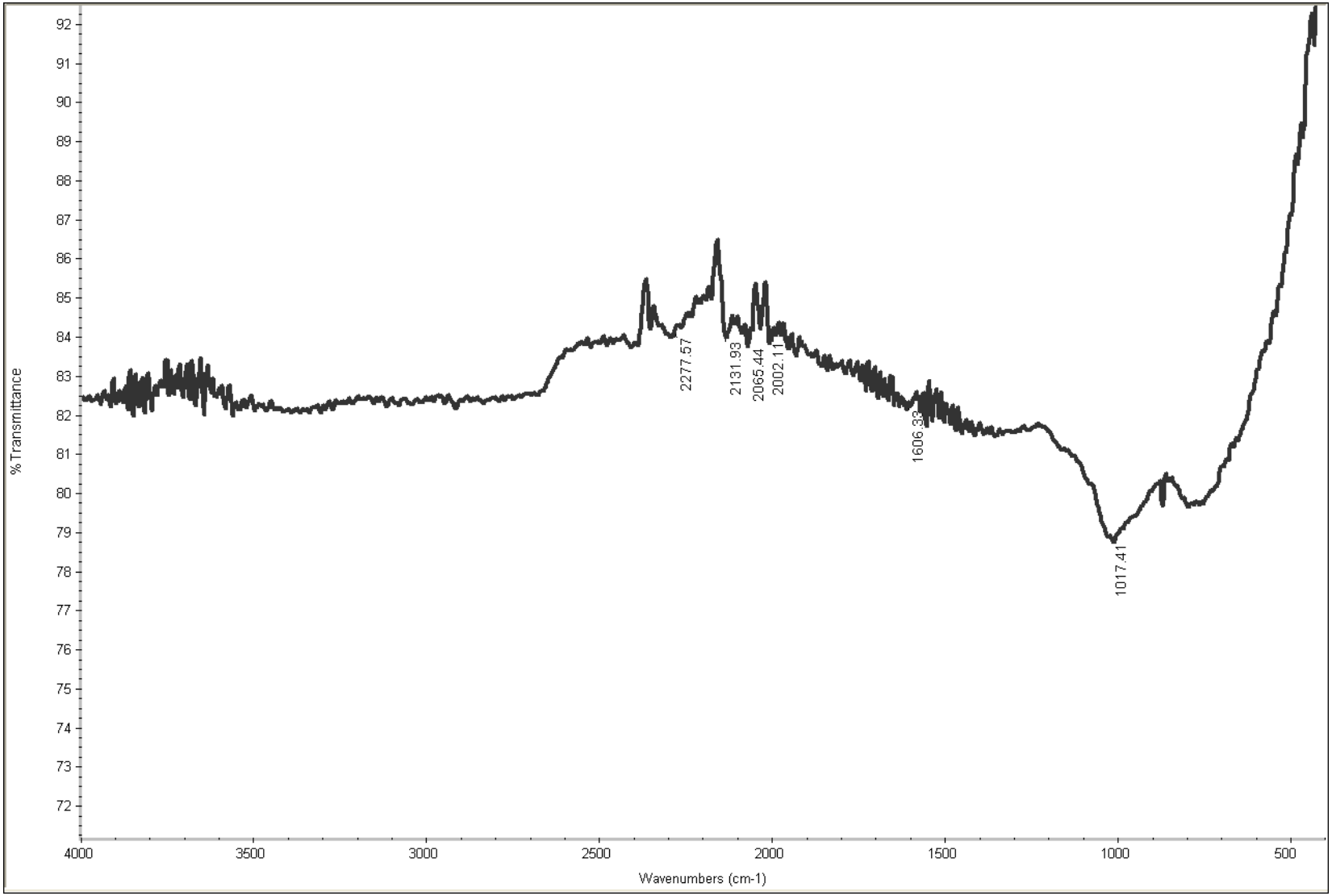

Figure 3.3. IR Spectrum of Pure Graphite.

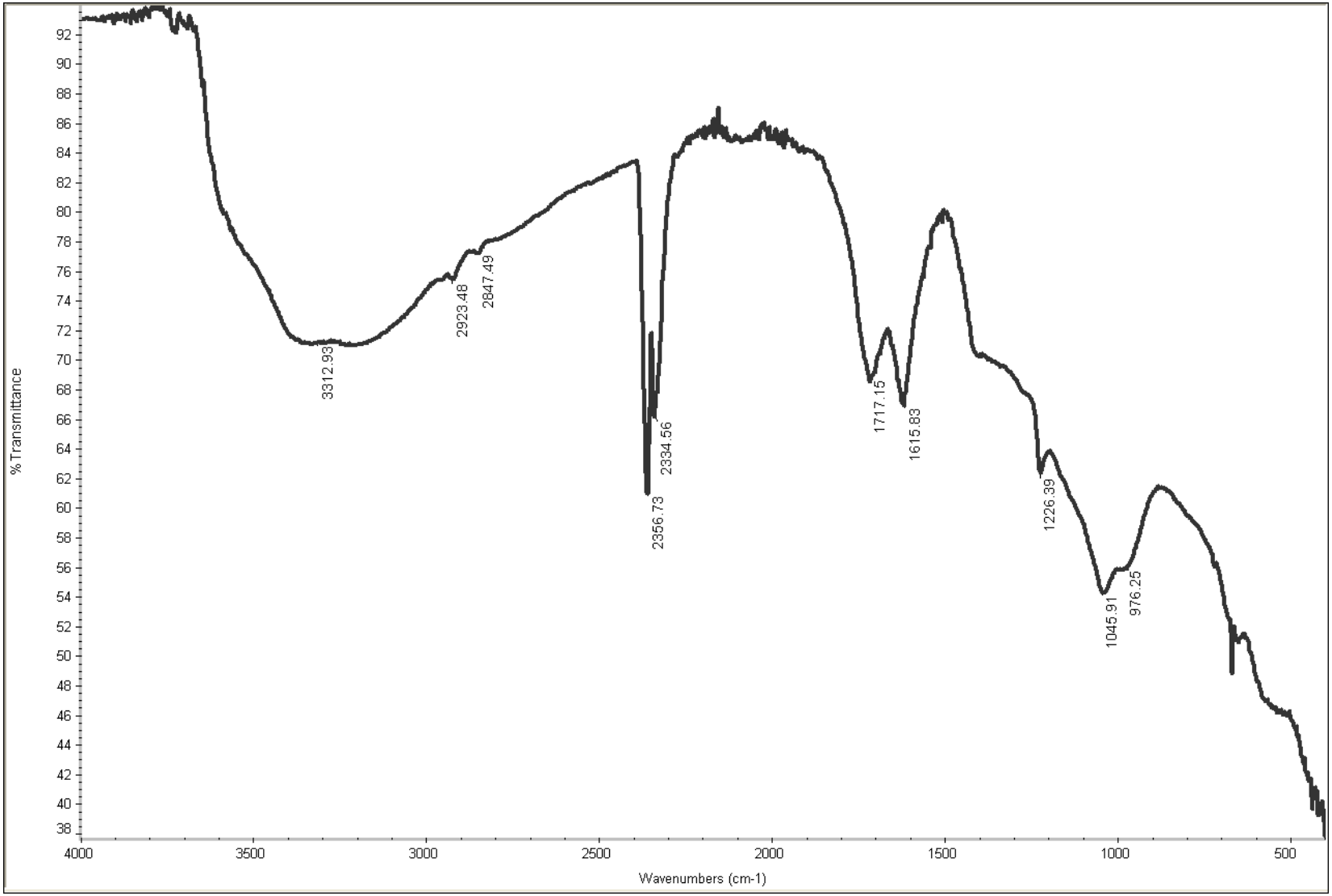

Figure 3.4. IR Spectrum of Graphite Oxide Before 1,6-Diamino-hexane Treatment.

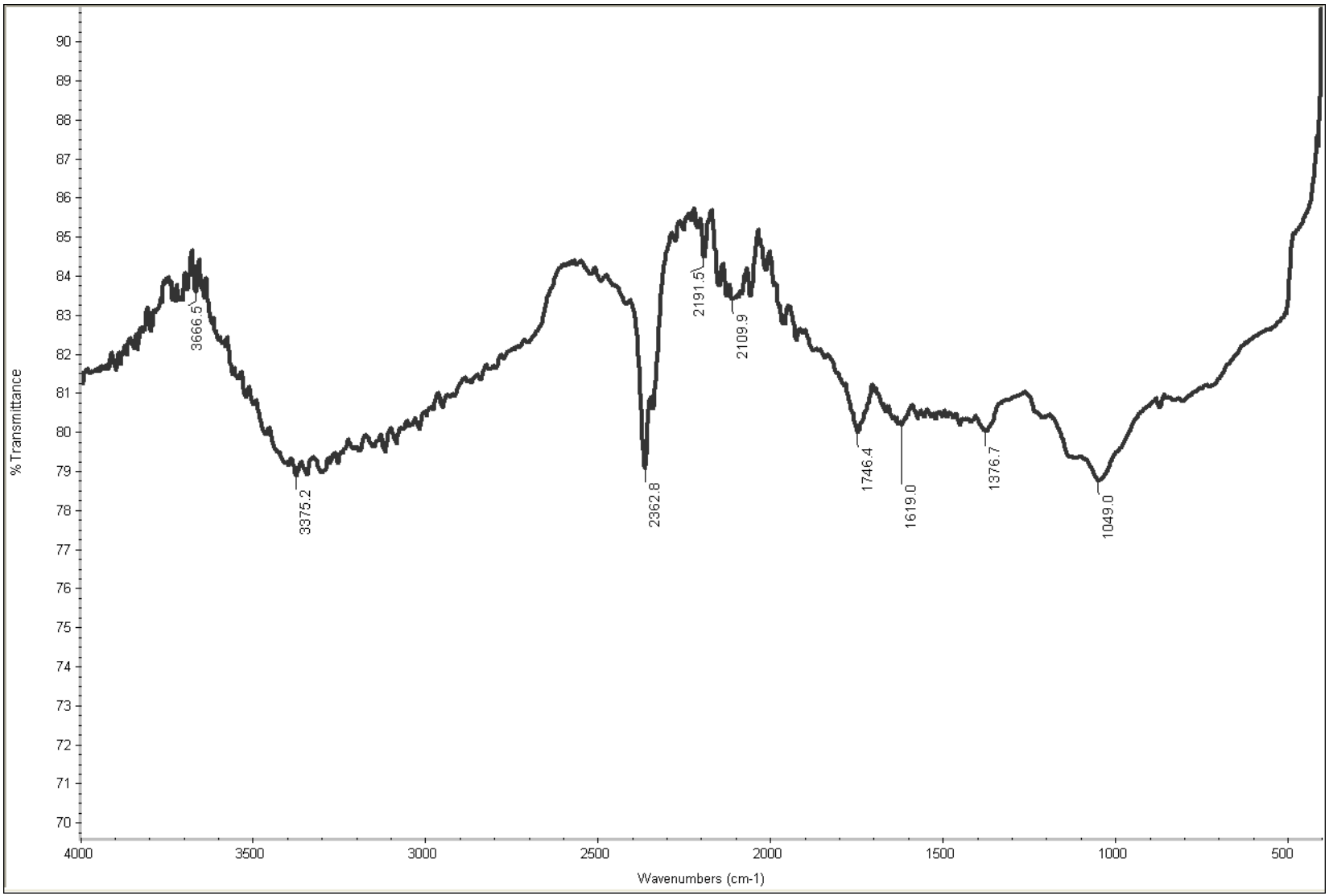

Figure 3.5. IR Spectrum of Hydroxylated Graphite.

4. RESULTS AND DISCUSSION

The objective of this research is to measure the thermal conductivity values of all the composites, to compare different fillers in increasing the overall thermal conductivity of the composites, to decide what shape of fillers is more advantageous in the thermal conductivity improvement of the composites, to have an idea about the interfacial properties between polymer matrix and the fillers, and finally, to combine all these purposes in one conclusion.

Thermal conductivity value of unfilled Surlyn® 1601 was found to be 0.76 W/m·K; however, in the literature, it is stated out that thermal conductivity of Surlyn® 1601 is 0.24 W/m·K [33]. This difference may be due to the degradation or oxidation of polymer chains during fabrication of the part, or oxidation of polymer chains by air before part preparation, or any impurities, inclusions that may have an effect on the thermal conductivity. The home-made thermal conductivity instrument may also have inherent measurement errors.

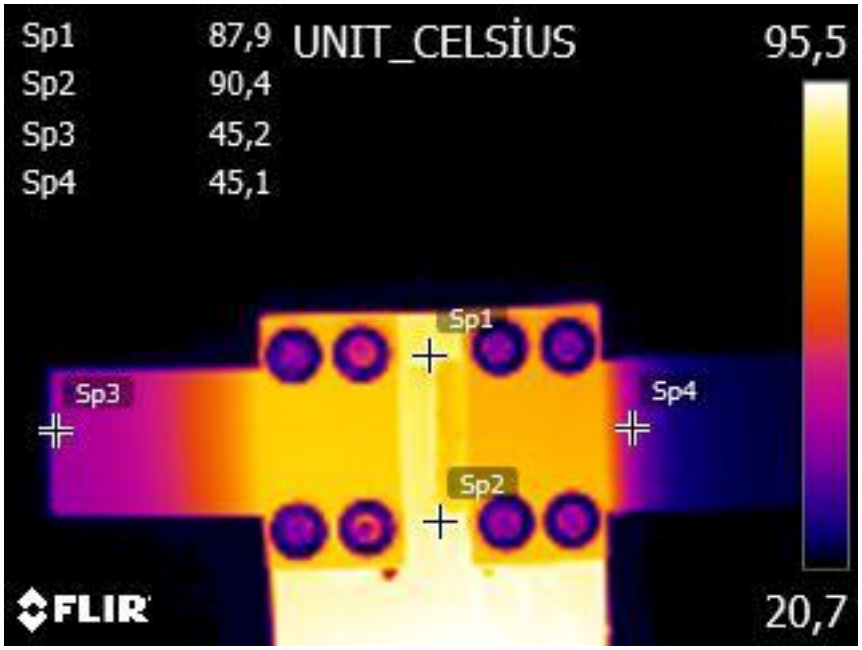

Figure 4.1. Thermal Camera View of Standard Stainless Steel Part (on the left) vs. Experimental Unfilled Surlyn®1601 Part (on the right).

The thermal conductivity comparison of Surlyn® 1601 polymer part with stainless steel part is given on the Figure 4.1. It is easily observed that while the system is being heated, heat can easily flow on the stainless steel part due to its much higher thermal conductivity value compared to the thermal conductivity value of the experimental polymer sample. However, heat flow on the polymeric sample seems to be very difficult because of its low thermal conductivity. Two isothermal points are chosen on both of the samples after the system reaches equilibrium, the ratio of the distances of these points to the edges touching heat path gives the ratio of the thermal conductivities of the samples. Of course, this comparator does not provide absolute thermal conductivity values. Actually, thermal conductivity measuring devices are very expensive; therefore, the comparator is an alternative cheaper way to use in measuring the thermal conductivities.

4.1. Aluminum Filled Surlyn® 1601 Composites

4.1.1. Thermal and Interfacial Properties of Untreated Aluminum Filled Surlyn® 1601 Composites

4.1.1.1. Thermal Conductivity Results. Aluminum powders with two different shapes of metallic particles were used as fillers in varying weight percentages in the composites. The reason for using different shapes of fillers is to interpret the thermal conductivity results according to the aspect ratio of the fillers. In ideal spherical particles, aspect ratio is approximately equal to 1 because the ratio of length to diameter is 1. The aspect ratio increases when the shape of the fillers changes from the spherical to another shape such as flakes, platelets and fibers [34]. The fillers used in these experiments were spherical aluminum and aluminum flakes.

Table 4.1 shows the thermal conductivity results of the composites including different amounts of spherical aluminum powder.

Table 4.1. Thermal Conductivity Results of the Composites Filled with Spherical Aluminum.

Filler Weight %	Thermal Conductivity (W/m·K)
10%	2.1
20%	2.4
30%	2.6
40%	2.7
50%	3.1

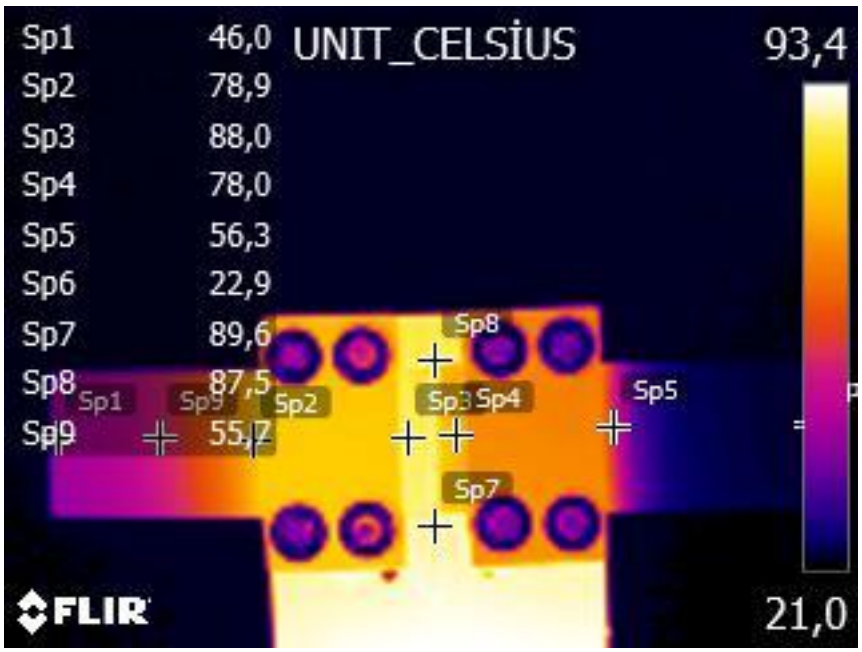

Figure 4.2. Thermal Camera View of Standard Stainless Steel Part (on the left) vs. 10% by Weight Untreated Spherical Aluminum Filled Surlyn®1601 Composite Part (on the right).

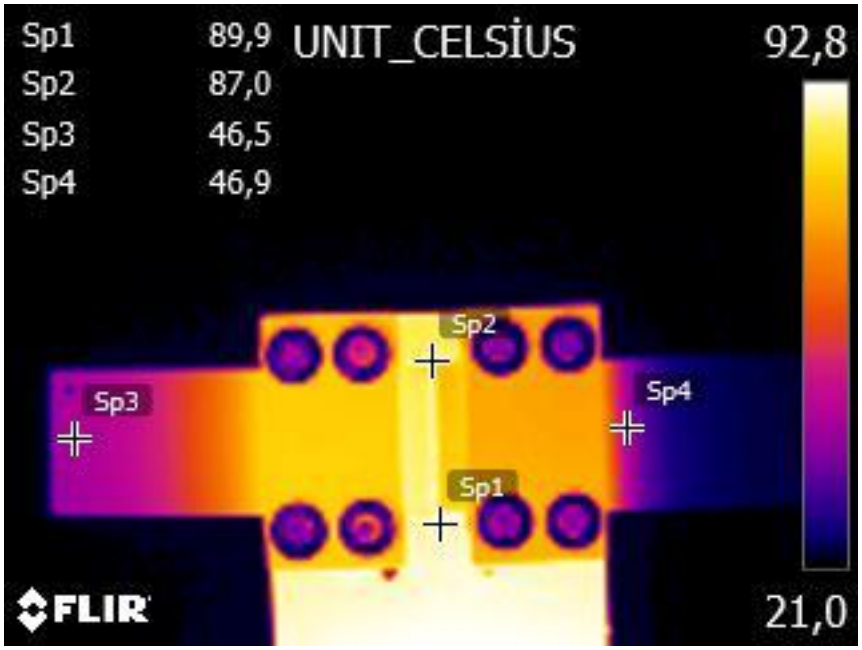

Figure 4.3. Thermal Camera View of Standard Stainless Steel Part (on the left) vs. 20% by Weight Untreated Spherical Aluminum Filled Surlyn®1601 Composite Part (on the right).

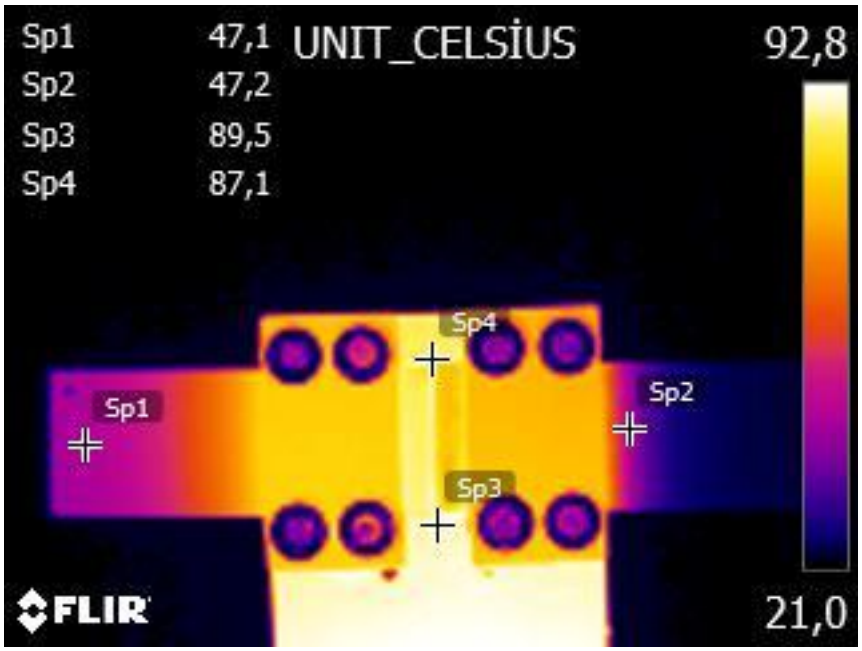

Figure 4.4. Thermal Camera View of Standard Stainless Steel Part (on the left) vs. 30% by Weight Untreated Spherical Aluminum Filled Surlyn®1601 Composite Part (on the right).

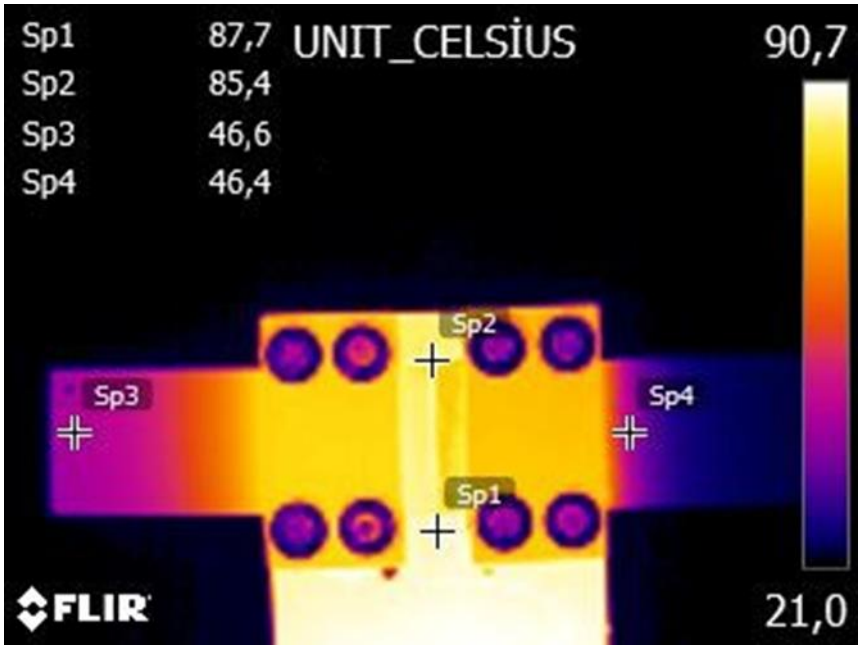

Figure 4.5. Thermal Camera View of Standard Stainless Steel Part (on the left) vs. 40% by Weight Untreated Spherical Aluminum Filled Surlyn®1601 Composite Part (on the right).

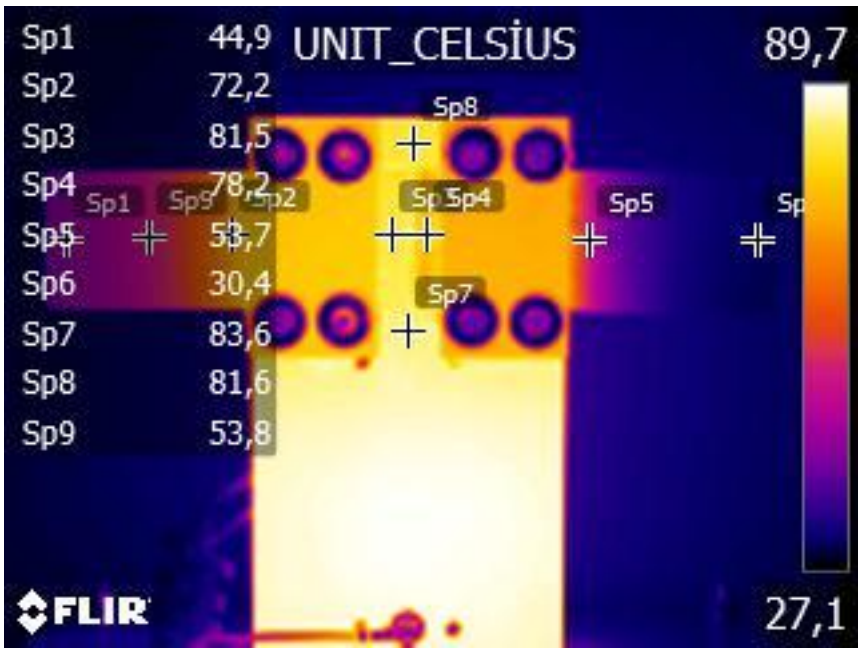

Figure 4.6. Thermal Camera View of Standard Stainless Steel Part (on the left) vs. 50% by weight Untreated Spherical Aluminum Filled Surlyn®1601 Composite Part (on the right).

As expected, the thermal conductivity increases as the weight ratio of the thermally conductive aluminum filler increases. Table 4.2 shows the thermal conductivity values of the composites containing 30% and 50% by weight aluminum flakes.

Table 4.2. Thermal Conductivity Results of the Composites Filled with Aluminum Flakes.

Filler Weight %	**Thermal Conductivity (W/m·K)**
30%	3.2
50%	4.0

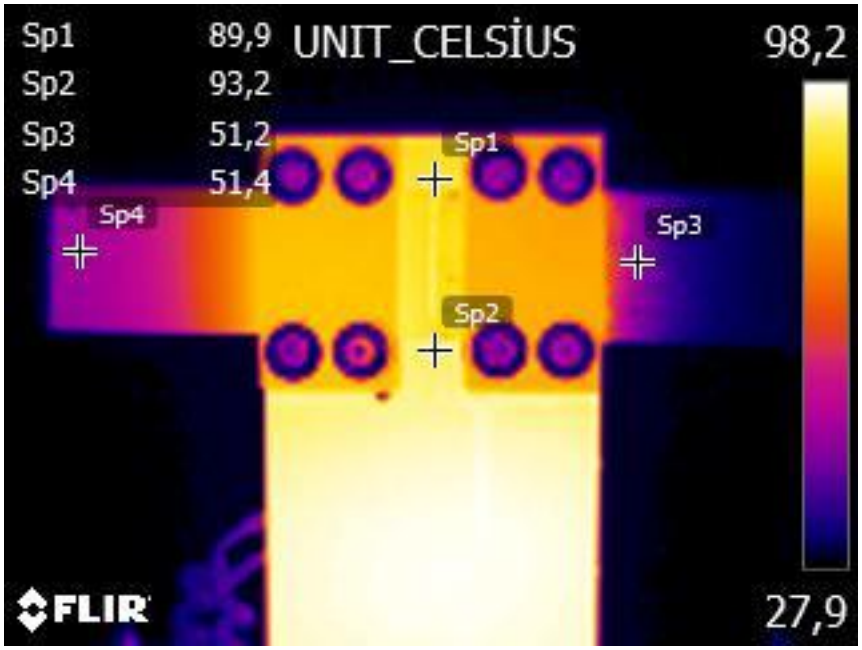

Figure 4.7. Thermal Camera View of Standard Stainless Steel Part (on the left) vs. 30% by Weight Untreated Aluminum Flake Filled Surlyn®1601 Composite Part (on the right).

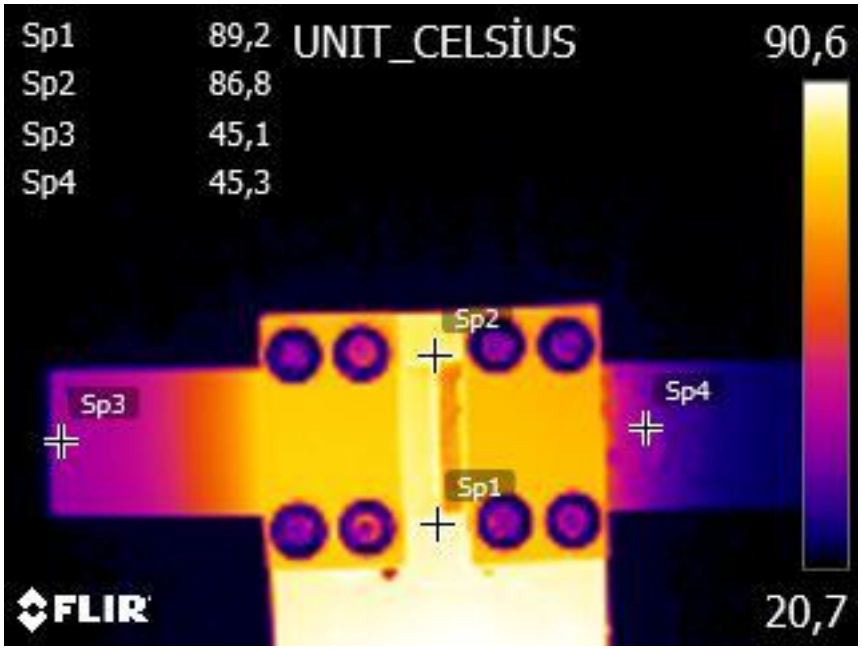

Figure 4.8. Thermal Camera View of Standard Stainless Steel Part (on the left) vs. 50% by Weight Untreated Aluminum Flake Filled Surlyn®1601 Composite Part (on the right).

It is easily observed that flake aluminum filled composites follow the same trend as spherical aluminum filled composites: Thermal conductivity increases with the increasing filler weight ratio. However, although the two kinds of aluminum fillers have the same thermal conductivity value (234 W/m·K), the composite with 30% aluminum flake fillers has a thermal conductivity of 3.2 W/m·K, while the composite with the same amount of spherical aluminum fillers has a thermal conductivity of 2.6 W/m·K. In the case of flake particles filled composites, filler particles are closer to each other compared to the case of spherical particles filled composites. In flake particles filled composites, highly thermally resistive regions are less, which will result in easier heat conduction, and therefore, higher composite thermal conductivity. We conclude that higher aspect ratio fillers give higher thermal conductivity in the final composite. In this work, we will follow the usual composite terminology and define the filler fraction as weight fraction. However, as Surlyn® 1601 has a density of 0,94 g /cm^3 and aluminum has a density of 2,7 g/cm^3, the volume fraction is lower than its weight fraction. For example, 30% w/w corresponds to 13% v/v.

4.1.1.2. Interfacial Properties. Interfacial properties between the polymer matrix and the filler play a very significant role in the enhancement of the thermal conductivity of the composites. If the interaction between the polymer matrix and the filler is poor, which causes interfacial heat resistance due to the existence of micro-voids between the interfaces of the filler and the matrix, then the enhancement of the thermal conductivity will be low. Interfacial properties are determined by scanning electron microscopy analyses of the fracture surfaces of the composites.

Spherical aluminum particles used in the composites were sieved into particles having diameters 5 micrometers or lower; therefore, it is impossible to detect the interaction of a single aluminum particle with the polymer matrix. However, the particles form clusters which are easy to observe with scanning electron microscopy. Figures 4.9, 4.10 and 4.11 show the SEM images of the spherical aluminum filled Surlyn® 1601 composite at 500x, 250x, 100x magnifications, respectively.

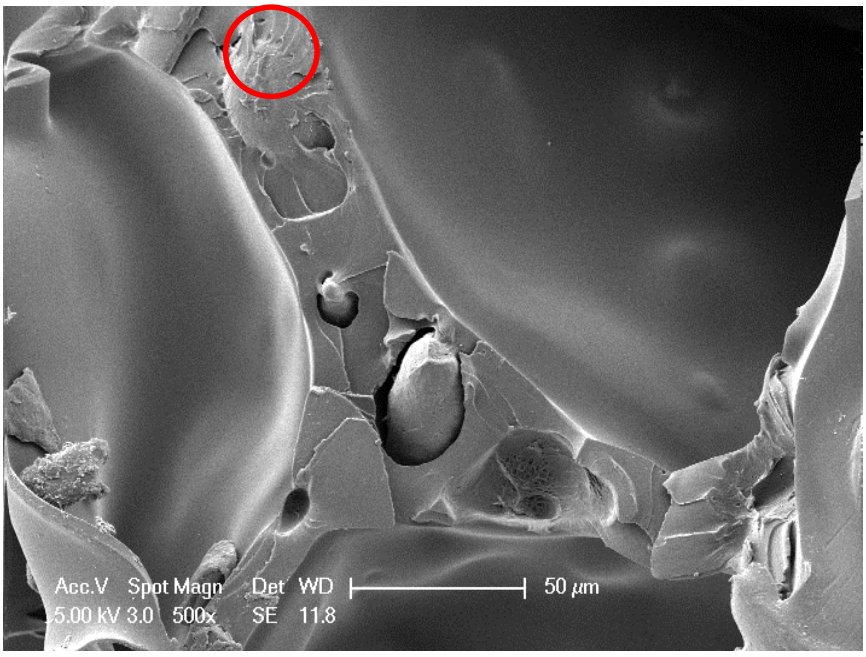

Figure 4.9. SEM Image of the Non-Treated Spherical Aluminum Filled Surlyn® 1601 Composite at 500x Magnification.

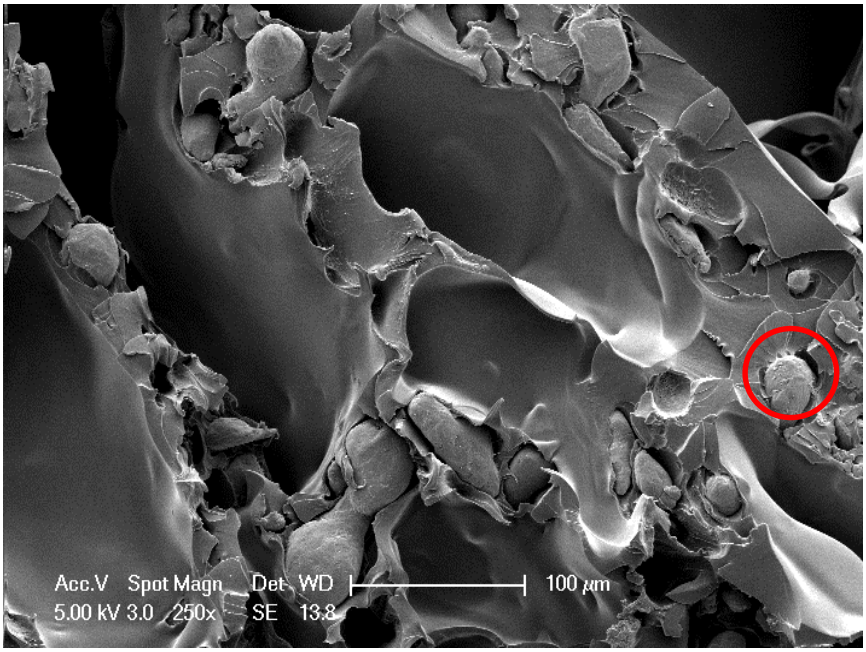

Figure 4.10. SEM Image of the Non-Treated Spherical Aluminum Filled Surlyn® 1601 Composite at 250x Magnification.

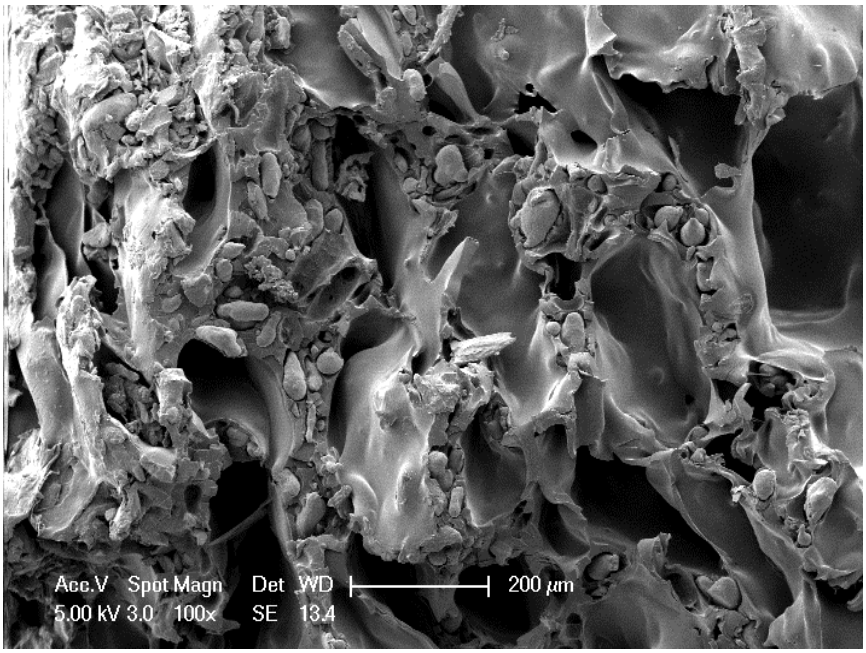

Figure 4.11. SEM Image of the Non-Treated Spherical Aluminum Filled Surlyn® 1601 Composite at 100x Magnification.

The reason for aluminum particles to form clusters is that metal-metal interactions overcome metal-polymer interactions; in other words, cohesive forces dominate adhesive forces. The polymer does not wet the metal surface. The voids that aluminum clusters sit in are larger than the sizes of the clusters. The micro-voids around the clusters are easily visible. These voids are the reason for low thermal conductivity and the phonon scattering at the interfacial zones. However, some clusters have some adhesion with polymer matrix as on Figure 4.10 with red circle. This is the proof that the proposed acid-base neutralization reaction between aluminum and Surlyn® 1601 matrix does take place. On Figure 4.9, the red circle shows the propagation of the cracks after breaking the composite. On Figure 4.11, air inclusions can be observed, which may be due to poor processing techniques, i.e. insufficient mixing and poor adhesion between the filler and the matrix. A vacuum equipped mixer, which was not available, would have yielded a sample with no air pockets. Air inclusions may also lead to the heat resistance and phonon scattering in such regions.

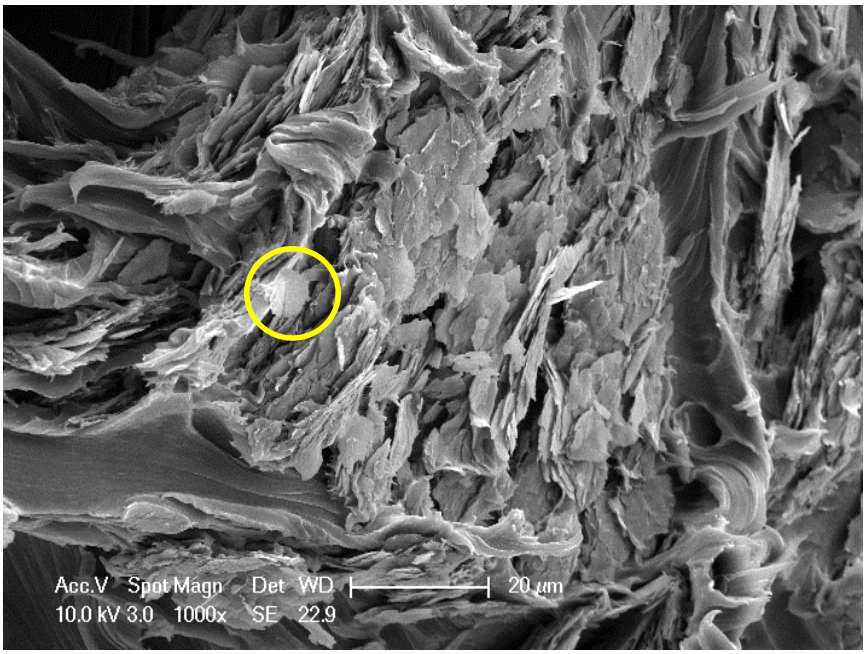

Figure 4.12. SEM Image of the Non-Treated Aluminum Flake Filled Surlyn® 1601 Composite at 1000x Magnification.

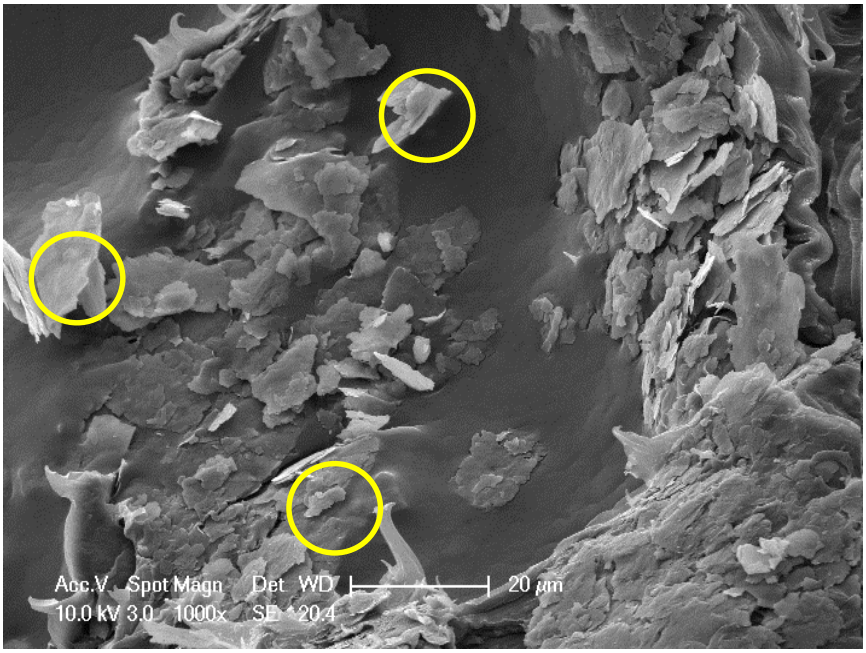

Figure 4.13. SEM Image of the Non-Treated Aluminum Flake Filled Surlyn® 1601 Composite at 1000x Magnification.

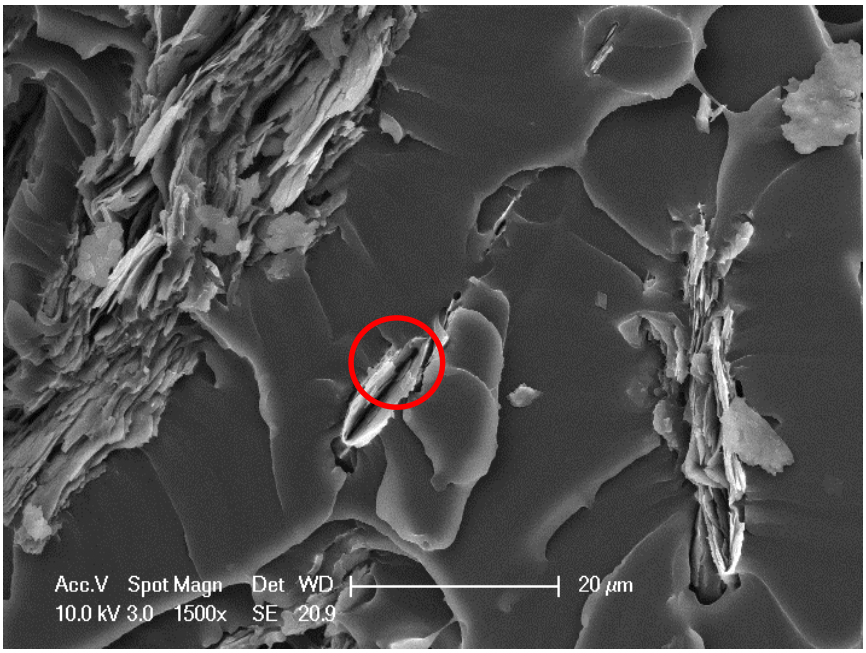

Figure 4.14. SEM Image of the Non-Treated Aluminum Flake Filled Surlyn® 1601 Composite at 1000x Magnification.

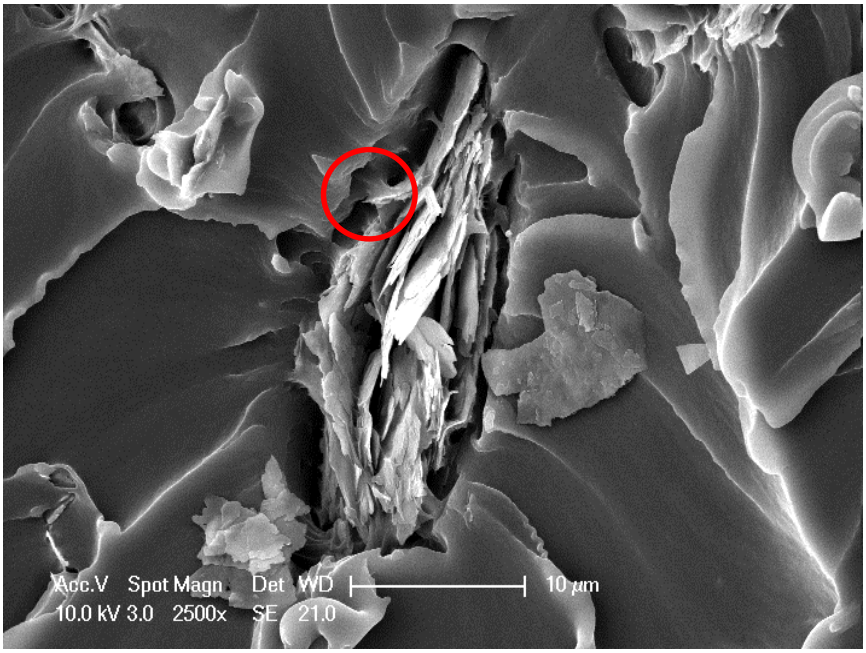

Figure 4.15. SEM Image of the Non-Treated Aluminum Flake Filled Surlyn® 1601 Composite at 2500x Magnification.

The diameter of the aluminum flake particles used in the experiments was large enough to be analyzed individually with the help of scanning electron microscopy. Figures 4.12, 4.13, 4.14 and 4.15 show the SEM images of the fractured surfaces of aluminum flake filled Surlyn® 1601 composites at 1000x, 1000x, 1500x, 2500x magnifications; respectively. Aluminum flakes tend to come together just as in the case of spherical aluminum particles filled composites. The reason can be again described by the fact that metal-metal interactions and polymer-polymer interactions overcome the metal-polymer interactions. There is some adhesion between the edges of the aluminum flake clusters and polymer matrix shown by red circles in figures 4.14 and 4.15. However, adhesion is not so good that some metallic particles are free; in other words, not bounded to the polymer matrix demonstrated by yellow circles in figures 4.12 and 4.13. Additionally, there are some micro sized voids between the polymer matrix and the aluminum flakes and between the aluminum flakes themselves. The reason for the voids between the polymer and the filler is the lack of good adhesion, whereas the voids between the flakes can be described by the shape of the particles; they do not sit on to the other particle well causing interfacial heat resistance and phonon scattering. In order to overcome such voids at the interfacial zones, it is the objective to improve the adhesion between the polymer matrix and filler by

surface treatment of aluminum particles. Due to the fact that aluminum flakes lead to higher composite thermal conductivity when compared to spherical aluminum, surface treatment steps will only be applied to aluminum flakes.

It should be noted that aluminum has a tendency to form oxides at the surface rapidly. Therefore, it is likely that both aluminum spheres and flakes are covered with a polar oxide layer which inhibits wetting.

4.1.2. Interfacial Properties and Thermal Conductivity Results of Surface Treated Aluminum Flake Filled Surlyn® 1601 Composites

As prescribed above, in order to improve the overall thermal conductivity of the composites, the problem of interfacial heat resistance and interfacial phonon scattering should be overcome by surface treatment of filler particles. For this purpose, aluminum flakes will be reacted with only 3-Aminopropyltriethoxysilane and the mixture of Michem® Prime 4983R and 3-Aminopropyltriethoxysilane.

4.1.2.1. SEM Analyses and Thermal Conductivity Result of 3-Aminopropyltriethoxysilane Treated Aluminum Flake Containing Surlyn® 1601 Composites. Improvement in the interfacial adhesion properties will improve the overall thermal conductivity of the composite; for this purpose, aluminum particles are treated with an aminosilane coupling agent. The reasons for choosing an aminosilane are that hydroxides on the surface of aluminum can be condensed with silanol groups after aminosilane is hydrolyzed and that amino group of the aminosilane can give an acid-base neutralization reaction with the carboxylic acid groups of Surlyn® 1601.

The proposed reaction between the surface of aluminum and the aminosilane is given on Figure 4.16. After the surface treatment step, the reaction between the surface treated aluminum and Surlyn® 1601 should take place as shown on Figure 4.17.

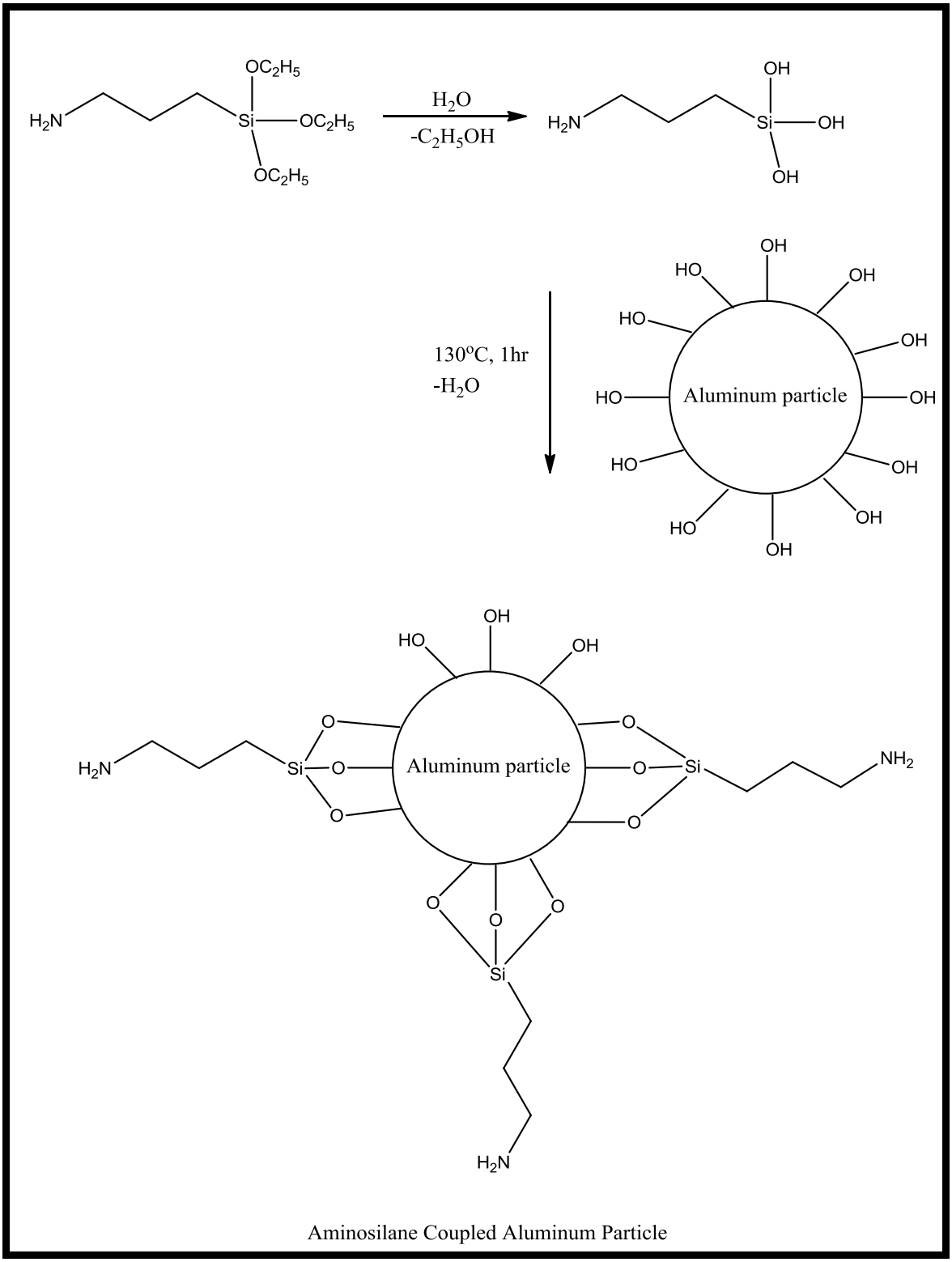

Figure 4.16. Surface Treatment Chemistry of Aluminum Particles.

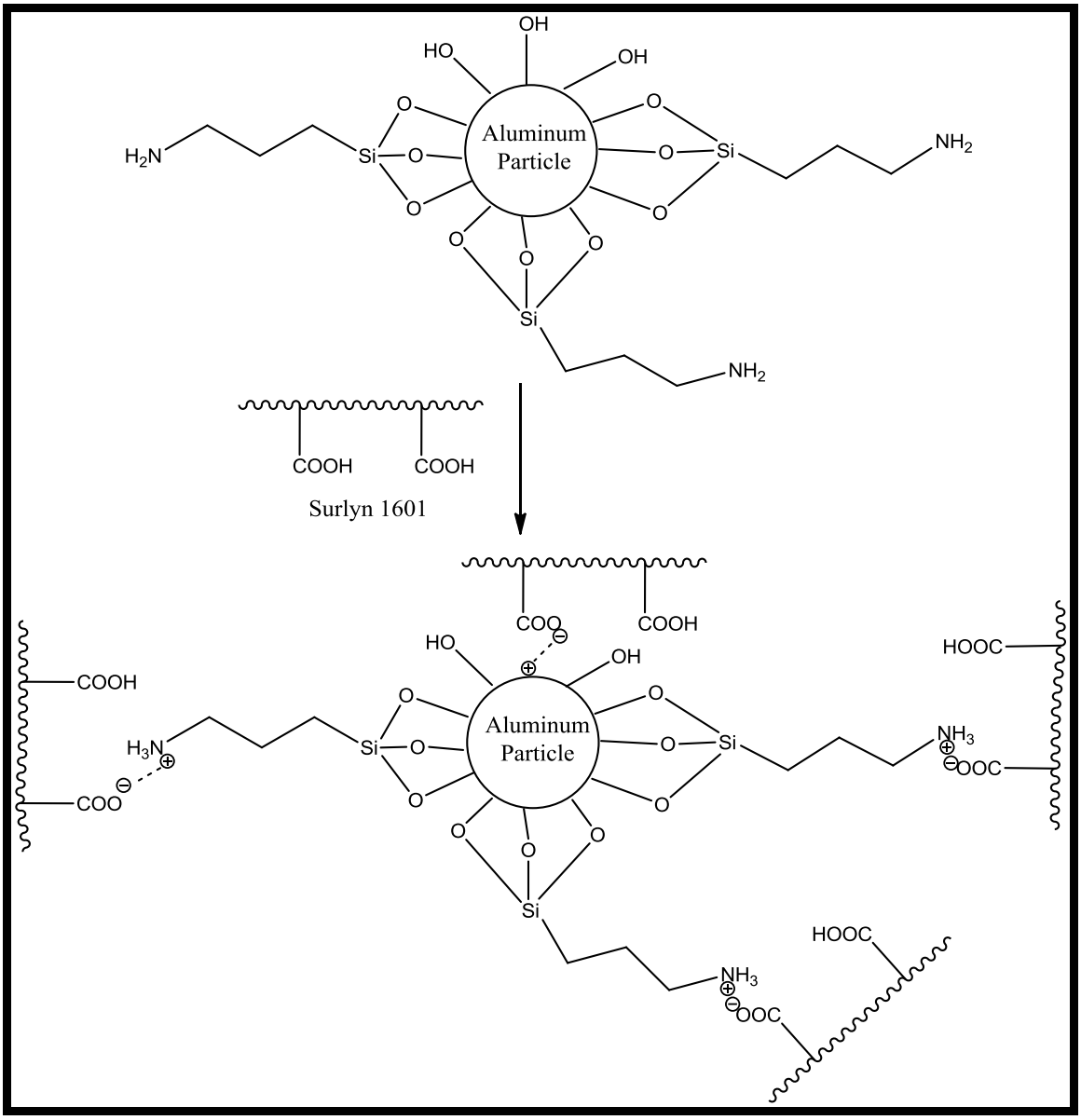

Figure 4.17. The Reaction between Aminosilane Treated Aluminum Surface and Surlyn® 1601.

First, the aminosilane is hydrolyzed at pH 5.5 to give silanol groups. The pH is adjusted with the help of acetic acid because it is volatile at the temperatures that condensation takes place between the surface of aluminum and silanol groups. The reaction in Figure 4.17 is an acid-base neutralization reaction. Amino groups of the aminosilane have basic character and are able to react with carboxylic acid groups of Surlyn® 1601. If the reactions proposed on figures 4.16 and 4.17 occur, there should be not only an enhancement in the adhesion of aluminum flakes to the polymer matrix but also

decrease in the number of micro-voids in the structure of the composite; and as a result, there should be an improvement in the overall thermal conductivity of the composite.

Figure 4.18, Figure 4.19, Figure 4.20, Figure 4.21 demonstrate the SEM images of the Surlyn® 1601 composites filled with 30% by weight aluminum flakes surface treated with 3-Aminopropyltriethoxysilane at 1500x, 2500x, 5000x, and 10000x magnifications, respectively.

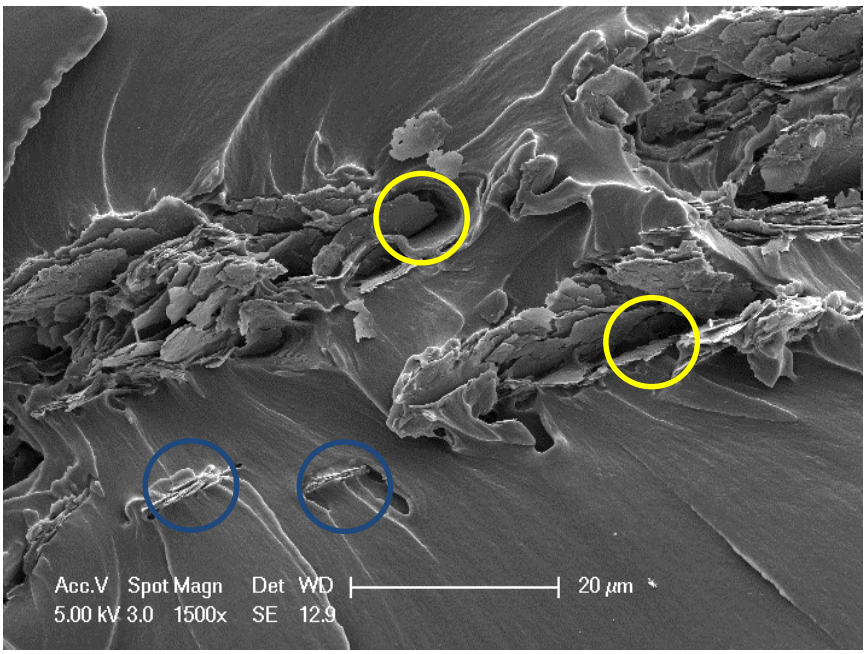

Figure 4.18. SEM Image of the Aminosilane Treated Aluminum Flake Filled Surlyn® 1601 Composite at 1500x Magnification.

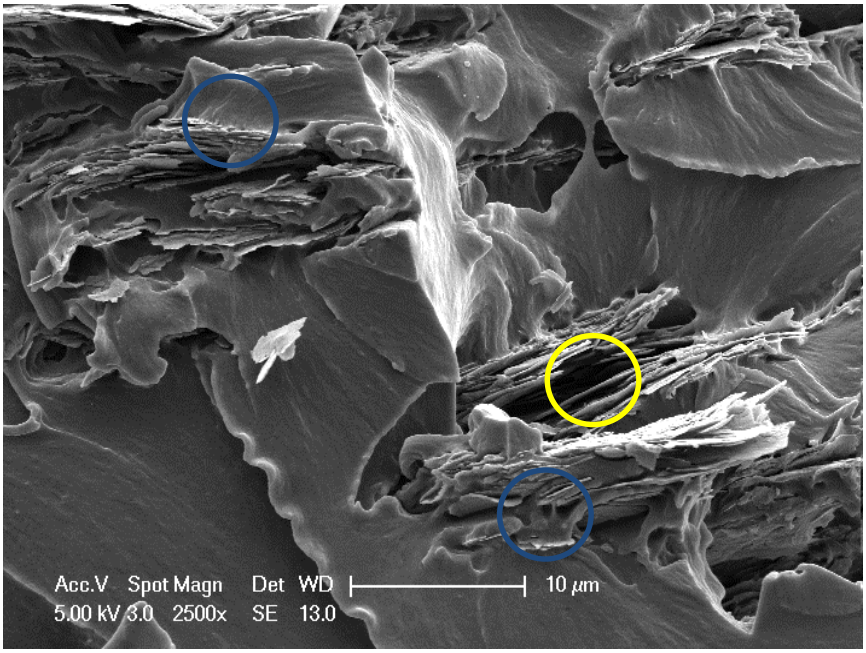

Figure 4.19. SEM Image of the Aminosilane Treated Aluminum Flake Filled Surlyn® 1601 Composite at 2500x Magnification.

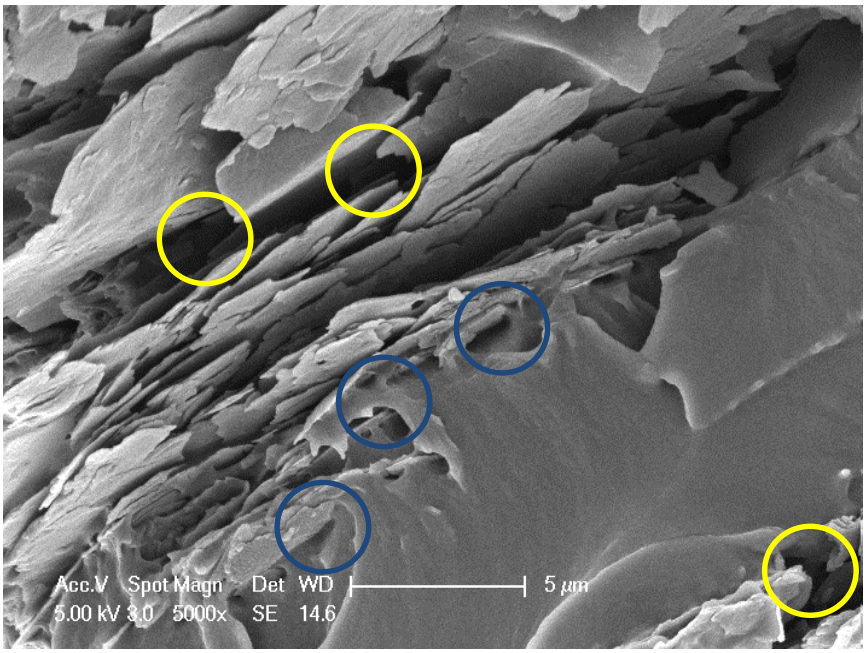

Figure 4.20. SEM Image of the Aminosilane Treated Aluminum Flake Filled Surlyn® 1601 Composite at 5000x Magnification.

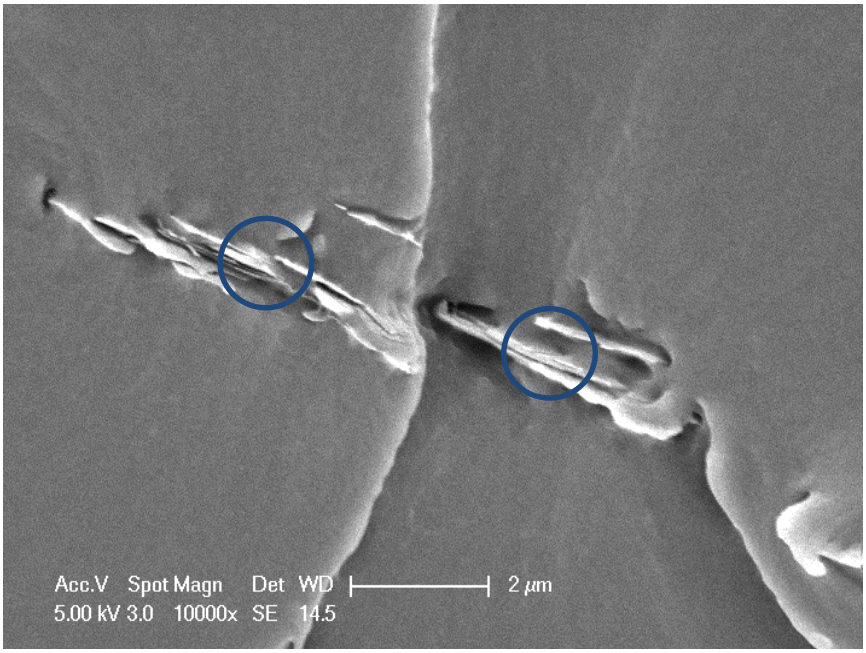

Figure 4.21. SEM Image of the Aminosilane Treated Aluminum Flake Filled Surlyn® 1601 Composite at 10000x Magnification.

SEM images prove that there is a good adhesion between aminosilane treated aluminum surface and the polymer matrix. Blue circles shown on the above images demonstrate the adhesion regions of polymer to the aluminum particles. There are almost no micro-voids between the aluminum particles and polymer matrix, the voids only occur between the aluminum particles, such voids are shown with yellow circles in the SEM images. Additionally, there is no evidence in the SEM images of any non-bounded aluminum particles in the structure of the composite. All these facts prove that aminosilane treatment of aluminum particles improves the adhesion between polymer matrix and aluminum. As a result, it is expected that thermal conductivity of the aminosilane coated aluminum flakes filled Surlyn® 1601 composite should have a larger thermal conductivity value compared to the non-coated aluminum flake filled Surlyn® 1601 composite at the same filler weight ratio.

Figure 4.22 shows the thermal conductivity comparison of aminosilane treated aluminum flake filled Surlyn® 1601 composite part at 30% filler weight ratio against standard stainless steel part.

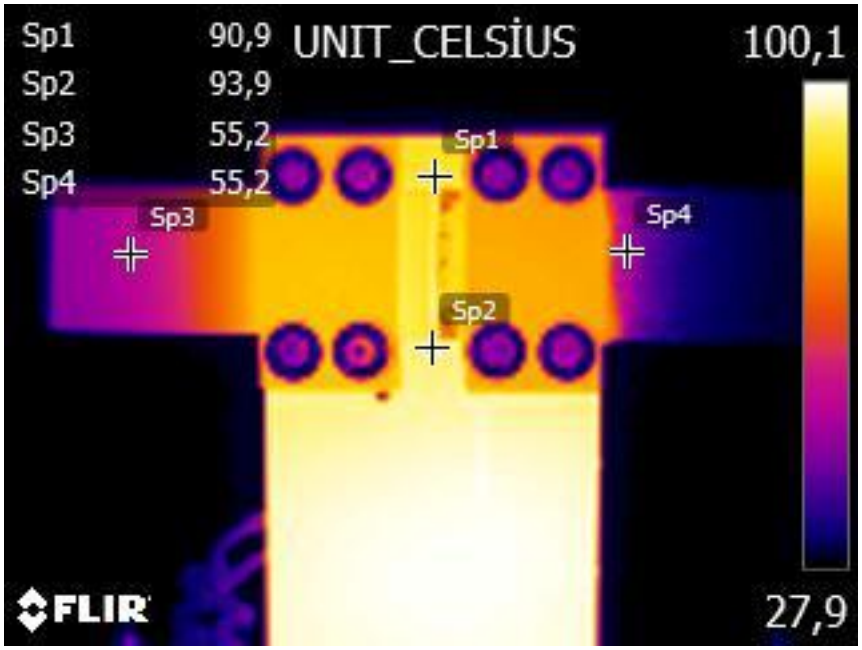

Figure 4.22. Thermal Camera View of Standard Stainless Steel Part (on the left) vs. 30% by Weight Aluminum Flake (aminosilane treated) Filled Surlyn®1601 Composite Part (on the right).

According to the calculations shown on the experimental part, the thermal conductivity value of aminosilane treated 30% aluminum flake filled Surlyn®1601 composite is found to be 4.0 W/m·K, which is higher than the thermal conductivity of the composite including 30% by weight non-treated aluminum flake filler which was found to be 3.2 W/m·K. It is concluded that aminosilane treatment improves the adhesion, decreases the number of voids in the structure, so decrease the highly thermally resistive regions in the structure. Therefore, there is an enhancement in the thermal conductivity of the composite.

4.1.2.2. SEM Analyses and Thermal Conductivity Result of Michem® Prime 4983R & Aminosilane Treated Aluminum Flake Containing Surlyn® 1601 Composite. The next aim is to solve the problem of micro-voids as much as possible. Aminosilane treatment showed an enhancement in the adhesion of polymer matrix and filler. However, the number of voids between the filler particles is not decreased completely. It was decided that an additional coupling agent could be used to increase wetting. This coupling agent was chosen to be a commercial polymer, Michem® Prime 4983R, which is an emulsion of poly

(ethylene-co-acrylic acid) [35]. The structure of Michem® Prime 4983R is given on Figure 4.23:

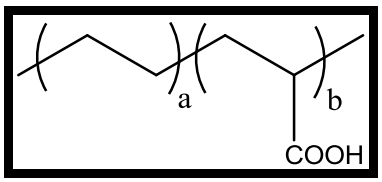

Figure 4.23. The Structure of Michem® Prime 4983R.

The reasons for choosing Michem® Prime 4983R are those polar carboxylic acid groups may give an acid-base neutralization reaction with the amino end of the silane, and the non-polar parts of Michem® Prime 4983R may have van der Waals interactions with non-polar parts of Surlyn® 1601 matrix and carboxylic acid groups of Surlyn® 1601 and Michem® Prime 4983R may have H-bonding interactions. Thus, the coupling reaction is converted to a cohesive force instead of an adhesive force.

The reactions between the mixture of these coupling agents and aluminum surface are given on Figure 4.24.

Van der Waals and H-bonding interactions as cohesive forces between Michem® Prime 4983R and Surlyn® 1601; additionally, ionic interactions between Michem® Prime 4983R and aluminum surface, and bond formation between aminosilane and aluminum surface as adhesive forces after Surlyn® 1601 is reacted with surface coated aluminum are demonstrated on Figure 4.25.

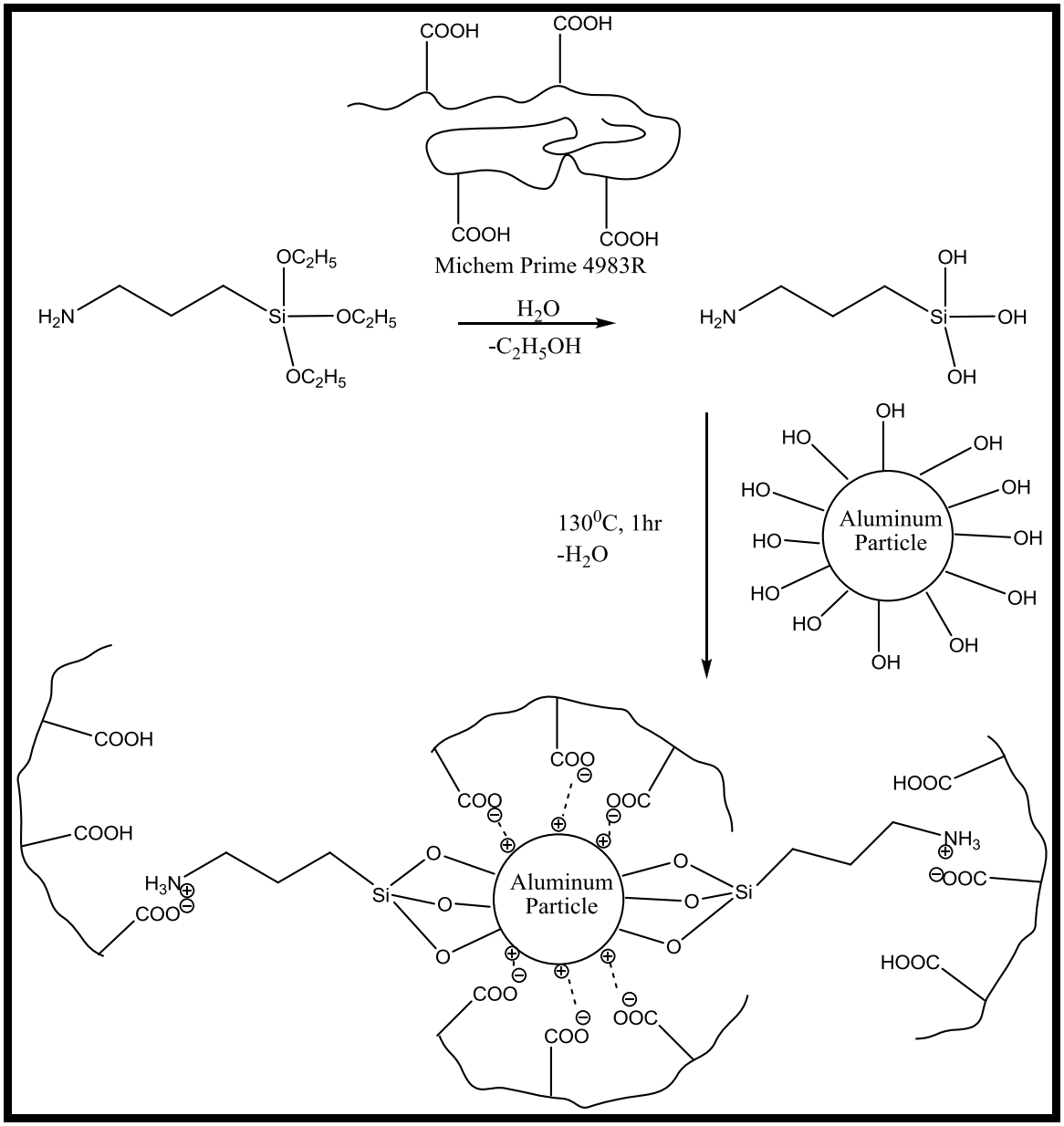

Figure 4.24. The Reactions between the Mixture of Coupling Agents and Aluminum Particles.

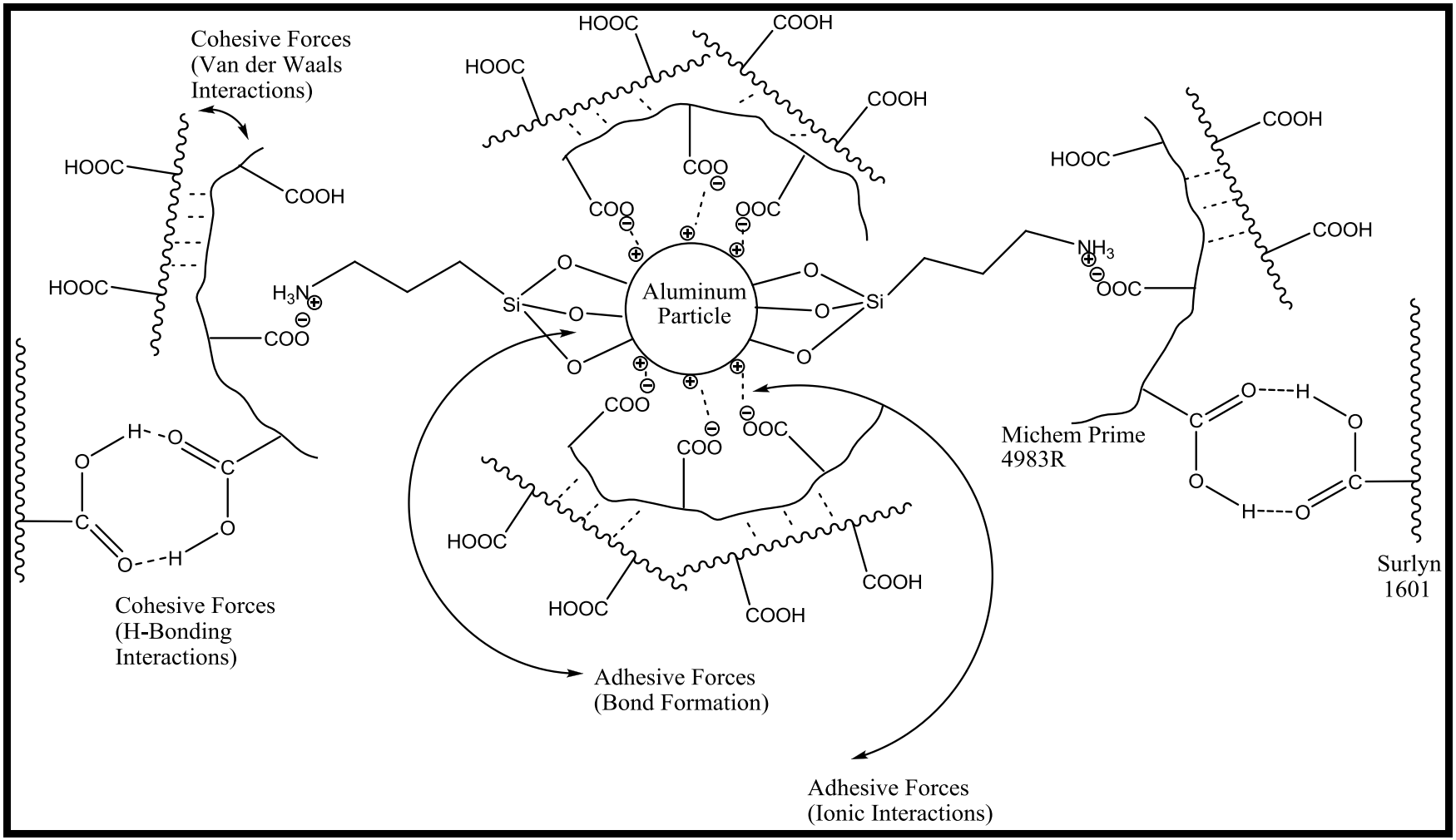

Figure 4.25. The Proposed Interactions between Aminosilane and Michem® Prime 4983R Treated Aluminum Surface and Surlyn® 1601.

In Figure 4.24, 3-Aminopropyltriethoxysilane is hydrolyzed with acetic acid in the presence of Michem® Prime 4983R. The resulting liquid is a suspension. After hydrolysis step, aluminum flakes are treated with this suspension, and then dried for a sufficient time. After that, treated aluminum flake powder is put into an oven at 130°C for 1 hour to give condensation reaction with silanol groups. Figure 4.25 shows the reaction between Surlyn® 1601 and surface treated aluminum flake. There are acid-base neutralization reactions between amino groups of aminosilane and methacrylic acid groups of Surlyn® 1601, and Van der Waals interactions between ethylene units of Surlyn® 1601 and Michem® Prime 4983R and H-bonding interactions between carboxylic acid groups of Surlyn® 1601 and Michem® Prime 4983R. Van der Waals and H-bonding interactions are shown with dotted lines. Figures 4.26, 4.27 and 4.28 show the SEM images of the Surlyn® 1601 composites filled with 30% by weight aluminum flakes surface treated with 3-Aminopropyltriethoxysilane and Michem® Prime 4983R at 250x, 1500x, and 1000x magnifications, respectively.

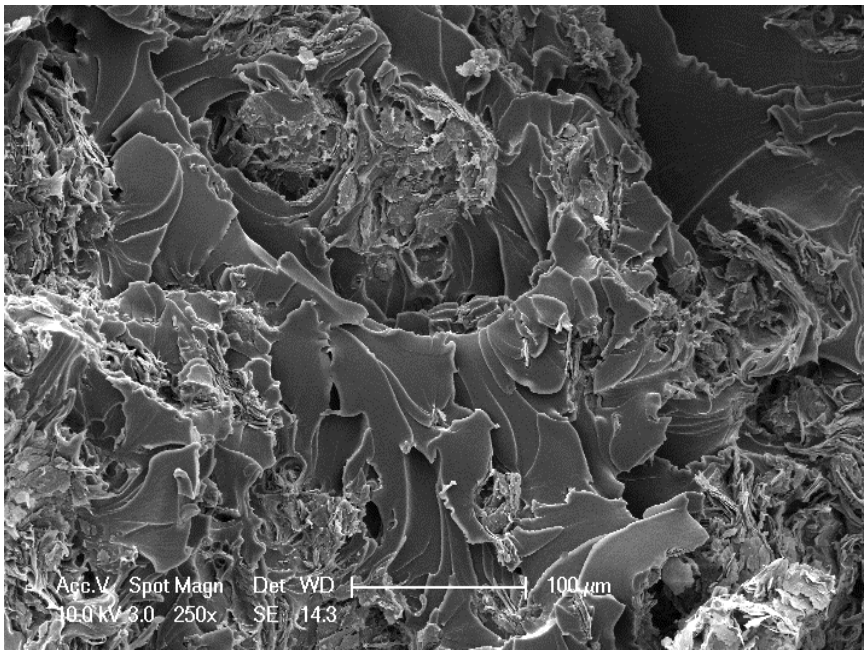

Figure 4.26. SEM Image of the Aminosilane and Michem® Prime 4983R Treated Aluminum Flake Filled Surlyn® 1601 Composite at 250x Magnification.

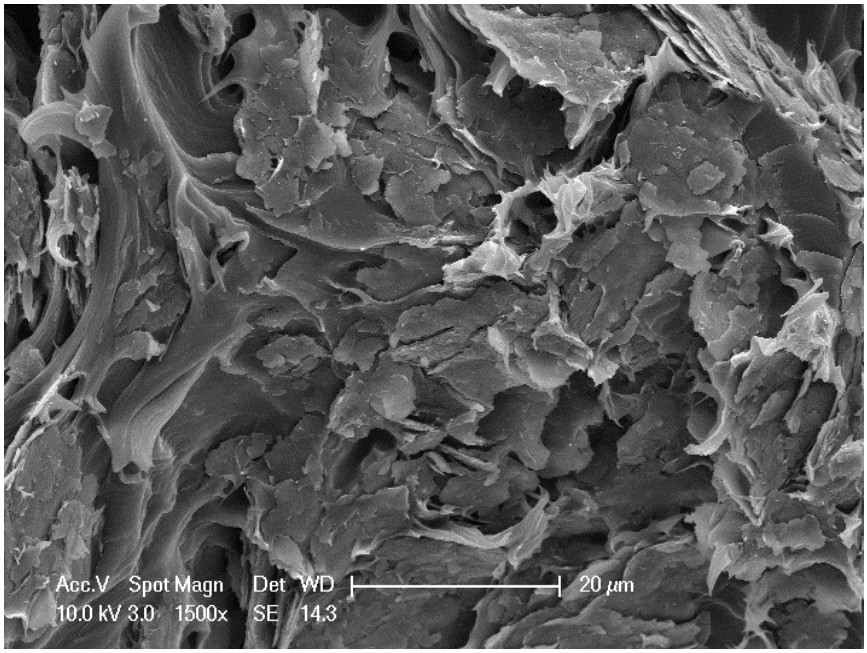

Figure 4.27. SEM Image of the Aminosilane and Michem® Prime 4983R Treated Aluminum Flake Filled Surlyn® 1601 Composite at 1500x Magnification.

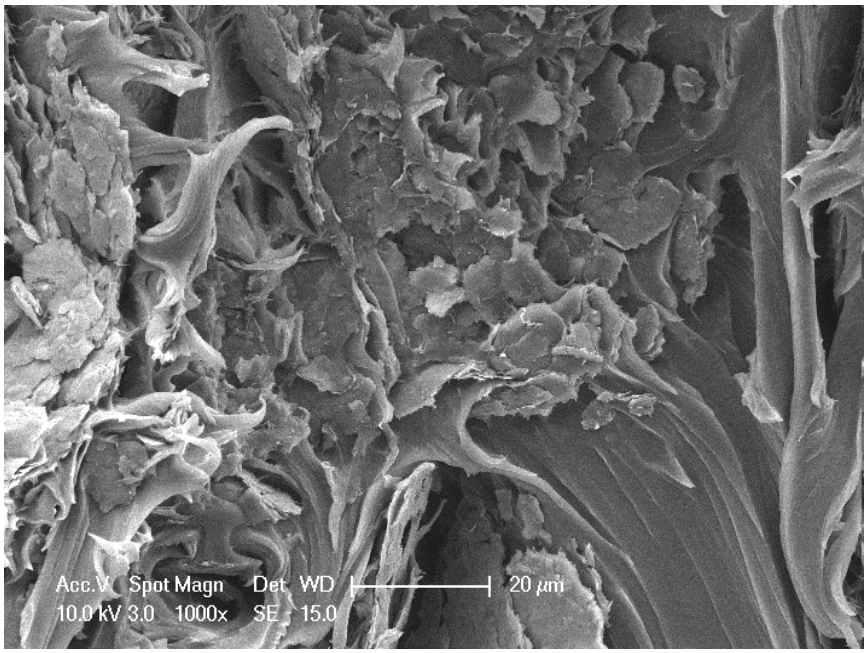

Figure 4.28. SEM Image of the Aminosilane and Michem® Prime 4983R Treated Aluminum Flake Filled Surlyn® 1601 Composite at 1000x Magnification.

SEM images shown on figures 4.26, 4.27 and 4.28 belong to the composites containing 30% by weight aminosilane and Michem® Prime 4983R surface treated aluminum flake. In Figure 4.26, aluminum flakes are observed to be buried under polymer, there are no free aluminum particles visible because the interaction is improved very efficiently. In figures 4.27 and 4.28, the adhesion of aluminum flakes are observed to be good; additionally, the voids between the polymer and the filler are minimized compared to untreated aluminum flake filled composites. Inter-filler voids are decreased efficiently because aluminum particles are covered with an organic layer, and there is van der Waals interactions between metallic particles in addition to metal-metal interactions. Although the voids in aminosilane and Michem® Prime 4983R treated aluminum flake filled composite are less compared to aminosilane treated aluminum flake filled composite, the thermal conductivity is lower than only aminosilane treated aluminum flake filled composite.

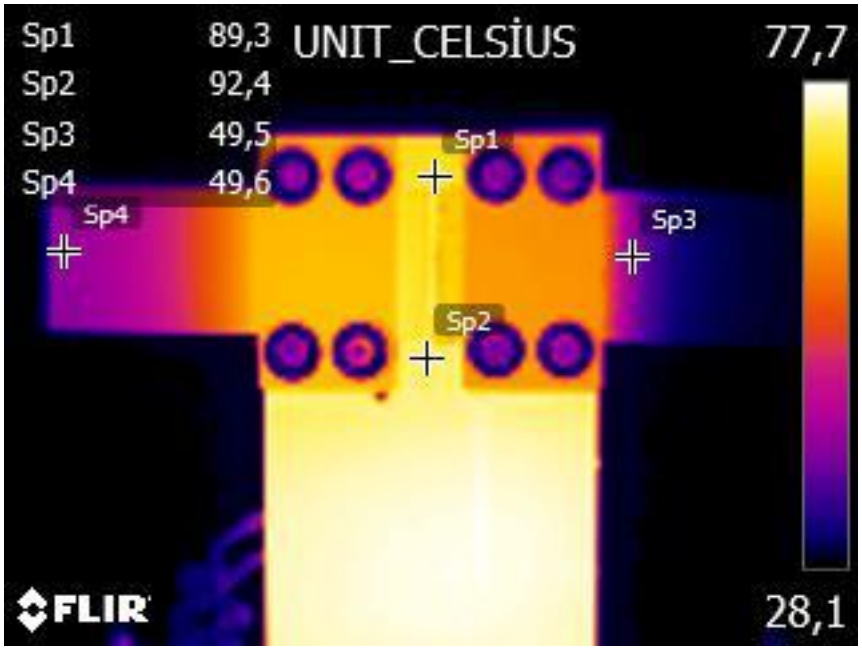

Figure 4.29. Thermal Camera View of Standard Stainless Steel Part (on the left) vs. 30% by Weight Aluminum Flake (Michem® Prime 4983R and aminosilane treated) Filled Surlyn®1601 Composite Part (on the right).

The thermal conductivity of 30% by weight aminosilane and Michem® Prime 4983R treated aluminum flake filled composite was found to be 3 W/m·K, lower than 30%

untreated aluminum flake containing composite. It is believed that heat flow regions of polymer covered aluminum particles are very thermally resistive. Organic layers between aluminum particles prevent aluminum particles to conduct heat to each other. While metal to polymer thermal conductivity may have increased, metal to metal thermal conductivity decreased resulting in an overall thermal conductivity decrease.

4.2. Graphite Filled Surlyn® 1601 Composites

The next step is to prepare composite including higher thermally conductive filler compared to aluminum; for this purpose, graphite is chosen. Graphite has a thermal conductivity value of 600 W/m·K, whereas aluminum has a thermal conductivity value of 234 W/m·K. In addition, graphite particles have flake like shapes. Moreover, graphite has the advantage of being non-corrosive compared to aluminum.

4.2.1. Thermal Conductivity Results and Interfacial Properties of Untreated Graphite Filled Surlyn® 1601 Composites

4.2.1.1. Thermal Conductivity Results. Table 4.3 shows the thermal conductivity results of Surlyn® 1601 composites including different amounts of untreated graphite. It is observed that as the graphite weight ratio increases, the thermal conductivity of the composite also increases. Moreover, thermal conductivity results of graphite filled composites are higher than the thermal conductivity of the spherical or flake aluminum filled composites at the same filler volume ratios even though aluminum particles are surface treated.

Table 4.3. Thermal Conductivity Results of the Composites Filled with Pure Graphite.

Filler Weight %	Thermal Conductivity (W/m·K)
10%	3.2
20%	4.2
30%	5.6
40%	6.8

Figures 4.30, 4.31, 4.32, and 4.33 show the thermal conductivity comparison of the varying weight percentages of pristine graphite filled composite parts over standard stainless steel part.

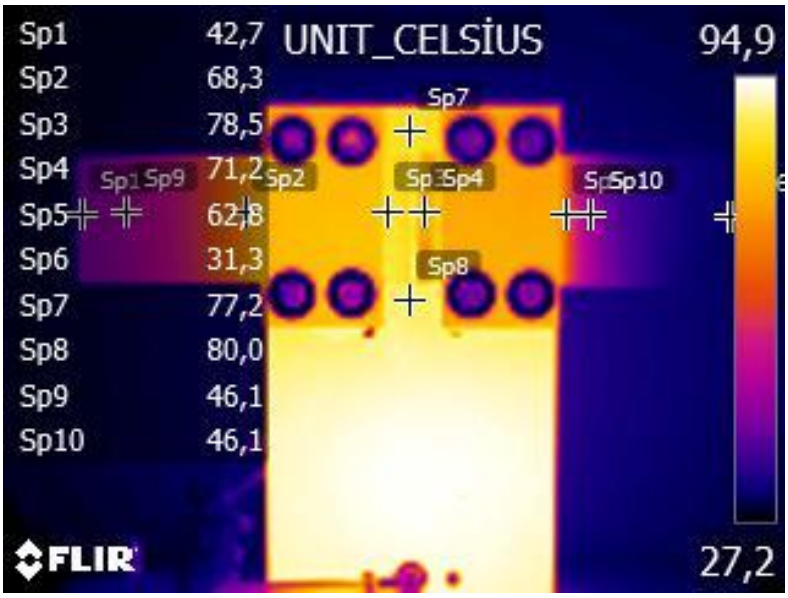

Figure 4.30. Thermal Camera View of Standard Stainless Steel Part (on the left) vs. 10% by Weight Graphite Filled Surlyn®1601 Composite Part (on the right).

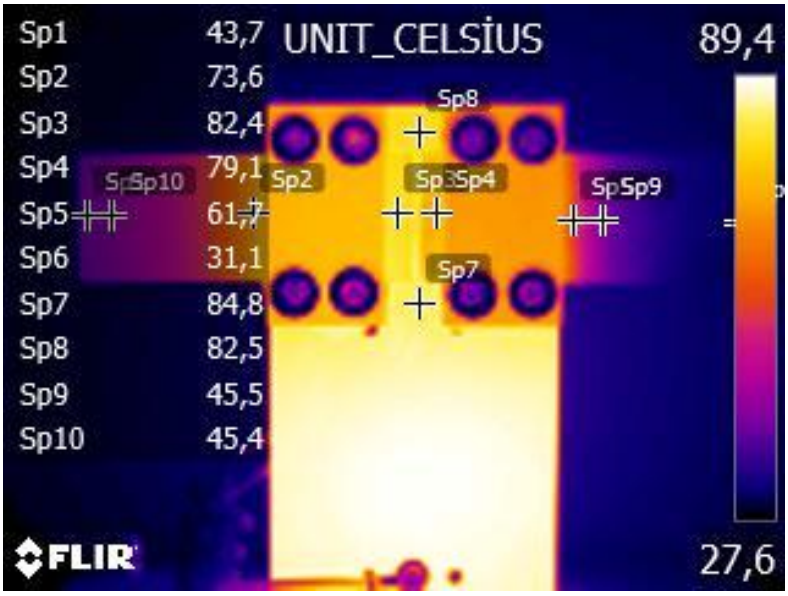

Figure 4.31. Thermal Camera View of Standard Stainless Steel Part (on the left) vs. 20% by Weight Graphite Filled Surlyn®1601 Composite Part (on the right).

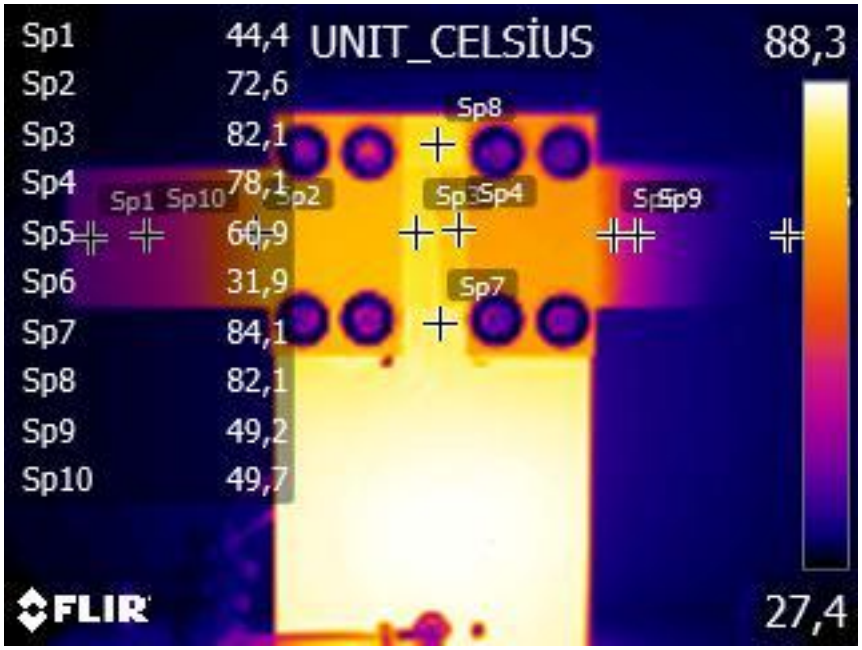

Figure 4.32. Thermal Camera View of Standard Stainless Steel Part (on the left) vs. 30% by Weight Graphite Filled Surlyn®1601 Composite Part (on the right).

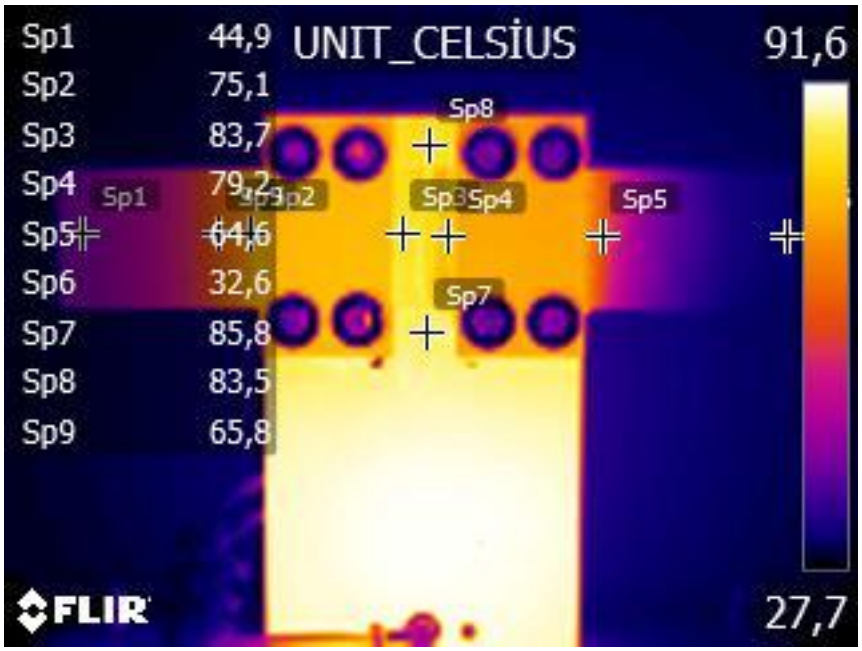

Figure 4.33. Thermal Camera View of Standard Stainless Steel Part (on the left) vs. 40% by Weight Graphite Filled Surlyn®1601 Composite Part (on the right).

4.2.1.2. Interfacial Properties. Graphite has layered, planar structure. It is composed of parallel graphene layers, and in the structure of graphene, there are fused aromatic carbon rings. Figure 4.34 shows the structure of one layer of graphite, which is called graphene [36].

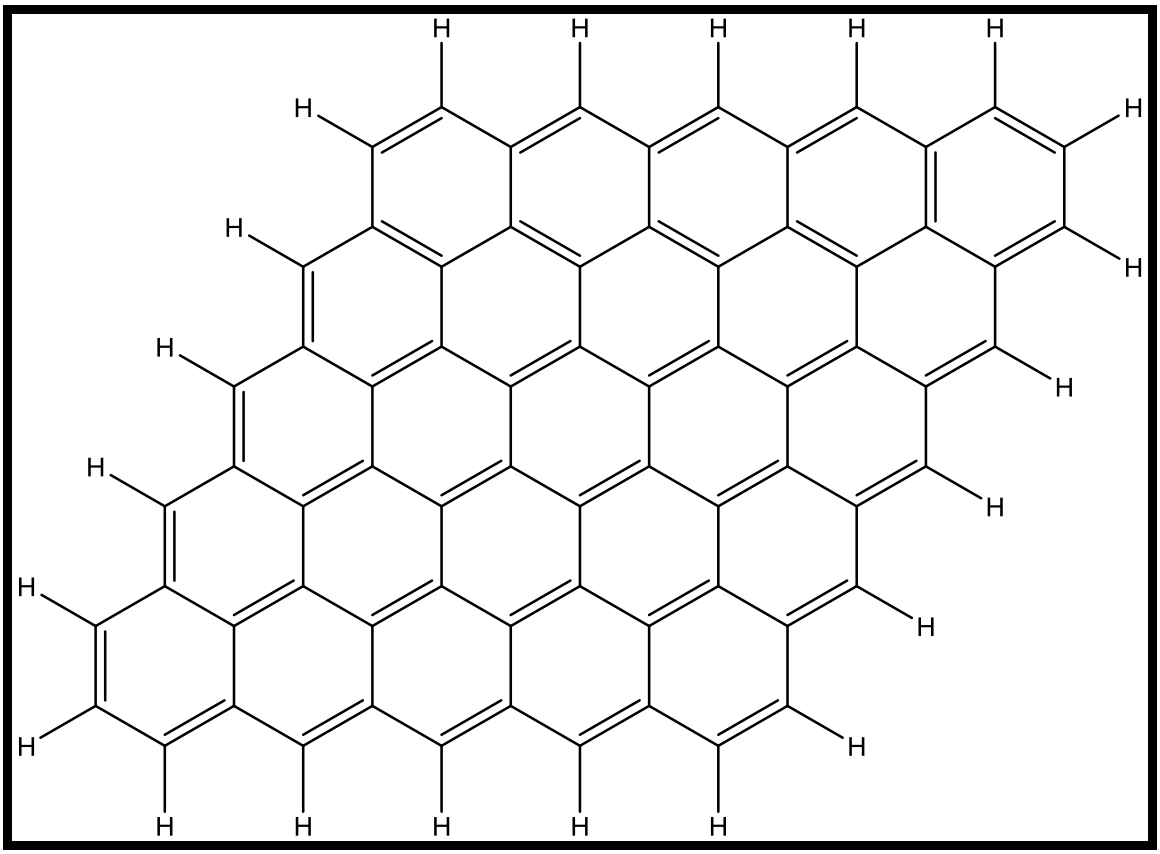

Figure 4.34. Structure of Graphene, One Layer of Graphite.

In spite of all carbon structure, graphite contains about 0.4% by weight hydrogen. The edges of graphene layers are terminated with hydrogen atoms [37, 38]. There are no reactive functional groups in graphite; therefore, a strong interaction with Surlyn® 1601 is not expected.

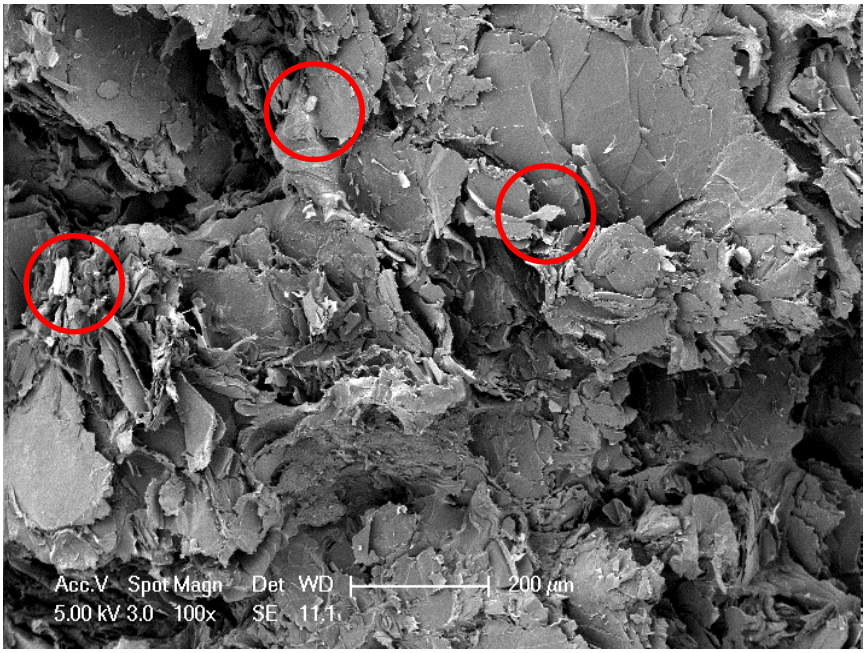

Figure 4.35. SEM Image of the Non-Treated Graphite Filled Surlyn® 1601 Composite at 100x Magnification.

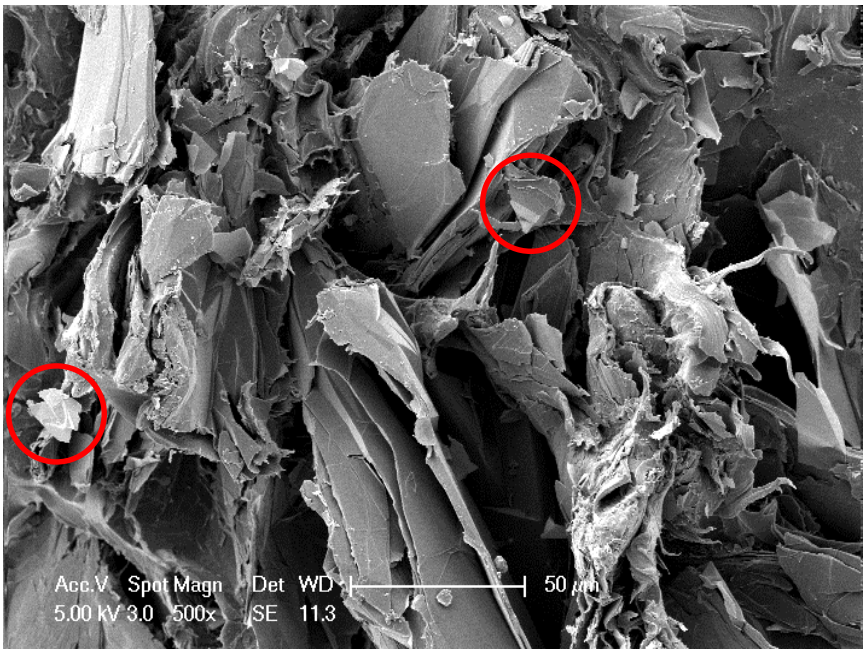

Figure 4.36. SEM Image of the Non-Treated Graphite Filled Surlyn® 1601 Composite at 500x Magnification.

Figures 4.35 and 4.36 show the SEM images of 30% by weight non-treated graphite filled Surlyn® 1601 composites at 100x and 500x magnifications, respectively. According to these SEM images, expectations about weak interfacial interactions between graphite and the polymer matrix are correct. There are lots of voids in the structure, and therefore, there is not a good adhesion between polymer matrix and graphite. Red circles show the free, unbound graphite particles in both of the above images. Consequently, the interaction between Surlyn® 1601 and graphite needs to be improved but as stated in the structure of graphite, there is no reactive functional groups on its structure. However, graphite is known to be oxidized at the surface to give reactive functional groups, such as alcohol, epoxy and carboxylic acid groups. Figure 4.37 shows the structure of graphene oxide, one layer of graphite oxide [39]. All the functional groups introduced by oxidation are capable of interaction with –COOH groups on Surlyn® 1601. However, the same groups should react much better with amino groups, so a diamine coupling agent could be used with oxidized graphite.

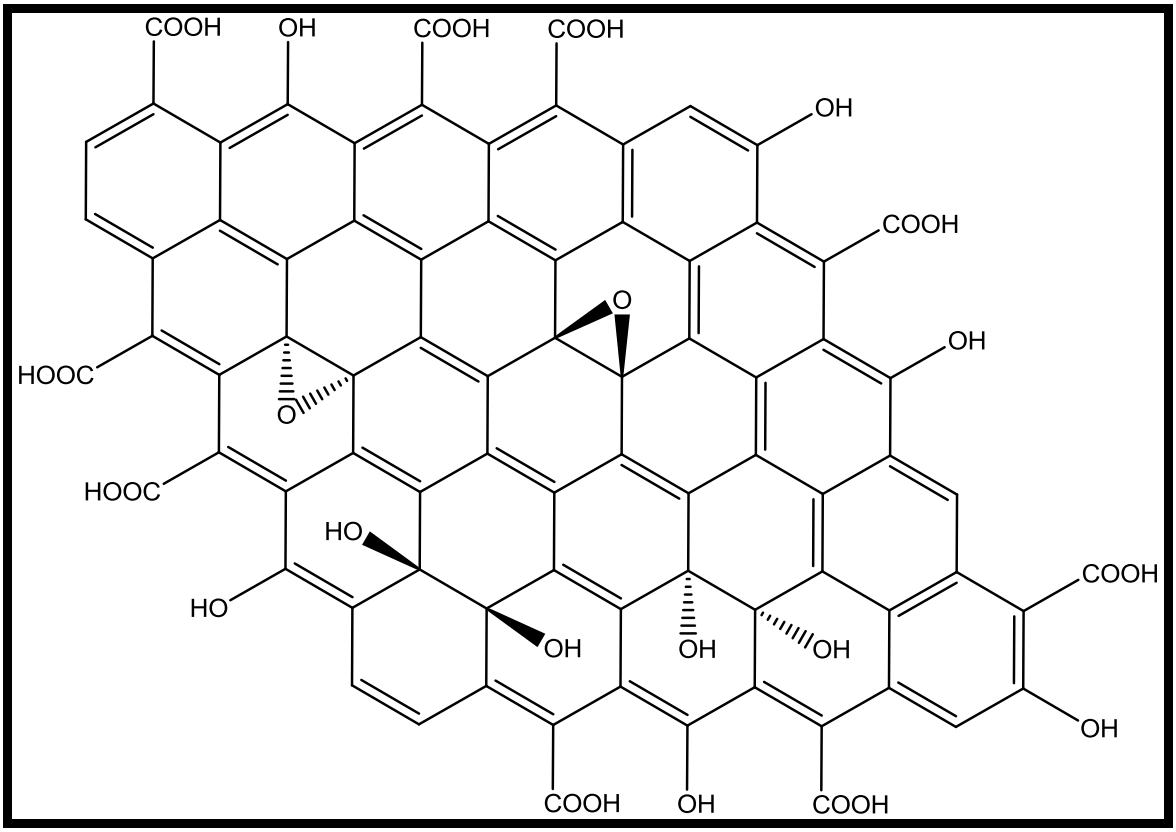

Figure 4.37. Structure of Graphene Oxide, One Layer of Graphite Oxide.

4.2.2. Thermal Conductivity Results and Interfacial Properties of Surface Treated Graphite Filled Surlyn®1601 Composites

4.2.2.1. SEM Analyses and Thermal Conductivity Result of 1,6-Diamino-hexane Treated Graphite Oxide Filled Surlyn® 1601 Composite. 1,6-Diamino-hexane has two basic amino groups that can be protonated by carboxylic acid structures in graphene oxide after treatment, this is an acid-base neutralization reaction. The amino groups are also reactive with epoxy groups *via* a ring opening addition reaction. The supposed reaction should give the product shown on Figure 4.38.

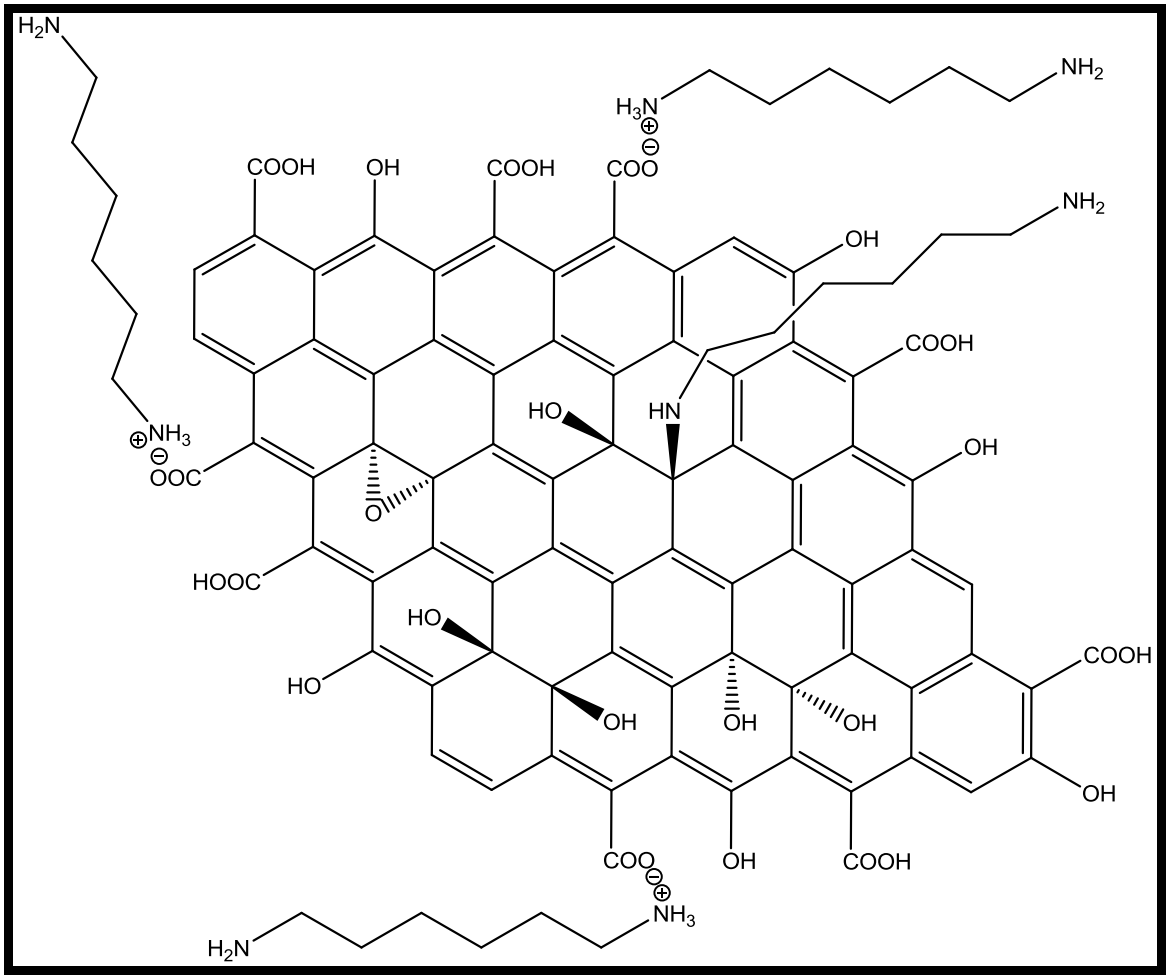

Figure 4.38. The Structure of Graphene Oxide After 1,6-Diamino-hexane Treatment.

By the use of a diamine we propose that one end of diamine should react with oxidized graphite and the other end should react with Surlyn® 1601, thus giving the desired filler-matrix adhesion.

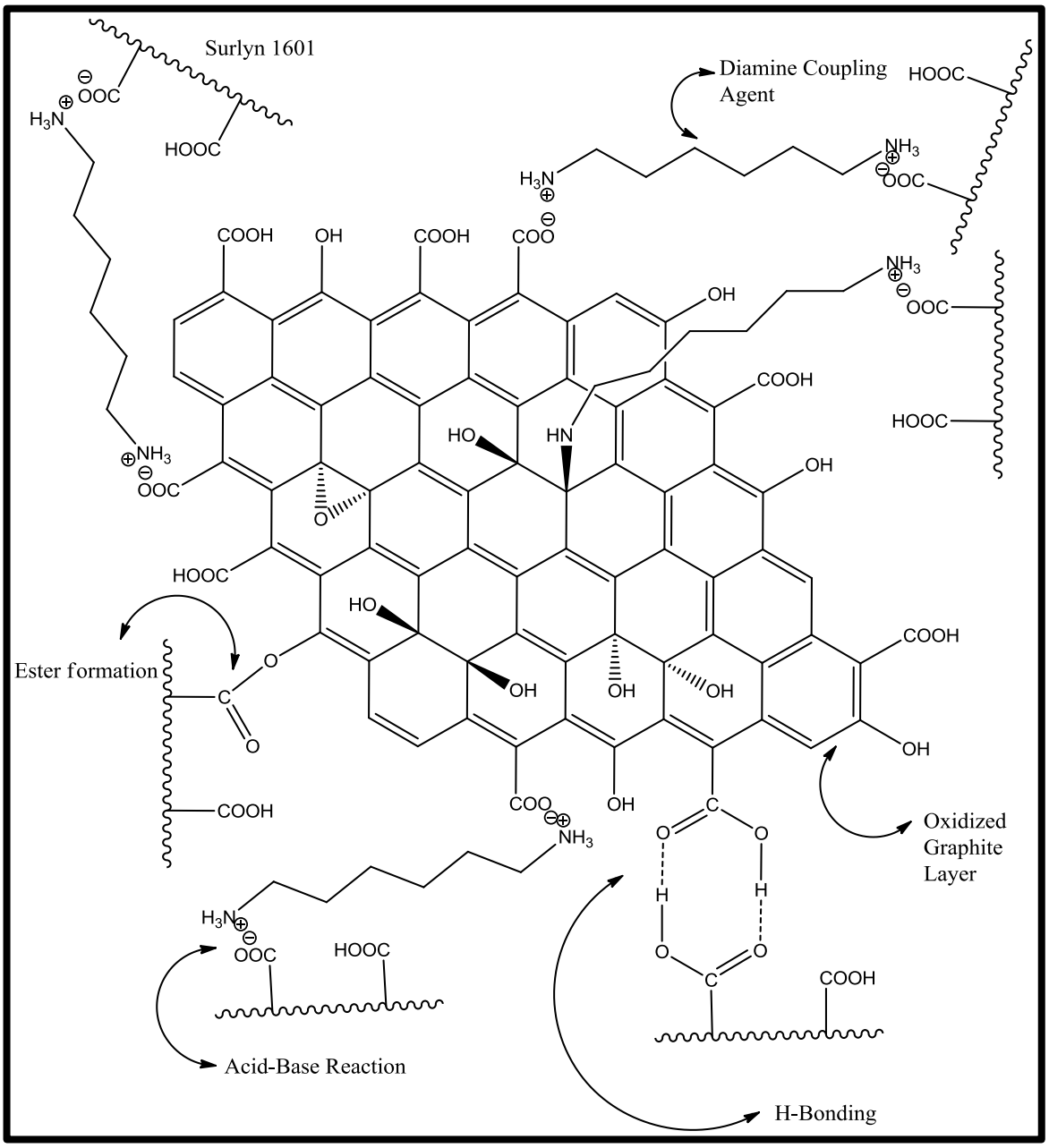

Figure 4.39. The Possible Network of 1,6-Diamino-hexane Coupled Graphite Oxide Reinforced Surlyn® 1601.

To obtain such a coupled sample, graphite is first oxidized, then dried and treated with 1,6-Diamino-hexane and dried again. In this step, any non-coupled diamine is

expected to evaporate. Then, 1,6-Diamino-hexane treated graphene oxide is extruded with Surlyn® 1601 and then molded, the interactions are shown on Figure 4.39. Firstly, there should be acid-base neutralization reactions between non-protonated amino end groups of 1,6-Diamino-hexane and acid groups of Surlyn® 1601. Additionally, there may be esterification reactions between alcohol ends of graphene oxide and acid groups of Surlyn® 1601. Lastly, hydrogen bonding interactions between carboxylic acid groups of graphite oxide and acid groups of Surlyn® 1601 should not be excluded. These are all possible reactions.

Figures 4.40, 4.41, 4.42 show the SEM images of 1,6-Diamino-hexane treated graphite oxide filled Surlyn® 1601 composite at 2000x, 5000x, 8000x magnifications, respectively.

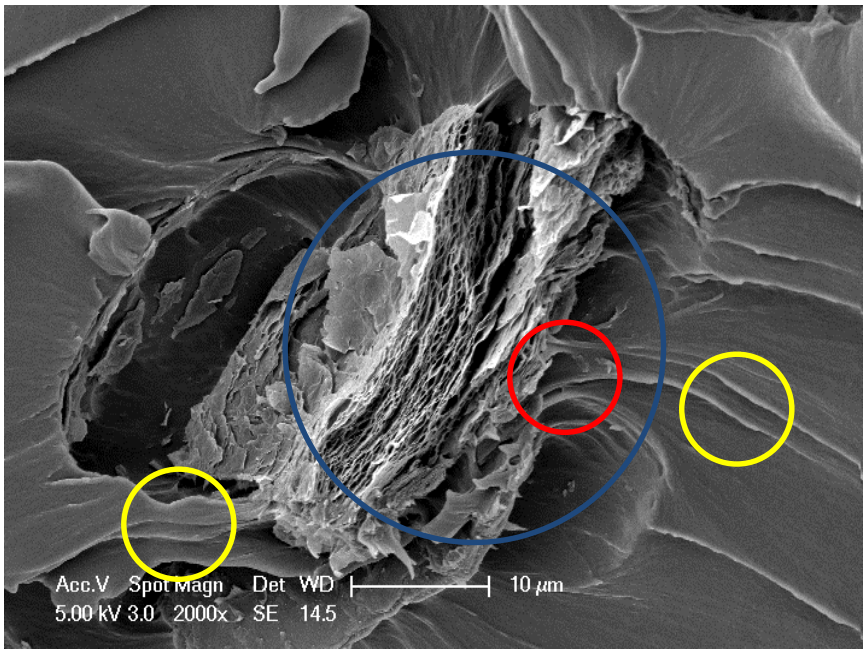

Figure 4.40. SEM Image of the 1,6-Diamino-hexane Treated Graphite Oxide Filled Surlyn® 1601 Composite at 2000x Magnification.

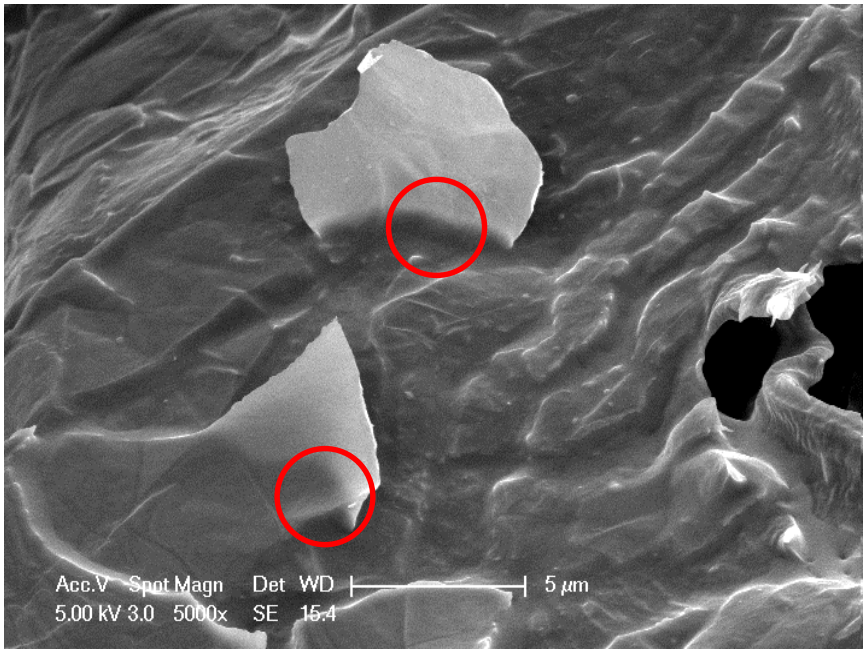

Figure 4.41. SEM Image of the 1,6-Diamino-hexane Treated Graphite Oxide Filled Surlyn® 1601 Composite at 5000x Magnification.

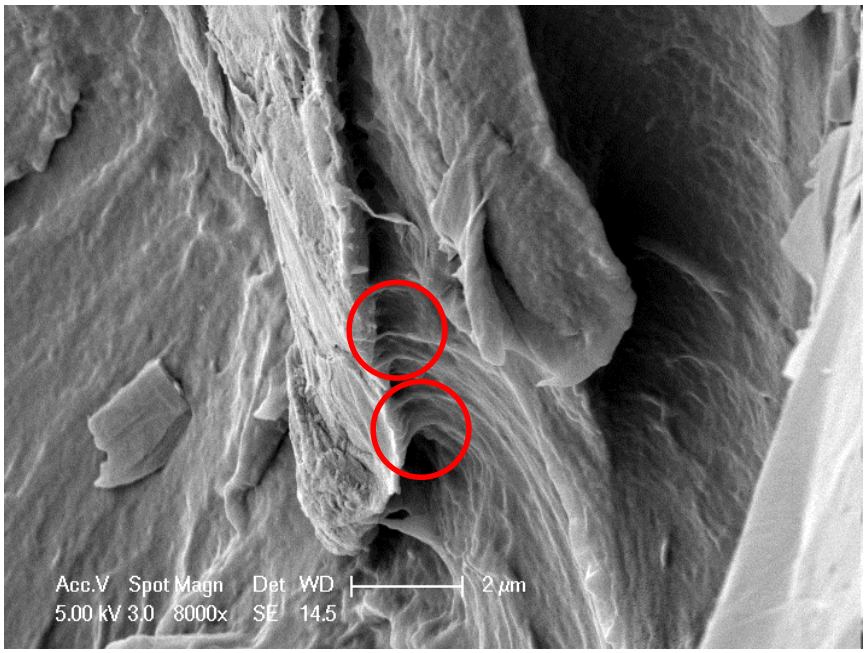

Figure 4.42. SEM Image of the 1,6-Diamino-hexane Treated Graphite Oxide Filled Surlyn® 1601 Composite at 8000x Magnification.

In Figure 4.40, the big blue circle shows the group of graphite oxide flakes. In the same SEM image, the red circle shows the adhesion between graphite oxide particles and polymer matrix. Graphite flakes tend to form clusters such as in the case of untreated aluminum and graphite oxide particles. Additionally, on this figure, the strain signs are designated as yellow circles. These strain signs prove that interfacial interactions between polymer matrix and the fillers are high. In Figure 4.41, the red circles show the graphite oxide particles having some regions buried under polymer matrix. In this picture again, there are graphite oxide flakes buried under polymer matrix completely. In Figure 4.42, there are some adhesion regions between the graphite oxide flake and the polymer matrix. As a result, interfacial interactions between the filler and the polymer matrix are dramatically improved by oxidizing graphite and treating it with 1,6-Diamino-hexane.

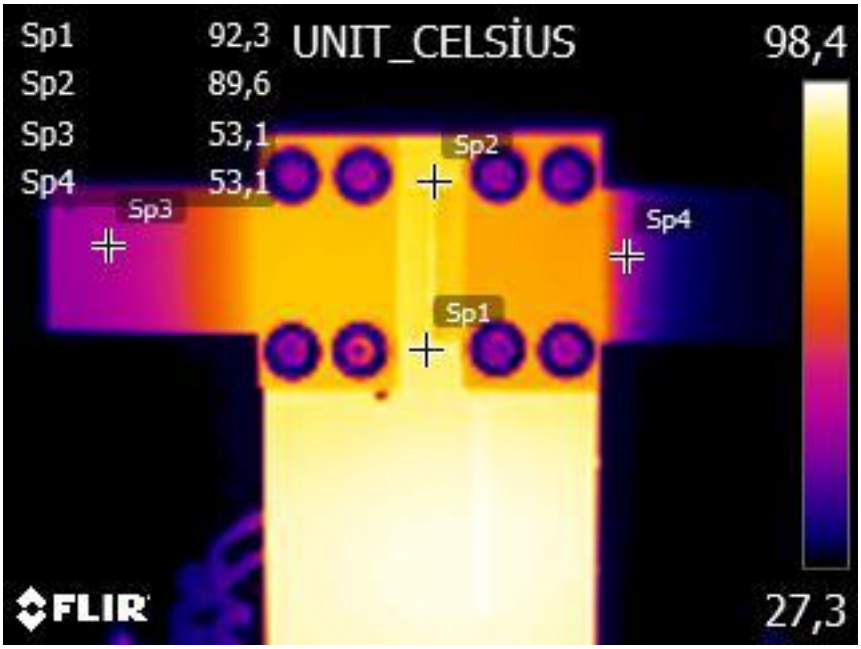

Figure 4.43. Thermal Camera View of Standard Stainless Steel Part (on the left) vs. 30% by Weight Graphite Oxide (1,6-Diamino-hexane treated) Filled Surlyn®1601 Composite Part (on the right).

Figure 4.43 demonstrates the thermal conductivity comparison of 30% by weight graphite oxide, which is treated by sufficient amount of 1,6-Diamino-hexane, filled Surlyn®1601 composite part over standard stainless steel part. Actually, due to the weight increase upon oxidation, 30% by weight 1,6-Diamino-hexane treated graphite oxide filled

composite is comparable to 20% by weight pristine graphite because of equal pure graphite content used in the composites. Thermal conductivity of 20% pristine graphite filled composite were found to be 4.2 W/m·K; however, thermal conductivity value of 30% surface treated graphite oxide filled composite is found to be 3.2 W/m·K. That is to say, although the interfacial interactions are enhanced, the thermal conductivity of the graphite oxide filled composite is lower than that of non-treated graphite filled composite at the same pure graphite concentration. This is because of the loss of extended conjugation in the structure of graphite oxide. According to the literature, when graphite is oxidized to graphite oxide, not only the edge groups but also the basal plane groups are oxygenated. The epoxy rings on the basal plane of the graphene oxide layers of graphite oxide disrupts the extended conjugation, and therefore, the electron movement, which is the actual reason of the decrease in the overall thermal conductivity of the composite. While graphite-polymer interactions are improved by oxidation, the thermal conductivity of graphite is reduced drastically.

4.2.2.2. SEM Analyses and Thermal Conductivity Result of Hydroxylated Graphite Filled Surlyn® 1601 Composite. The Fenton chain reactions are given on Figure 4.44 [40]:

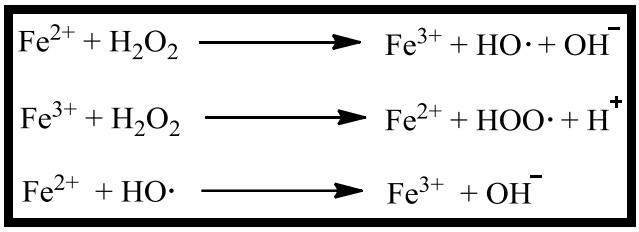

Figure 4.44. Fenton Chain Reactions.

When pure graphite is reacted with Fenton's reagents, the hydroxyl radical produced should attack the unsaturated -C=C- bonds of graphite at the edges. Only one hydroxyl radical may be added to the graphite not disturbing the conjugation, or two hydroxyl radicals may attack one double bond forming a diol-like structure, and this diol like structure may be further oxidized to diketone like structures. Figure 4.45 indicates the reaction of graphite with hydroxyl radical produced by Fenton's reactions. Methacrylic acid groups of Surlyn® 1601 may give esterification reactions with hydroxyl groups of hydroxylated graphite. There is also a possibility of having H-bonding interactions

between acid groups of the polymer and the alcohol groups of the filler. Methacrylate groups of Surlyn® 1601 may give Michael-addition reactions with α,β-unsaturated ketone like structures. Figure 4.46 shows all possible interactions of hydroxylated graphite with Surlyn® 1601.

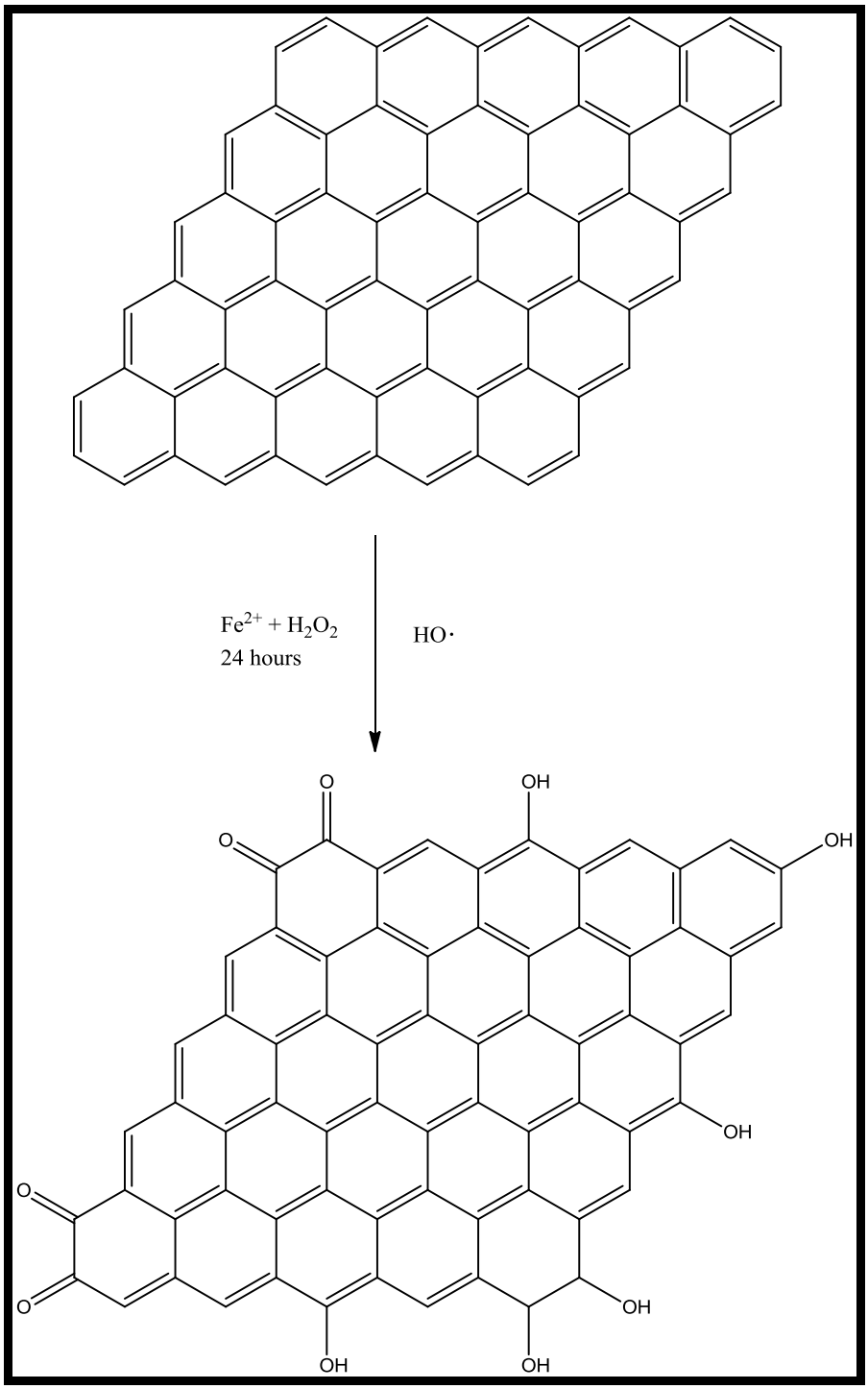

Figure 4.45. Fenton Oxidation of Graphite.

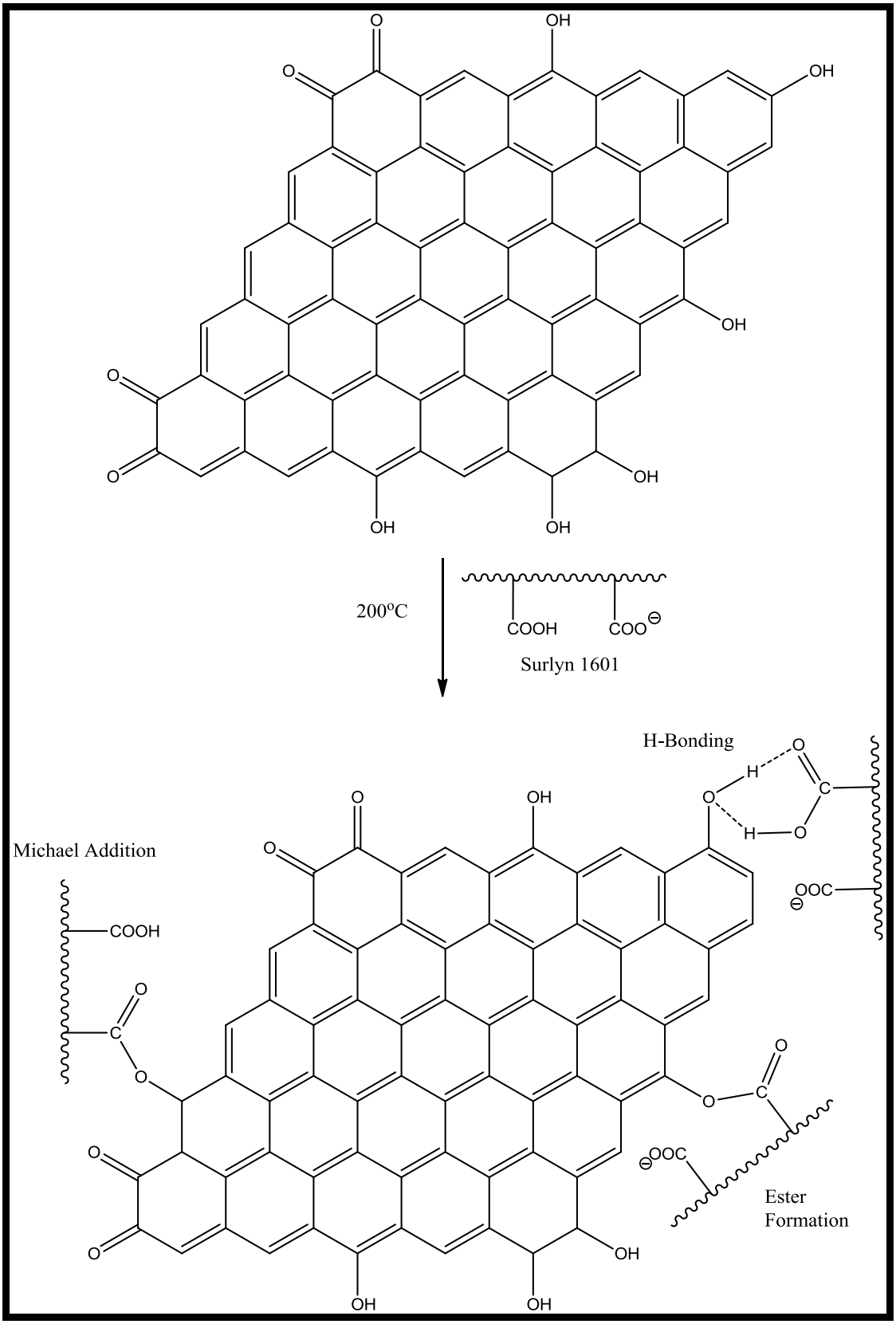

Figure 4.46. Possible Reactions and Interactions between Surlyn® 1601 and Hydroxylated Graphite.

If the reactions proposed in figures 4.45 and 4.46 take place, there will be an enhancement in the adhesion of graphite flakes to the polymer matrix. Figures 4.47, 4.48, 4.49 and 4.50 show the SEM images of the fractured surfaces of Surlyn® 1601 composite filled with 30% by weight hydroxylated graphite flakes at 250x, 1000x, 1500x and 2500x magnifications, respectively.

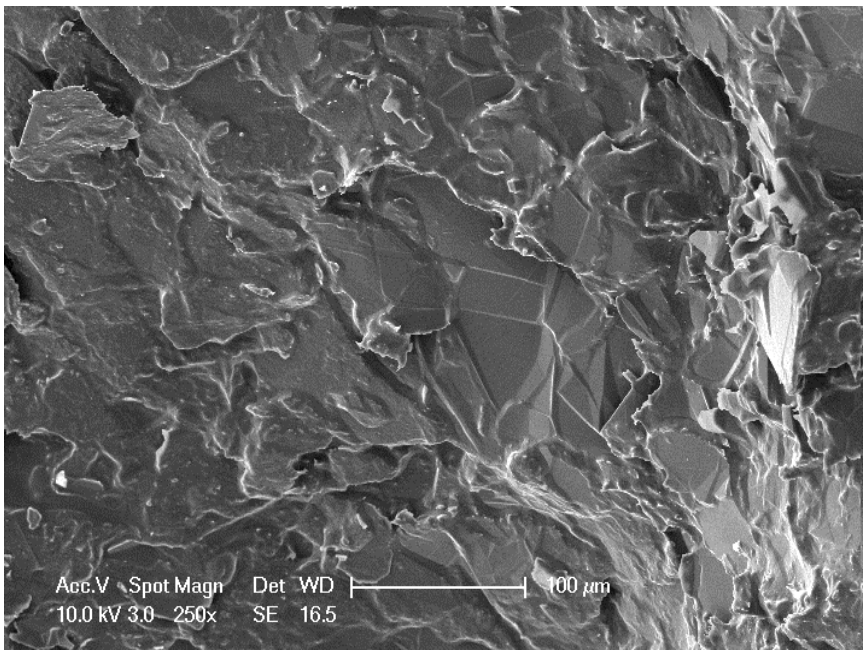

Figure 4.47. SEM Image of Hydroxylated Graphite Filled Surlyn® 1601 Composite at 250x Magnification.

In Figure 4.47, there is not any free graphite flake particle visible. Either they are buried under polymer matrix or they have adhesion regions to polymer matrix. There is also not much air inclusions and micro-voids visible which are due to the poor compatibility between the polymer and the filler. In Figure 4.48, the red circles show the adhesion regions of graphite flakes to the polymer matrix. There are some small particles on graphite flakes shown by blue circles; these are most probably the polymer residues after the composite part is fractured. This is an indication of the good interaction between the polymer matrix and the filler.

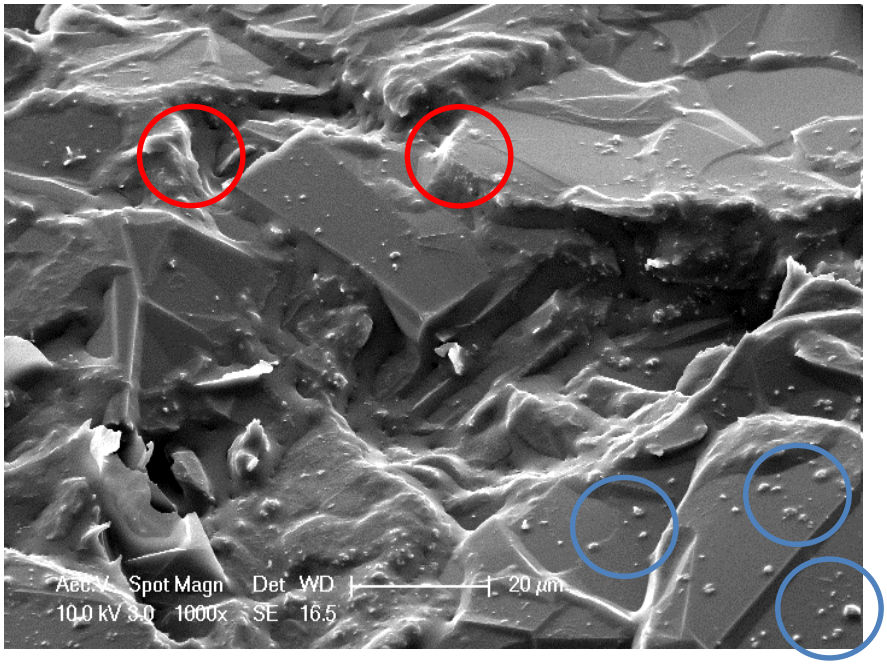

Figure 4.48. SEM Image of Hydroxylated Graphite Filled Surlyn® 1601 Composite at 1000x Magnification.

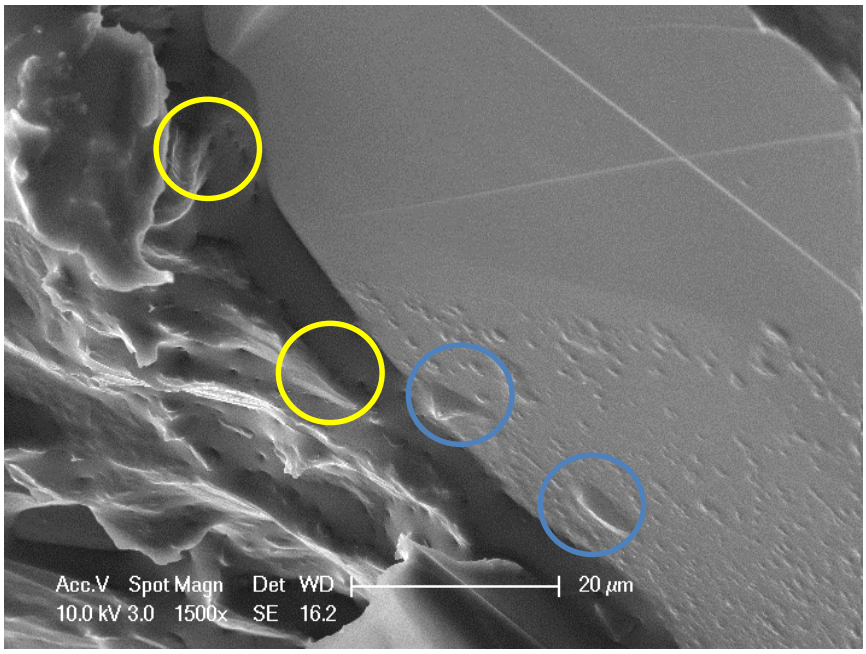

Figure 4.49. SEM Image of Hydroxylated Graphite Filled Surlyn® 1601 Composite at 1500x Magnification.

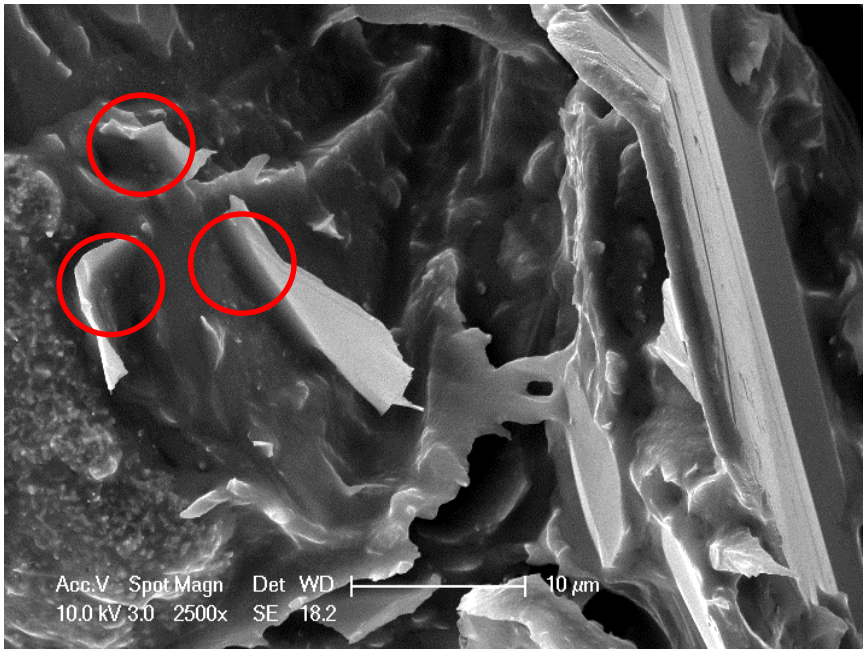

Figure 4.50. SEM Image of Hydroxylated Graphite Filled Surlyn® 1601 Composite at 2500x Magnification.

In Figure 4.49, there is a big graphite flake visible, and the adhesion points of this flake to the polymer matrix are shown by yellow circles. In the same image, the polymer residues on the graphite flake are shown by yellow circles. In Figure 4.50, there is some graphite flakes of which some parts are buried under polymer matrix are shown with red circles. There are no micro-voids or air inclusions near the flakes meaning that the polymer matrix and the hydroxylated graphite flakes are nearly compatible to each other.

Figure 4.50 demonstrates the thermal conductivity comparison of 30% by weight hydroxylated graphite filled Surlyn®1601 composite part over standard stainless steel part. The thermal conductivity of 30% by weight hydroxylated graphite filled Surlyn® 1601 composite is calculated to be 5.8 W/m·K, which is higher than those of 30% by weight pure graphite filled Surlyn® 1601 (5.6 W/m·K) and 30% by weight diamine coupled oxidized graphite filled Surlyn® 1601 (3.2 W/m·K) composites. Hydroxylated graphite filled composite has higher thermal conductivity compared to the others because the interfacial adhesion is improved with not much disturb on the conjugation of graphite structure; therefore, interfacial phonon scattering is decreased, having a result of an enhancement of the overall thermal conductivity of the composite.

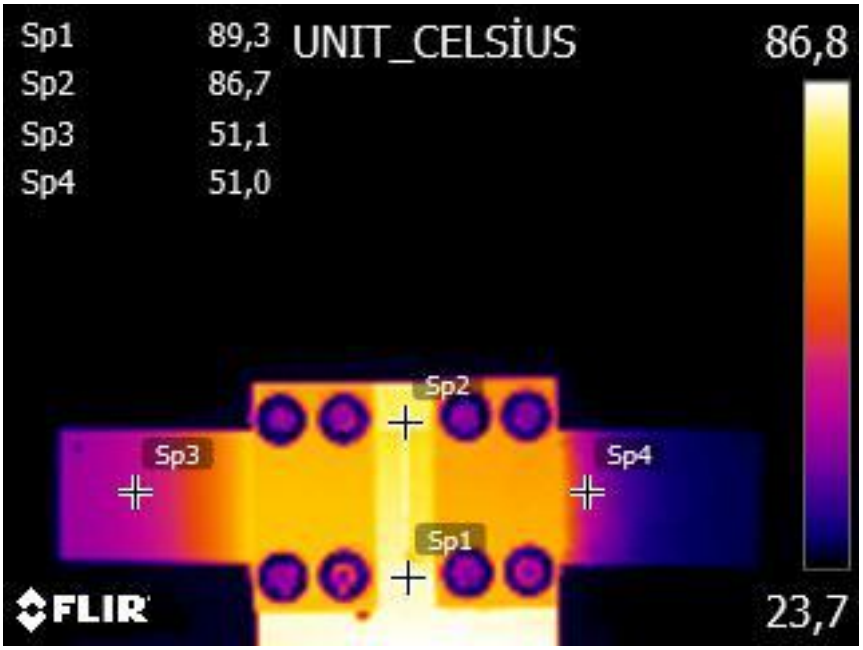

Figure 4.51. Thermal Camera View of Standard Stainless Steel Part (on the left) vs. 30% by Weight Hydroxylated Graphite Filled Surlyn®1601 Composite Part (on the right).

4.3. Carbon Fiber Filled Surlyn® 1601 Composites

Carbon fiber was chosen as another type of fillers used in these experiments for its advantage of having a higher aspect ratio compared to graphite flakes. It is easier for the filler particles to touch another at lower concentrations when fibers are used instead of spherical or flake shaped particles. Percolation threshold is reached at lower filler volume loading if fibers are used as fillers. Carbon fiber has exactly the same structure with non-oxidized graphite except that the graphite sheet is rolled into the shape of a fiber and that the edges of carbon fiber are oxidized during manufacture; for that reason, it may have some reactive functional groups with the polymer matrix. The edge groups of carbon fiber may be 1,4 diketone, quinone, hydroquinone and dicarboxylic acid like structures. Figure 4.51 shows the parallel sheets-like structure of graphite and rolled sheets-like structure of carbon fiber.

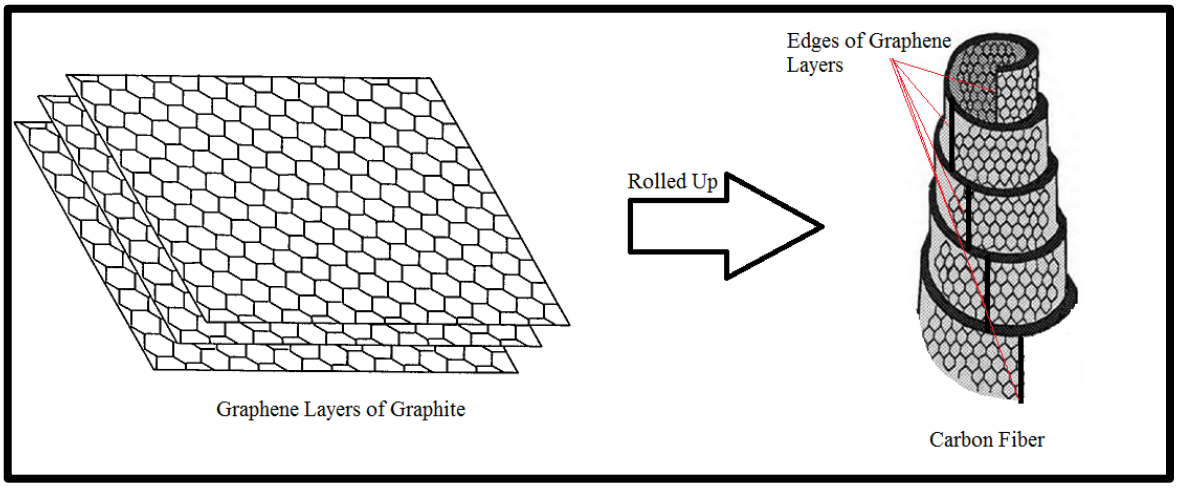

Figure 4.52. Structure of Graphite and Carbon Fiber.

These reactive groups may have some reactions with methacyrlic acid groups of Surlyn® 1601. This may be another advantage of carbon fiber over graphite. However, it has also some disadvantages over graphite. One disadvantage may be that thermal conductivity of carbon fiber used in these experiments, which is PAN-based carbon fiber, is not as high as graphite, it is only 20W/m·K. In general, PAN-based carbon fibers exhibit much lower thermal conductivity than other types of carbon fibers such as pitch-based and vapor-grown carbon fibers due to the fact that pitch-based carbon fiber and vapor grown carbon fiber have highly ordered microstructure compared to the structure of PAN-based carbon fiber [41]. Using PAN-based carbon fiber may not lead to high composite thermal conductivity although the shape factor is seemed to be advantageous. Another disadvantage of using carbon fiber is related to filler packing factor. Packing factor decreases when particle shape changes from spherical to flake, to fiber; and fibers have the lowest value of packing factor [42]. Therefore, it is not possible to reach very high filler loadings when fibers are used as fillers. One more disadvantage of using carbon fiber instead of graphite is that carbon fiber reinforced composite manufacturing is very difficult because fibers make entanglements which causes high melt viscosity during processing.

4.3.1. Thermal Conductivity Results

Table 4.4 shows the thermal conductivity results of Surlyn® 1601 composites including different amounts of untreated carbon fiber.

Table 4.4. Thermal Conductivity Results of the Composites Filled with Carbon Fiber.

Filler Weight %	Thermal Conductivity (W/m·K)
5%	2.3
10%	2.5
15%	2.7
20%	2.8

As the carbon fiber weight percentage increases in the composite, the thermal conductivity increases. However, filler loading above 20% by weight was very difficult to produce because very high viscosity was reached during process. Additionally, while 10% untreated graphite filled composite has a thermal conductivity value of 3.2 W/m·K, 10% untreated carbon fiber filled composite has a thermal conductivity value of 2.5 W/m·K. The difference in thermal conductivities is larger when filler loading is about 20%. 20% untreated carbon fiber filled composite has a thermal conductivity value of 2.8 W/m·K, whereas the composite containing 20% untreated graphite has a thermal conductivity value 4.2 W/m·K. Therefore, increasing carbon fiber filler loading does not increase the thermal conductivity of the composite effectively.

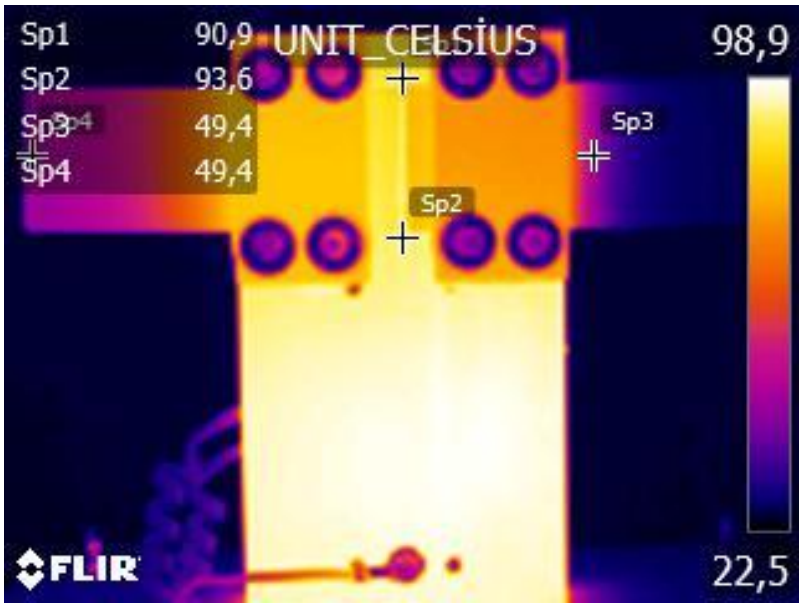

Figure 4.53. Thermal Camera View of Standard Stainless Steel Part (on the left) vs. 5% by weight Carbon Fiber Filled Surlyn®1601 Composite Part (on the right).

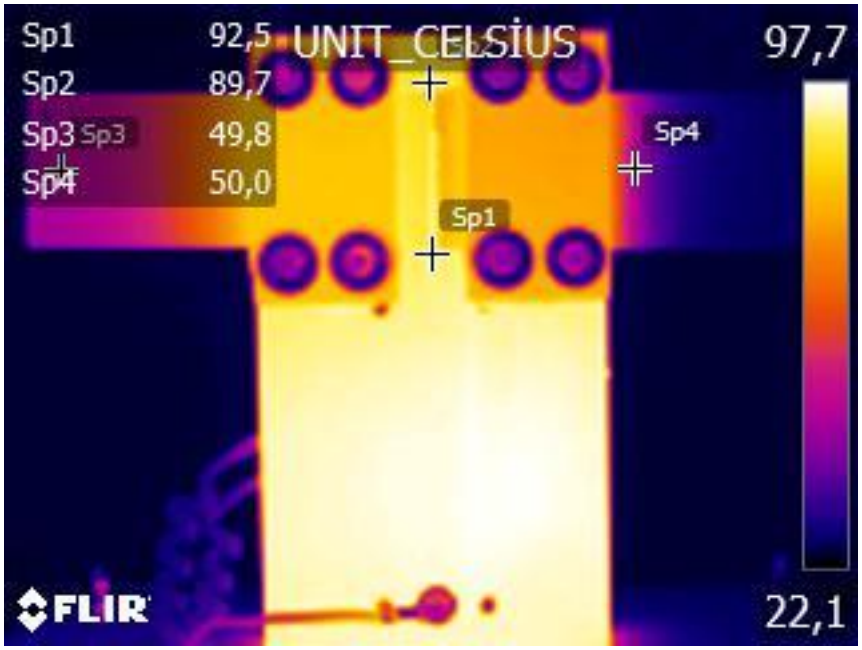

Figure 4.54. Thermal Camera View of Standard Stainless Steel Part (on the left) vs. 10% by Weight Carbon Fiber Filled Surlyn®1601 Composite Part (on the right).

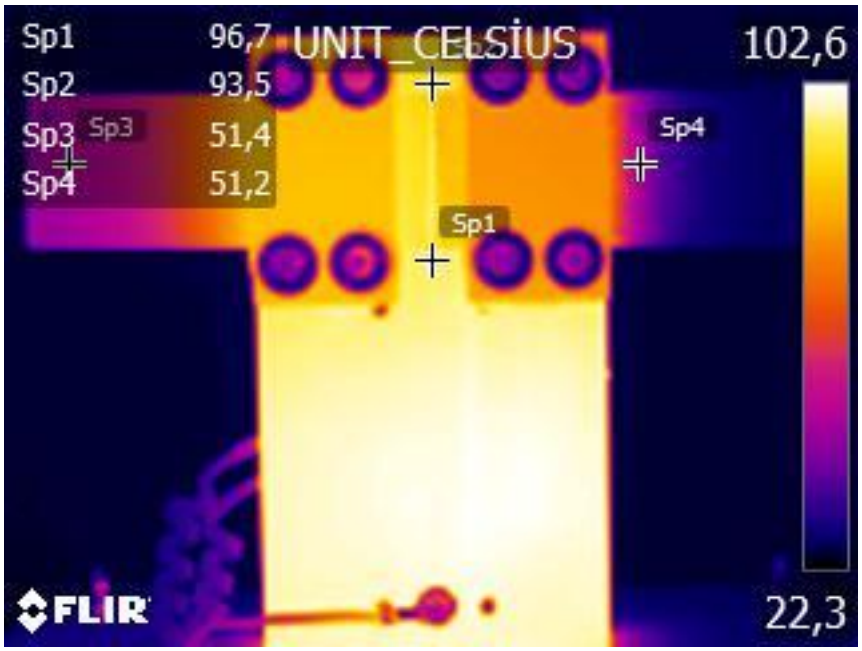

Figure 4.55. Thermal Camera View of Standard Stainless Steel Part (on the left) vs. 15% by Weight Carbon Fiber Filled Surlyn®1601 Composite Part (on the right).

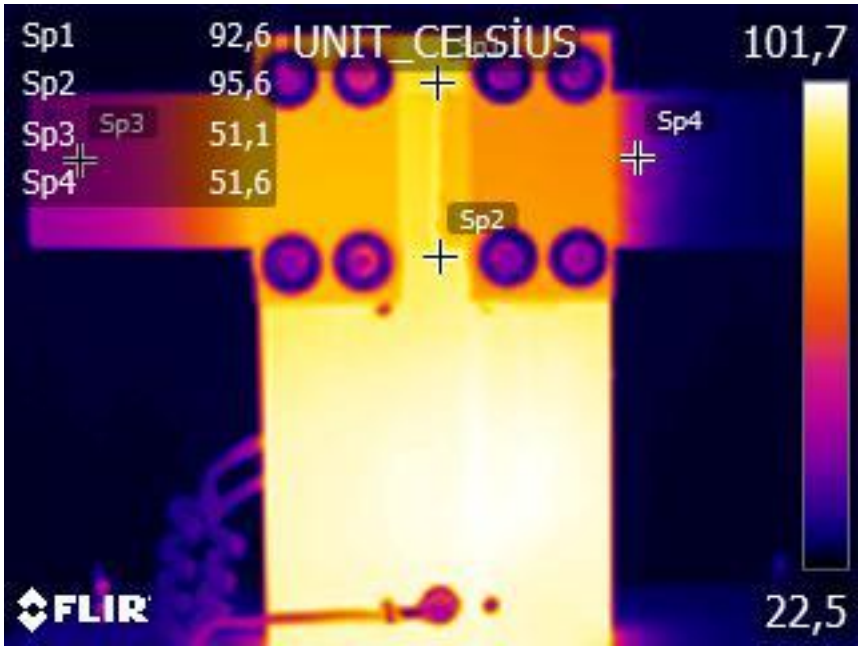

Figure 4.56 Thermal Camera View of Standard Stainless Steel Part (on the left) vs. 20% by Weight Carbon Fiber Filled Surlyn®1601 Composite Part (on the right).

4.3.2. Interfacial Properties

As stated above, carbon fiber consists of successive aromatic carbon rings except that the edges of the graphene sheets are oxidized during manufacture; for that reason, it may have some reactive functional groups. The edge groups of carbon fiber may be 1,4 diketone, quinone, hydroquinone and dicarboxylic acid like structures which may react with methacyrlic acid or methacrylate groups of Surlyn® 1601. Figures 4.46, 4.47, 4.48 and 4.49 show the SEM images of the fractured surfaces of carbon fiber filled Surlyn® 1601 composites at 100x, 250x, 350x, 200x magnifications; respectively.

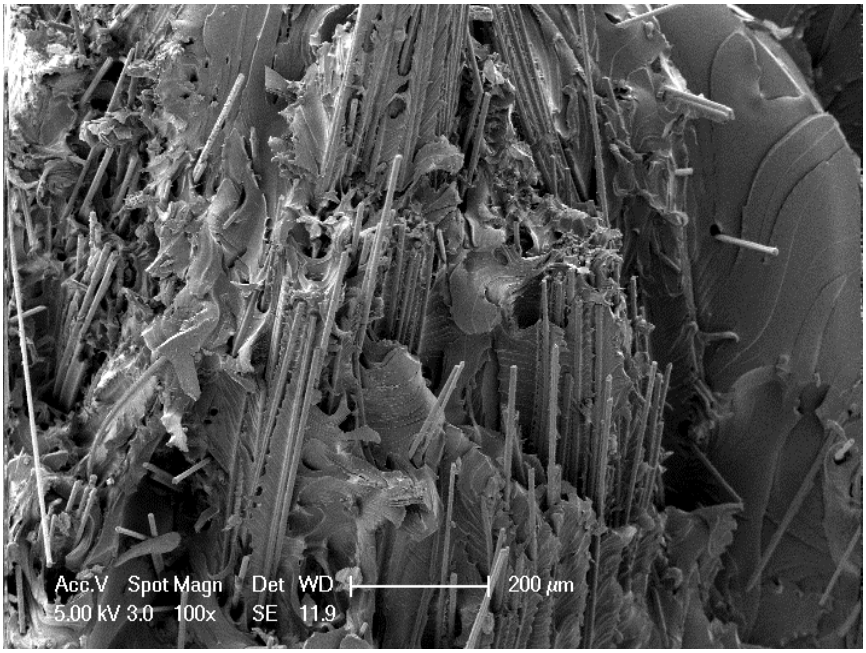

Figure 4.57. SEM Image of the Non-Treated Carbon Fiber Filled Surlyn® 1601 Composite at 100x Magnification.

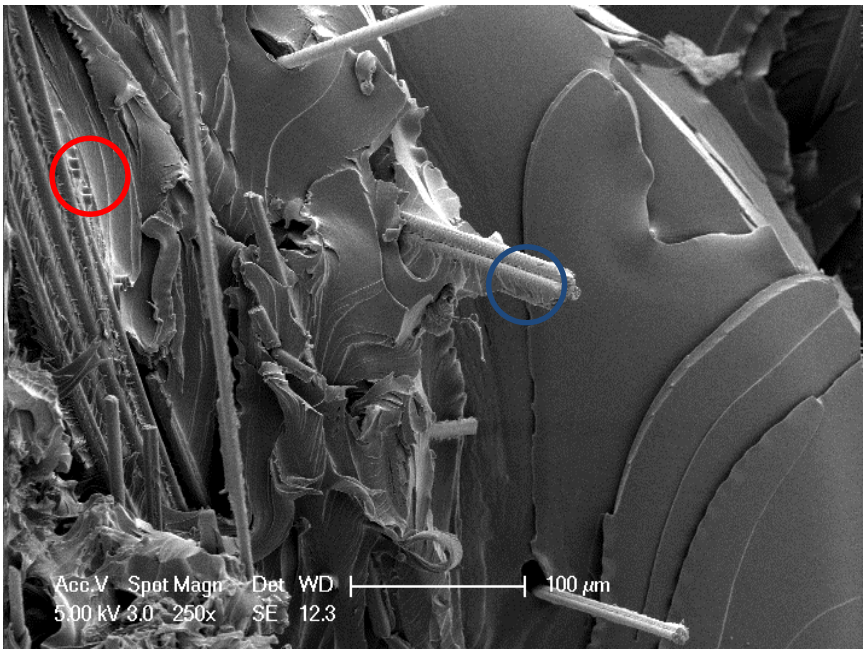

Figure 4.58. SEM Image of the Non-Treated Carbon Fiber Filled Surlyn® 1601 Composite at 250x Magnification.

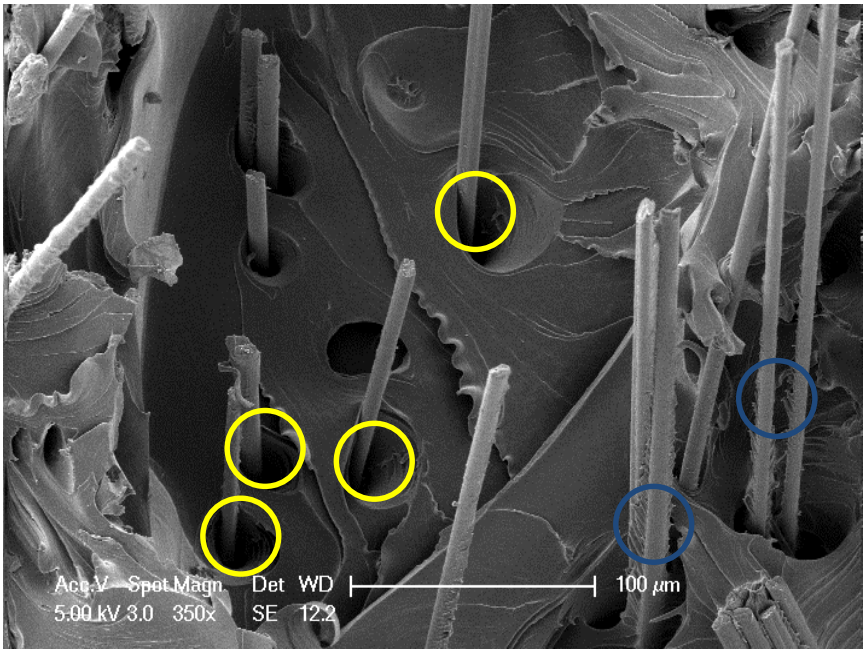

Figure 4.59. SEM Image of the Non-Treated Carbon Fiber Filled Surlyn® 1601 Composite at 350x Magnification.

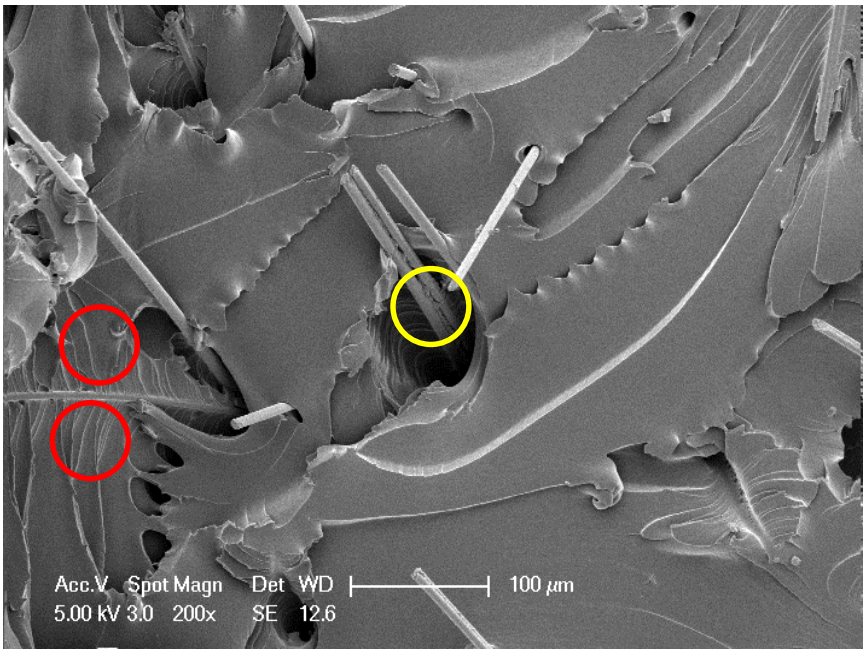

Figure 4.60. SEM Image of the Non-Treated Carbon Fiber Filled Surlyn® 1601 Composite at 200x Magnification.

Red circles on above SEM images show the strain signs on the polymer matrix during breaking the composite. This is an indication of the existence of an interaction between non-treated carbon fiber and Surlyn® 1601 polymer matrix. Another indication of the interaction may be that carbon fiber is wetted by the polymer matrix after fracture shown by blue circles on above figures. At some regions, there are some voids, in these voids; there are one or more carbon fibers. In such voids, the interactions are observed to be weak, shown by yellow circles. If the voids were as small as possible, even adherent to carbon fibers, then the interactions would be excellent. However, there are some smaller voids, too. That is to say, there are some good and moderate interactions at some regions between polymer matrix and carbon fiber. It should be added that the carbon fiber used was optimized for epoxy resins during manufacture. Polarity of epoxy resins is much higher than Surlyn® 1601.

For the fact that the adhesion between the carbon fiber and the matrix is good enough and the thermal conductivity enhancement of carbon fiber addition to the filler is not very effective, there is no need to make surface modification of carbon fiber.

5. CONCLUSIONS

Conclusions drawn from this work are as follows:

Addition of highly thermally conductive fillers such as aluminum, graphite and carbon fiber to the polymer matrix results in an increase of the thermal conductivity. As the weight ratio of such additives increases, the thermal conductivity of the composite is further increased.

Using high aspect ratio aluminum fillers instead of lower aspect ratio aluminum fillers results in higher thermal conductivity. Although the flake aluminum and the spherical aluminum have exactly the same thermal conductivity value, flake aluminum filled composites have higher thermal conductivity compared to the spherical aluminum filled composites at the same filler weight ratios.

Interfacial heat resistance and phonon scattering are important problems affecting the thermal conductivity of the composite negatively; therefore, they should be minimized. In order to minimize such problems, the attractive interactions between the polymer matrix and the filler should be excellent. Treating aluminum flakes with an aminosilane increases the adhesion between the polymer and the filler; therefore, at the same filler weight ratio, aminosilane treated aluminum flake filled composite has higher thermal conductivity compared to non-treated aluminum flake filled composite.

Although treating aluminum flakes with an aminosilane and an organic polymer emulsion Michem® Prime 4983R seems to be enhance the adhesion very much, the thermal conductivity of the composite is lower than non-treated aluminum flake filled composite at the same filler weight ratio. The reason may be that when the organic polymer Michem® Prime 4983R coupled aluminum flakes touch other, the thermal insulation of the polymeric coating decreases conductivity.

Using fillers with higher thermal conductivity increases thermal conductivity of the composite. Graphite filled composites have higher thermal conductivity values compared

to spherical aluminum and flake aluminum filled composites at the same filler weight ratios.

Oxidizing graphite *via* Modified Hummers Method is an efficient way to have reactive functional groups such as carboxylic acid groups, alcohol groups and epoxy rings on graphite structure; however, such groups exist not only on the edge plane of the graphene sheets but also on the basal plane of these sheets. Consequently, these functional groups results in the loss of the extended conjugation of the whole graphite structure disturbing electron movement and increase the distance between the graphene sheets of graphite, which are the causes of the thermal conductivity decrease of the filler. Therefore, although the interfacial adhesion is improved by using oxidized graphite instead of pure graphite in the composite, the overall thermal conductivity of the composite is not enhanced.

Hydroxylation of graphite *via* Fenton Oxidation is an alternative way to create reactive functional groups on graphite. These functional groups may be hydroxyl groups, diol structures, α,β-unsaturated ketone and diketone like structures. Fenton Oxidation method does not affect the basal plane structure of graphite, only the edge groups are oxidized, which does not disturb the conjugation of the whole structure; only conjugation near the edges may be disturbed. Using Fenton hydroxylated graphite instead of pure graphite improves the interfacial adhesion, decreases the phonon scattering at the interfacial zones; therefore, overall the thermal conductivity of the composite is improved.

Although they have nearly the same structure, thermal conductivity of graphite used in these experiments is higher than thermal conductivity of PAN-based carbon fiber used in these experiments. This is because of the precursors used in the carbon fiber manufacturing process; however, carbon fiber has the advantages of higher aspect ratio and better adhesion to the polymer matrix over graphite. Graphite filled composites have higher thermal conductivity values compared to carbon fiber filled composites at the same filler volume ratios. This may be due to 30 fold thermal conductivity difference of graphite and carbon fiber.

Packing factor, or namely, filling limit, is a disadvantage of high aspect ratio fillers such as whiskers and fibers. Therefore, it is not possible to use high levels of fillers when high aspect ratio fillers are used because the melt viscosity of the polymer becomes impractically high.

Table 5.1 gives the numerical value of the thermal conductivities obtained in this research. Each data point is obtained from at least 5 measurements.

Table 5.1. Summary of the Thermal Conductivity Values of the Composites in W/m·K.

Filler Type/Filler Loading	**5%**	**10%**	**15%**	**20%**	**30%**	**40%**	**50%**
Spherical Al		2.1		2.4	2.6	2.7	3.1
Flake Al					3.2		4.0
Aminosilane Treated Al Flake					4.0		
Michem® Prime 4983R + Aminosilane Treated Flake Al					3.0		
Graphite		3.2		4.2	5.6	6.8	
Diamine Treated Graphite Oxide					3.2		
Hydroxylated Graphite					5.8		
Carbon Fiber	2.3	2.5	2.7	2.8			

REFERENCES

1. Serway, R. A., J. W., Jewett, *Physics*, 6th Edition, Thomson Brooks/Cole, London, 2001.

2. Tsekmes, I. A., R., Kochetov, P. H. F., Morshuis, J. J., Smit, "Modeling the Thermal Conductivity of Polymeric Composites Based on Experimental Observations", *IEEE Transactions on Dielectrics and Electrical Insulation*, Vol. 21, No. 2, pp. 412-423, 2014.

3. Junior, A. F., D. J., Shanafield, "Thermal conductivity of polycrystalline nitride (AlN) ceramics", *Ceramica*, Vol. 50, No. 315, pp. 247-253, 2004.

4. Serway, R. A., J. W., Jewett, *Physics*, 6th Edition, Thomson Brooks/Cole, London, 2001.

5. Hong, J., D. W., Park, S. E., Shim, "A Review on Thermal Conductivity of Polymer Composites Using Carbon-Based Fillers: Carbon Nanotubes and Carbon Fibers", *Carbon Letters*, Vol. 11, No. 4, pp. 347-356, 2010.

6. Weber, E. H., *Development and Modeling of Thermally Conductive Polymer/Carbon Composites*, Ph.D. Thesis, Michigan Technological University, 2001.

7. Han, Z., A., Fina, "Thermal conductivity of carbon nanotubes and their polymer nanocomposites: A review", *Progress in Polymer Science*, Vol. 36, No. 7, pp. 914-944, 2011.

8. Huang, X., P., Jiang, T., Tanaka, "A Review of Dielectric Polymer Composites with High Thermal Conductivity", *IEEE Electrical Insulation Magazine*, Vol. 27, No. 4, pp. 8-16, 2011.

9. Tsekmes, I. A., R., Kochetov, P. H. F., Morshuis, J. J., Smit, "Thermal Conductivity of Polymeric Composites: A Review", *International Conference on Solid Dielectrics*, IEEE, Bologna, 2013.

10. Mamunya, Ye. P., V. V., Davydenko, P., Pissis, E. V., Lebedev, "Electrical and Thermal Conductivity of Polymers Filled with Metal Powders", *European Polymer Journal*, Vol. 38, pp. 1887-1897, 2002.

11. Lee, G. W., M., Park, J., Kim, J. I., Lee, H. G., Yoon, "Enhanced Thermal Conductivity of Polymer Composites Filled with Hybrid Filler", *Composites*, Part A, Vol. 37, pp. 727-734, 2006.

12. Heiser, J. A., J. A., King, "Thermally conductive carbon filled Nylon 6,6", *Polymer Composites*, Vol. 25, No. 2, pp. 186-193, 2004.

13. Kumar, N., *Comprehensive Physics XII*, Laxmi Publications, New Delhi, 2003.

14. Callister, W. D., *Materials Science and Engineering*, Seventh Edition, John Wiley and Sons Inc., New York, 2007.

15. Vettoor, S. V., "*Electrical Conduction and Superconductivity*", 2003, http://www.ias.ac.in/resonance/Volumes/08/09/0041-0048.pdf , [Accessed October 2015].

16. Dai, L., *Intelligent Macromolecules for Smart Devices*, Springer, London, 2004.

17. Stauffer, D., A., Aharony, *Introduction to percolation theory*, Revised Second Edition, Taylor and Francis, London, 1994.

18. Mamunya, Y., A., Boudenne, N., Lebovka, L., Ibos, Y., Candau, M., Lisunova, "Electrical and thermophysical behaviour of PVC-MWCNT nanocomposites", *Composites Science and Technology*, Vol. 68, pp. 1981-1988, 2008.

19. Callister, W. D., *Materials Science and Engineering*, Seventh Edition, John Wiley and Sons Inc., New York, 2007.

20. Jin, J., Y., Lin, M., Song, C., Gui, S., Leesirisan, "Enhancing the electrical conductivity of polymer composites", *European Polymer Journal*, Vol. 49, Issue 5, pp. 1066-1072, 2013.

21. Horibe, H., T., Kamimura, K., Yoshida, "Electrical Conductivity of Polymer Composites Filled with Carbon Black", *Japanese Journal of Applied Physics*, Vol. 44, Part 1, No. 4A, pp. 2025-2029, 2005.

22. Squitieri, V., "Thermally Conductive Materials", United States Patent, US 4869954 A, 1989.

23. Janssen, R. H. C., F. V., Van, "Heatsinks of Thermally Conductive Plastic Materials", European Patent, EP 2254940 B1, 2014.

24. Crawford, M. L., B. W., Peterson, M. D., McKnight, "Enhanced Thermally-Conductive Cushioning Foams by Addition of Graphite", United States Patent, US 20140182063 A1, 2014.

25. Wang, Z., T., Iizuka, M., Kozako, Y., Ohki, T., Tanaka, "Development of Epoxy/BN Composites with High Thermal Conductivity and Sufficient Dielectric Breakdown Strength Part I – Sample Preparations and Thermal Conductivity", *IEEE Transactions on Dielectrics and Electrical Insulation*, Vol. 18, Issue: 6, pp. 1963-1972, 2011.

26. Weber, E. H., *Development and Modeling of Thermally Conductive Polymer/Carbon Composites*, Ph.D. Thesis, Michigan Technological University, 2001.

27. Reynolds, P. J., *A Surlyn® Ionomer as a Self-Healing and Self-Sensing Composite*, MRes Thesis, University of Birmingham, 2011.

28. Fall, R., *Puncture Reversal of Ethylene Ionomers – Mechanistic Studies*, MSc Thesis, Virginia State University, 2001.

29. DuPont™, *DuPont™ Surlyn® Thermoplastic Resins*, 2014, http://www.dupont.com//content/dam/dupont/products-and-services/packaging-materials-and-solutions/packaging-materials-and-solutions-landing/documents/surlyn_properties_overview_.pdf, [Accessed October 2015].

30. MatWeb Material Property Data, *DuPont™ Surlyn® 1601 Sodium Ionomer Resin for Blown and Cast Film*, 2011, http://www.matweb.com/search/DataSheet.aspx?MatGUID=05ab70e3d1ca488eae578546c238588e&ckck=1, [Accessed October 2015].

31. Chen, J., B., Yao, C., Li, G., Shi, "An improved Hummers method for eco-friendly synthesis of graphene oxide", *Carbon*, Vol. 64, pp. 225-229, 2013.

32. Bradley, R. H., K., Cassity, R., Andrews, M., Meier, S., Osbeck, A., Andreu, C., Johnston, A., Crossley, "Surface studies of hydroxylated multi-wall carbon nanotubes", Applied Surface Science, Vol. 258, Issue 11, pp. 4835-4843, 2012.

33. MatWeb Material Property Data, *DuPont™ Surlyn® 1601 Sodium Ionomer Resin for Blown and Cast Film*, 2011, http://www.matweb.com/search/DataSheet.aspx?MatGUID=05ab70e3d1ca488eae578546c238588e&ckck=1, [Accessed October 2015].

34. Chauhan, D., N., Singhvi, R., Singh, "Effect of Geometry of Particles on the Effective Thermal Conductivity of Two-Phase Systems", *International Journal of Modern Nonlinear Theory and Application*, Vol. 1, pp. 40-46, 2012.

35. Michelman™ Technical Data Sheet, *Michem® Prime 4983R*, 2015, http://www.michelman.com/products/download/?pcode=MP4983R, [Accessed October 2015].

36. Jaksich, J. A., *Fullerenes and Graphene: Super Molecules of Nanotechnology*, 2014, http://www.decodedscience.org/fullerenes-graphene-super-molecules-nanotechnology/49012, [Accessed October 2015].

37. Delhaes, P., *Graphite and Precursors*, Taylor & Francis, Amsterdam, 2001.

38. Enoki, T., "Role of edges in the electronic and magnetic structures of nanographene", *Physica Scripta*, Vol. 2012, pp. 1-14, 2012.

39. He, H., J., Klinowski, M., Forster, A., Lerf, "A new structural model for graphite oxide", Chemical Physics Letter, Vol. 287, Issues 1-2, pp. 53-56, 1998.

40. Li, W., Y., Bai, Y., Zhang, M., Sun, R., Cheng, X., Xu, Y., Chen, Y., Mo, "Effect of hydroxyl radical on the structure of multi-walled carbon nanotubes", *Synthetic Metals*, Vol. 155, Issue 3, pp. 509-515, 2005.

41. Mortensen, A., *Concise Encyclopedia of Composite Materials*, Second Edition, Elsevier, Amsterdam, 2006.

42. Chan, E. H., *Development and Characterization of Thermally Conductive Polymeric Composites for Electronic Packaging Applications*, Master of Applied Science and Engineering, University of Toronto, 2011.